GJ/TMC-17
UC-70A

CALIBRATION-PAD PARAMETER ASSIGNMENTS FOR IN-SITU GAMMA-RAY MEASUREMENTS OF RADIUM, THORIUM, AND POTASSIUM

November 1985

U.S. DEPARTMENT OF ENERGY
ASSISTANT SECRETARY FOR NUCLEAR ENERGY

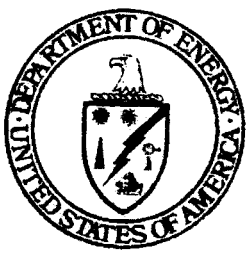

Office of Remedial Action and Waste Technology
Technical Measurements Center
Grand Junction Projects Office, Colorado

Printed in the United States of America
Available from
National Technical Information Service
U.S. Department of Commerce
5285 Port Royal Road
Springfield, VA 22161

NTIS price codes
Printed copy: A04
Microfiche copy: A01

Mary Gerry White, TMC Program Manager
Office of Remedial Action and Waste Technology
Larry Ball, Project Officer
Grand Junction Projects Office
John R. Duray, Project Manager
Technical Measurements Center

GJ/TMC-17
UC-70A

CALIBRATION-PAD PARAMETER ASSIGNMENTS FOR IN-SITU GAMMA-RAY MEASUREMENTS OF RADIUM, THORIUM, AND POTASSIUM

David C. George
Edward F. Novak
Randall K. Price
Technical Measurements Center

November 1985

Prepared for
U.S. Department of Energy
Office of Remedial Action and Waste Technology

Bendix Field Engineering Corporation
Grand Junction, Colorado
Under Contract No. DE-AC07-76GJ01664
with
U.S. Department of Energy
Grand Junction Projects Office
Idaho Operations

CONTENTS LISTING

CONTENTS LISTING (continued)

APPENDICES
(on microfiche, in pocket, back inside cover)

LIST OF ILLUSTRATIONS

LIST OF TABLES

LIST OF TABLES (continued)

ABSTRACT

The U.S. Department of Energy (DOE) Office of Remedial Action and Waste Technology has as one of its goals the standardization of field measurements made by remedial action contractors throughout the country. In support of this goal, the Technical Measurements Center (TMC) was established at the DOE Grand Junction, Colorado, Projects Office, and tasked with developing and/or recommending measurement methods for use in support of remedial action programs. One part of this technical support is the provision of calibration facilities for standardization of field measurements. This report presents results of a study conducted to assign calibration parameters to 59 calibration 'pads' maintained by the Department of Energy at seven permanent and three temporary (remedial action) sites across the United States. The pads are concrete cylinders, roughly 5 feet in diameter and 2 feet high, and are enriched in radium-226, thorium-232, and/or potassium-40. They are used to calibrate those portable field instruments that are used by remedial action contractors to make direct, in-situ measurements of radium-226, thorium-232, and potassium-40.

Calibration parameters were assigned to the pads by combining the results of two sets of measurements. First, physical samples collected from the pads were assayed in the laboratory using a high-resolution germanium detector. The samples were prepared by crushing, drying, and sealing against loss of radon-222. Calibration of the laboratory-measurement system provides traceability of the results to nationally recognized standards. Second, gamma-ray flux emanating from the pads was measured in the field using a high-resolution germanium detector. These results provide consistency among the assignments, such that a calibration performed on one set of pads will be statistically identical to that performed on another set. Ancillary field measurements were made of secular equilibrium in the pads, of moisture content in the pads, and of instrument performance, especially dead time. Results of these ancillary measurements were used to correct the laboratory- and field-measurement data. Both sets of data were then subjected to a regression analysis from which the final calibration-pad assignments were derived. These assignments, together with the raw data and detailed explanation of the assignment process, are presented in this report.

1.0 EXECUTIVE SUMMARY

1.1 PROBLEM DEFINITION AND APPROACH

The objective of this study was to assign calibration parameters to 59 calibration pads located at Grand Junction, Colorado, and at six secondary field sites and three uranium-mill-tailings remedial action sites across the United States. These pads are maintained by the U.S. Department of Energy (DOE) for purposes of instrument and measurement calibration. Each of the 59 pads included in this study is described in Table 1-1 with respect to its designation, location, property serial (tag) number, size, and primary source of enrichment (George and Knight, 1982). Fundamental calibration parameters to be assigned to the pads are concentrations by dry weight (specific activities) of radium-226, thorium-232, and potassium-40. Secondary parameters assigned to the pads are moisture content, radon-222 exhalation, and dry bulk density. The secondary parameters may be used to correct instrument response to the fundamental parameters.

Parameters assigned to the pads must meet two requirements: First, the values must be traceable to national standards, and, second, the values must be consistent from pad to pad. The consistency requirement ensures that calibration of a specific instrument performed on one pad will be statistically the same as a calibration of the same instrument performed on another pad. In the past, calibration parameter assignments for certain pads were determined directly from laboratory measurements of physical samples collected from the pads. For the 'E' series of pads listed in Table 1-1, assignments were made by Mathews and Kosanke (1978). For the 'W' series of pads in Table 1-1 (the large pads located at the Walker Field Airport, Grand Junction), assignments were made by Ward (1978) and by Stromswold (1978). For the other pads listed in the table, no prior published assignments have been made. In all cases, past assignments have been based solely on laboratory measurements using gamma-ray spectroscopy. The intent of this present study was to not only repeat the laboratory measurements, but to obtain in-situ measurements of gamma-ray count rates from each of the pads and to correlate both sets of data in order to make 'best' estimates of the needed parameters, while balancing the sometimes conflicting goals of traceability to standards and consistency of calibrations. The scope of the study also included obtaining a set of separate, independent measurements to test and verify the assignments.

Table 1-1. Description of the Calibration Pads

Pad	Location	Tag Number	Size[a] (ft)	Primary Enrichment[b]
E1	Grand Jct.,	GJO-10253	3.5 x 1.5	Ra-226, 25 pCi/g
E2	Colorado	GJO-10254		Ra-226, 80 pCi/g
E4		GJO-10255		Ra-226, 400 pCi/g
E5		GJO-10256		Ra-226, 900 pCi/g
CE2	Casper,	GJO-10130		Ra-226, 80 pCi/g
CE4	Wyoming	GJO-10131		Ra-226, 400 pCi/g
GE2	Grants, New	GJO-10132		Ra-226, 80 pCi/g
GE4	Mexico	GJO-10133		Ra-226, 400 pCi/g
TE2	George West,	GJO-10134		Ra-226, 80 pCi/g
TE4	Texas	GJO-10135		Ra-226, 400 pCi/g
W1	Walker Field,	GJO-3019	30 x 40 x	None, Normal Concrete
W2	Grand Jct.,	GJO-3019	1.5	K-40, 50 pCi/g
W3	Colorado	GJO-3019		Th-232, 5 pCi/g
W4		GJO-3019		Ra-226, 12 pCi/g
W5		GJO-3019		Ra-226, 8 pCi/g; Th-232, 2 pCi/g; K-40, 35 pCi/g
H1	Grand Jct.,	GJO-12417	4.0 x 1.67	None, Normal Concrete
H2	Colorado	GJO-12413		K-40, 50 pCi/g
H3		GJO-12414		Ra-226, 160 pCi/g
H4		GJO-12415		Th-232, 70 pCi/g
H5		GJO-12416		Ra-226, 100 pCi/g; Th-232, 20 pCi/g; K-40, 40 pCi/g
PK	Grand Jct.,	GJO-X11602	5.0 x 2.0	K-40, 50 pCi/g
PL	Colorado	GJO-X11609		Ra-226, 90 pCi/g
PH		GJO-X11616		Ra-226, 400 pCi/g
PT		GJO-X11623		Th-232, 30 pCi/g
PB		GJO-X11630		None, Ottawa Sand
CPK	Casper,	GJO-X11603	5.0 x 2.0	K-40, 50 pCi/g
CPL	Wyoming	GJO-X11610		Ra-226, 90 pCi/g
CPH		GJO-X11617		Ra-226, 400 pCi/g
CPT		GJO-X11624		Th-232, 30 pCi/g
CPB		GJO-X11631		None, Ottawa Sand

[a]Two dimensions indicate cylindrical configuration listed as diameter by height. Three dimensions indicate rectangular configuration listed as length by width by thickness.

[b]The specific activities only indicate approximate 'order-of magnitude' activities. Assigned values are presented in Table 1-2.

Table 1-1. Description of the Calibration Pads (continued)

Pad	Location	Tag Number	Size[a] (ft)	Primary Enrichment[b]
GPK	Grants, New Mexico	GJO-X11604	5.0 x 2.0	K-40, 50 pCi/g
GPL		GJO-X11611		Ra-226, 90 pCi/g
GPH		GJO-X11618		Ra-226, 400 pCi/g
GPT		GJO-X11625		Th-232, 30 pCi/g
GPB		GJO-X11632		None, Ottawa Sand
TPK	George West, Texas	GJO-X11605	5.0 x 2.0	K-40, 50 pCi/g
TPL		GJO-X11612		Ra-226, 90 pCi/g
TPH		GJO-X11619		Ra-226, 400 pCi/g
TPT		GJO-X11626		Th-232, 30 pCi/g
TPB		GJO-X11633		None, Ottawa Sand
SPK	Spokane, Washington	GJO-X11606	5.0 x 2.0	K-40, 50 pCi/g
SPL		GJO-X11613		Ra-226, 90 pCi/g
SPH		GJO-X11620		Ra-226, 400 pCi/g
SPT		GJO-X11627		Th-232, 30 pCi/g
SPB		GJO-X11634		None, Ottawa Sand
RPK	Reno, Nevada	GJO-X11607	5.0 x 2.0	K-40, 50 pCi/g
RPL		GJO-X11614		Ra-226, 90 pCi/g
RPH		GJO-X11621		Ra-226, 400 pCi/g
RPT		GJO-X11628		Th-232, 30 pCi/g
RPB		GJO-X11635		None, Ottawa Sand
MPK	Morgantown, West Virginia	GJO-X11608	5.0 x 2.0	K-40, 50 pCi/g
MPL		GJO-X11615		Ra-226, 90 pCi/g
MPH		GJO-X11622		Ra-226, 400 pCi/g
MPT		GJO-X11629		Th-232, 30 pCi/g
MPB		GJO-X11636		None, Ottawa Sand
NPL	Niagara Falls, New York	GJO-X11637	5.0 x 2.0	Ra-226, 15 pCi/g
NPH	Middlesex, New Jersey	GJO-X11639		Ra-226, 50 pCi/g
PPL	Salt Lake City, Utah	GJO-X11638	5.0 x 2.0	Ra-226, 15 pCi/g
PPH		GJO-X11640		Ra-226, 50 pCi/g

[a]Two dimensions indicate cylindrical configuration listed as diameter by height. Three dimensions indicate rectangular configuration listed as length by width by thickness.

[b]The specific activities only indicate approximate 'order-of-magnitude' activities. Assigned values are presented in Table 1-2.

In summary, this study involved the acquisition of three major data sets:

- Gamma-ray measurements made on each of the pads using a high-resolution (high-purity germanium) detector.
- Gamma-ray measurements (laboratory assays) of physical samples from the pads.
- Gamma-ray measurements made on each of the pads using a sodium iodide detector.

The first two data sets were used to generate the parameter assignments. The third set was used only to check, and thus verify, those assignments.

1.2 DATA COLLECTION AND REDUCTION

1.2.1 Parameter Assignment

Data sets were generated from the following measurements:

- Measurements of gamma-ray count rates observed on the pads, made using a high-purity germanium detector. Net count rates were determined for the following gamma-ray photopeaks:

  -- 1461 keV from K-40
  -- 1765 keV from Bi-214
  -- 2615 keV from Tl-208
  -- 1001 keV from Pa-234m

- Measurements of in-situ moisture content, made using a neutron-neutron moisture gauge.
- Laboratory measurements of dry-weight concentrations of K-40, Ra-226, and Th-232, made on samples from the pads using a lithium-drifted germanium [Ge(Li)] gamma-ray spectroscopy system, calibrated against New Brunswick Laboratory (NBL) uranium and thorium standards and a potassium standard made locally from K_2CO_3. Measurements were made for the following gamma-ray photopeaks:

  -- 1461 keV from K-40
  -- 1765 keV from Bi-214
  -- 2615 keV from Tl-208

Laboratory measurements of dry bulk density were also made.

The data sets were reduced as follows:

- A correction for gamma-ray attenuation by moisture was computed from the neutron-neutron measurements and from the dry bulk density.
- A correction for Rn-222 exhalation was computed from a ratio comparison of the in-situ count rates at 1001 keV with those at 1765 keV (and from ancillary measurements of relative detector efficiency and from laboratory measurements of relative gamma-ray branching ratios).
- The observed count rates were corrected for dead time of the measurement system, for moisture content, and for Rn-222 exhalation.
- A regression analysis was performed on the data set of laboratory assays versus the set of corrected in-situ count rates. From this regression, best estimates of K-40, Ra-226, and Th-232 concentrations (and their uncertainties) were made.

1.2.2 Parameter Verification

The following data set was collected:

- Measurements of gamma-ray count rates on the pads, made using a sodium iodide detector, 4 inches in diameter by 4 inches high, collimated with an external shield. Observed count rates were measured for the following spectral windows:

  -- 1320 to 1575 keV (principally K-40 at 1461 keV)
  -- 1650 to 2390 keV (principally Bi-214 at 1765 and 2204 keV)
  -- 2475 to 2765 keV (principally Tl-208 at 2615 keV)

The data were reduced as follows:

- The observed count rates were corrected for system dead time, for moisture content, and for Rn-222 exhalation. The last two corrections were derived from the data obtained to generate parameter assignments (cf. Section 1.2.1).

- A calibration factor for the detector was determined using the corrected count-rate data and the parameter assignments for the pads. Since all the pads were included, the calibration coefficients were overdetermined and a 'best' calibration factor was determined through regression analysis.

- Using that calibration factor, count rates expected from each pad were calculated from the assigned parameters. A comparison was then made between the expected count rates and the observed count rates for each pad. The uncertainties in the expected and observed count rates were also compared.

1.3 RESULTS AND CONCLUSIONS

Table 1-2 presents the calibration-pad parameter assignments, expressed in dry-weight concentrations, for Ra-226, K-40, and Th-232. These assignments are reasonable, based on the observations summarized in Table 1-3 and discussed below. However, the uncertainties in the assignments are larger than one would like to see for calibration 'standards,' especially for the radium concentrations in the pads enriched in radium.

The uncertainties in the radium assignments are particularly large because the measurements of radon exhalation made for this study were very uncertain. However, even if the measurements could have been made with complete certainty, it is important to note that the state of exhalation of a given pad changes with meteorologic conditions, as demonstrated in measurements made on the 'W' pads at Walker Field (Stromswold, 1978; Novak, 1985). A fairly large uncertainty for the radium assignments is therefore qualitatively justified in the sense that the (unknown) particular state of exhalation of a given pad will always have a direct effect on the calibration factors determined for specific instruments. As is further discussed in Section 6.3, the radium assignments agree with the laboratory values more closely than what is indicated by the assignments' uncertainties. Nevertheless, we conclude that the large uncertainties for the radium assignments are justified for calibration purposes, even though the radium-226 concentrations could be determined with smaller uncertainties than the assigned values. It is apparent, and we recommend, that further work be done to measure the radon exhalation from the pads, except from the Walker Field pads, and to determine the variation in exhalation associated with each pad.

Table 1-2. Parameter Assignments for the Calibration Pads

Pad	Assigned Concentration (pCi/g)[a]		
	Ra-226	Th-232	K-40
E1	25.21 ± 6.68	0.67 ± 0.10	13.30 ± 0.72
E2	80.34 ± 14.12	0.79 ± 0.10	13.83 ± 0.98
E4	395.84 ± 46.92	0.66 ± 0.12	11.43 ± 1.48
E5	871.45 ± 97.72	0.75 ± 0.12	14.27 ± 2.18
H1	0.84 ± 0.90	0.67 ± 0.10	10.95 ± 0.62
H2	0.67 ± 0.90	0.08 ± 0.06	54.00 ± 1.56
H3	161.83 ± 20.40	0.66 ± 0.08	11.31 ± 0.86
H4	11.03 ± 4.00	67.90 ± 1.24	10.76 ± 1.48
H5	102.59 ± 17.42	19.57 ± 0.54	37.75 ± 1.60
PK	1.16 ± 0.78	0.04 ± 0.06	50.96 ± 1.50
PL	85.71 ± 14.16	0.64 ± 0.10	15.78 ± 1.02
PH	374.36 ± 47.06	0.60 ± 0.10	15.80 ± 1.58
PT	6.63 ± 3.06	31.28 ± 0.86	14.92 ± 1.08
PB	0.0 ± 0.3	0.0 ± 0.3	0.0 ± 0.1
W1	0.82 ± 1.02	0.67 ± 0.10	12.67 ± 0.72
W2	1.92 ± 1.54	0.87 ± 0.12	45.58 ± 1.82
W3	1.70 ± 1.38	4.92 ± 0.26	17.07 ± 0.82
W4	12.07 ± 5.64	1.04 ± 0.12	17.56 ± 0.98
W5	8.36 ± 3.52	1.91 ± 0.16	34.68 ± 1.46
NPL	15.83 ± 5.32	0.64 ± 0.10	10.92 ± 0.72
PPL	15.08 ± 5.54	0.62 ± 0.10	10.84 ± 0.66
NPH	44.20 ± 9.72	0.73 ± 0.10	11.13 ± 0.82
PPH	49.34 ± 10.78	0.63 ± 0.10	10.97 ± 0.86
GE2	83.13 ± 15.42	0.70 ± 0.10	12.93 ± 1.02
GE4	396.66 ± 49.70	0.80 ± 0.12	12.20 ± 1.48
GPK	0.58 ± 0.82	0.01 ± 0.06	51.53 ± 1.46
GPL	87.78 ± 14.32	0.50 ± 0.10	15.58 ± 1.02
GPH	375.74 ± 45.14	0.61 ± 0.10	15.93 ± 1.62
GPT	6.57 ± 3.14	30.23 ± 0.80	14.94 ± 1.02
GPB	0.0 ± 0.3	0.0 ± 0.3	0.0 ± 0.1
TE2	83.53 ± 15.10	0.66 ± 0.10	13.17 ± 0.98
TE4	398.74 ± 50.36	0.51 ± 0.10	11.44 ± 1.58
TPK	0.69 ± 0.86	0.00 ± 0.06	52.81 ± 1.46
TPL	87.02 ± 14.68	0.57 ± 0.10	15.49 ± 1.02
TPH	385.36 ± 47.52	0.45 ± 0.10	14.85 ± 1.42
TPT	5.96 ± 2.96	31.21 ± 0.82	15.03 ± 1.08
TPB	0.0 ± 0.3	0.0 ± 0.3	0.0 ± 0.1
MPK	0.22 ± 0.56	0.02 ± 0.06	52.45 ± 1.46
MPL	89.88 ± 14.42	0.56 ± 0.10	15.88 ± 1.02
MPH	384.23 ± 47.08	0.50 ± 0.10	16.11 ± 1.48
MPT	7.01 ± 3.14	32.03 ± 0.76	15.78 ± 1.08

[a]Uncertainties are two sigmas (95 percent confidence level).

Table 1-2. Parameter Assignments for the Calibration Pads (continued)

Pad	Assigned Concentration (pCi/g)[a] Ra-226	Th-232	K-40
MPB	0.0 ± 0.3	0.0 ± 0.3	0.0 ± 0.1
RPK	0.69 ± 0.86	0.04 ± 0.06	52.01 ± 1.60
RPL	85.01 ± 7.76	0.62 ± 0.10	16.12 ± 1.02
RPH	373.97 ± 46.02	0.53 ± 0.10	15.76 ± 1.52
RPT	6.40 ± 3.02	31.60 ± 0.74	15.40 ± 1.08
RPB	0.0 ± 0.3	0.0 ± 0.3	0.0 ± 0.1
SPK	0.58 ± 0.78	0.01 ± 0.06	51.64 ± 1.46
SPL	93.67 ± 15.36	0.59 ± 0.10	15.97 ± 1.02
SPH	374.28 ± 46.62	0.57 ± 0.10	14.88 ± 1.48
SPT	6.68 ± 3.18	30.80 ± 0.78	14.45 ± 1.02
SPB	0.0 ± 0.3	0.0 ± 0.3	0.0 ± 0.1
CE2	81.45 ± 14.42	0.79 ± 0.12	13.63 ± 0.98
CE4	409.93 ± 50.90	0.66 ± 0.10	12.29 ± 1.58
CPK	0.76 ± 0.90	0.04 ± 0.06	51.36 ± 1.46
CPL	91.77 ± 15.20	0.54 ± 0.10	15.44 ± 1.02
CPH	360.65 ± 43.82	0.55 ± 0.10	14.99 ± 1.58
CPT	6.07 ± 2.92	30.18 ± 0.78	14.13 ± 1.02
CPB	0.0 ± 0.3	0.0 ± 0.3	0.0 ± 0.1

[a]Uncertainties are two sigmas (95 percent confidence level).

Table 1-3. Observations on Parameter Assignments According to Pad Type

Pad Type[a]	Observations on Assigned Calibration Parameters[b]		
	K-40	Ra-226	Th-232
K	Concentrations: 45-55 pCi(K-40)/g. Uncertainties: <4%. Agreement with lab to <2 pCi(K-40)/g.	Concentrations: <1 pCi(Ra-226)/g except 1.9 pCi/g in W2. Uncertainties: Large, as expected for small concentrations.	Concentrations: 0.0-0.1 pCi(Th-232)/g except W2=0.9 pCi(Th-232)/g. Uncertainties: Large, as expected for small concentrations.
Ra	Concentrations: 10-17 pCi(K-40)/g. Uncertainties: 5-15%. Agreement with lab to <2 pCi(K-40)/g.	Concentrations: 25-900 pCi(Ra-226)/g. Uncertainties: 10-35%, inverse to radium concentration. Agreement with lab to about 5%.	Concentrations: 0.5-1.0 pCi(Th-232)/g. Uncertainties: 10-15%. Up to 30% disparity with lab values, but few lab assays made.
Th	Concentrations: 10-16 pCi(K-40)/g. Uncertainties: 5-15%. Agreement with lab to <2 pCi(K-40)/g.	Concentrations: approx. 6.5 pCi(Ra-226)/g except W3=1.7 pCi/g and H4=11 pCi/g. Uncertainties: Large due to uncertain Rn-222 exhalation. Agreement with lab to 7%.	Concentrations: 5-70 pCi(Th-232)/g. Uncertainties: 2-3% except W3=5%. Agreement with lab to 6% except H4=10%.

[a]Based on the primary source of enrichment in the pad.

[b]Uncertainties cited are two sigmas (95 percent confidence interval), expressed in percent of concentration being discussed.

The potassium assignments are in good agreement with laboratory assays, the assignment being within 2 pCi(K-40)/g of the laboratory value in every case. We believe this order of precision, and uncertainty, is as good as, or better than, the level of accuracy and uncertainty which can be attained with commonly used field instrumentation (spectrometers equipped with sodium iodide detectors). We conclude therefore that the potassium assignments are reasonably accurate and precise.

The thorium assignments are the most relatively certain of all the assignments, though the laboratory measurements suffered due to the difficulty in observing the 2615-keV photopeak for many of the samples from the radium-enriched pads. On the other hand, the 2615-keV photopeak was easily observable for the in-situ measurements, and was measured relatively precisely. We conclude that the thorium assignments are reasonably accurate and precise.

The assignments for the barren pads (PB, GPB, TPB, MPB, RPB, SPB, and CPB) are zero because we were unable to measure their radioelement concentrations, even on samples in the laboratory. Furthermore, we implicitly assumed the concentrations in the barren pads to be zero by using them to determine background count rates. In reality, the concentrations in these pads are not zero, but are small enough to be negligible. The associated uncertainties were assigned through subjective analyses and informal discussions with laboratory personnel.

Measurements for verification of the assignments were disappointing. Measurements of background count rates were apparently contaminated. We suspect that the contamination resulted from a neutron source carried on the truck containing the sodium iodide detector system. The poor measurements of background essentially invalidated many of the other measurements, except those of the primary enriched element in each pad. Furthermore, we suspect that the procedure used to set the gain of the system, and to stabilize it, did not permit the system to perform as well as we had hoped, and also contributed to some of the problems encountered in data analysis. The chief value of these data, therefore, was the determination that there are no obvious 'flyers' in the assigned concentrations, at least for the principal enriched element in each pad. Using the data obtained from the verification measurements, we were able to verify the assignments only to within 12 percent for the potassium content of the potassium pads, 12 percent for the apparent radium content of the radium pads, and 7.5 percent for the thorium content of the thorium pads.

1.4 USING THE RESULTS FOR ROUTINE CALIBRATIONS

During the course of this study, correction factors were determined for radon-222 exhalation and moisture content; they are presented in Table 1-4. Measurements to derive these factors were performed concurrently with those conducted for purposes of assigning parameter concentrations. The factors therefore reflect the conditions of the pads at those times. The same conditions may not be present at any other time. However, it may not be possible or practical to measure prevailing conditions, in order to determine corrections, each time the pads are used for calibration. On the other hand, both radon-222 exhalation and moisture content directly influence field measurements of radioelement concentrations. We therefore suggest two possible approaches when using the calibration models.

1. Ignore the corrections while performing both calibration and field measurements. If the exhalation and moisture conditions in the field were coincidentally the same as those in the set of calibration models used, then no error would result in the field measurements of radioelement concentrations. If the conditions in the field were not the same as those in the models, then an error would result in the estimation of radioelement concentrations measured in the field. The error inherent in these field estimates would be related to the departure of conditions in the field from those in the models at the time of calibration. Although this method of accounting for moisture and exhalation may not be wholly satisfactory, it is no worse than making an error related to, for example, the total amount of moisture or exhalation.

2. Apply corrections while performing calibration based on conditions in the models at that time, and apply analogous corrections to the field measurements based on ambient conditions in the field. This approach, though scientifically attractive, may be impractical or technically ineffective if, for example, the moisture content or radon exhalation, or both, varies considerably over the field site.

In the case of either approach, it is beneficial to know or estimate the moisture and exhalation conditions in the calibration models. This is true of the first approach described above because conditions in the field are not measured and are therefore assumed to be the same as those in the models, whether known or estimated. Use of the second approach dictates the need to know moisture and exhalation conditions in the pads at the time of calibration. Should it be impossible or impractical to

measure prevailing conditions at the time of calibration, the correction factors cited in Table 1-4 may be used. It is important to note, however, that the uncertainties in those factors are fairly large; and since these uncertainties propagate into the final radioelement concentrations inferred from the field measurements, the user may wish to make every attempt to obtain the necessary instruments and measure the moisture content and radon-222 exhalation in the models at the time of calibration, in order to determine more precise corrections.

Table 1-4. Correction Factors Derived During This Study for the Calibration Pads

Pad	Correction Factor[a]	
	Radon-222 Exhalation	Moisture Content[b]
E1	1.364 ± 0.185	1.068 ± 0.008
E2	1.151 ± 0.102	1.074 ± 0.008
E4	1.105 ± 0.065	1.086 ± 0.010
E5	1.093 ± 0.058	1.065 ± 0.007
H1	1.022 ± 0.574	1.110 ± 0.013
H2	1.022 ± 0.591	1.084 ± 0.010
H3	1.063 ± 0.067	1.106 ± 0.012
H4	1.022 ± 0.188	1.057 ± 0.006
H5	0.980 ± 0.092	1.082 ± 0.009
PK	1.368 ± 0.863	1.082 ± 0.009
PL	1.232 ± 0.104	1.104 ± 0.012
PH	1.282 ± 0.074	1.103 ± 0.012
PT	1.368 ± 0.310	1.094 ± 0.011
PB	1.000 ± 0.000[c]	1.000 ± 0.000[c]
W1	1.171 ± 0.601	1.148 ± 0.017
W2	1.171 ± 0.431	1.144 ± 0.016

[a]Uncertainties are one sigma (68 percent confidence level). See Sections 4.2 and 4.3 for further details on these factors.

[b]The moisture correction factors cited here are those for Ra-226. Correction factors for Th-232 and K-40 are nearly, but not exactly, the same (see Section 4.2).

[c]It is assumed that the barren pads contain no measurable radium; hence, no radon would be produced and the exhalation correction factor is assumed to be unity, with zero uncertainty. Similarly, it is assumed that the Ottawa sand used to construct the pads contains negligible moisture; hence, the moisture correction factor is also assumed to be unity, with zero uncertainty.

Table 1-4. Correction Factors Derived During This Study for the Calibration Pads (continued)

Pad	Correction Factor[a]	
	Radon-222 Exhalation	Moisture Content[b]
W3	1.171 ± 0.466	1.119 ± 0.014
W4	1.171 ± 0.272	1.143 ± 0.016
W5	1.171 ± 0.233	1.137 ± 0.016
NPL	1.471 ± 0.233	1.100 ± 0.011
PPL	1.254 ± 0.190	1.100 ± 0.011
NPH	1.213 ± 0.134	1.108 ± 0.012
PPH	1.470 ± 0.150	1.113 ± 0.013
GE2	1.175 ± 0.105	1.141 ± 0.016
GE4	1.218 ± 0.071	1.089 ± 0.010
GPK	1.368 ± 0.904	1.071 ± 0.008
GPL	1.405 ± 0.114	1.096 ± 0.011
GPH	1.332 ± 0.076	1.082 ± 0.009
GPT	1.368 ± 0.306	1.085 ± 0.010
GPB	1.000 ± 0.000[c]	1.000 ± 0.000[c]
TE2	1.272 ± 0.108	1.110 ± 0.013
TE4	1.248 ± 0.075	1.133 ± 0.015
TPK	1.368 ± 0.819	1.073 ± 0.008
TPL	1.384 ± 0.119	1.092 ± 0.010
TPH	1.466 ± 0.083	1.091 ± 0.010
TPT	1.368 ± 0.317	1.091 ± 0.010
TPB	1.000 ± 0.000[c]	1.000 ± 0.000[c]
MPK	1.368 ± 1.499	1.072 ± 0.008
MPL	1.413 ± 0.110	1.085 ± 0.010
MPH	1.387 ± 0.080	1.074 ± 0.008
MPT	1.368 ± 0.302	1.074 ± 0.008
MPB	1.000 ± 0.000[c]	1.000 ± 0.000[c]
RPK	1.368 ± 0.819	1.092 ± 0.011
RPL	1.254 ± 0.107	1.085 ± 0.010
RPH	1.358 ± 0.079	1.084 ± 0.010

[a]Uncertainties are one sigma (68 percent confidence level). See Sections 4.2 and 4.3 for further details on these factors.

[b]The moisture correction factors cited here are those for Ra-226. Correction factors for Th-232 and K-40 are nearly, but not exactly, the same (see Section 4.2).

[c]It is assumed that the barren pads contain no measurable radium; hence, no radon would be produced and the exhalation correction factor is assumed to be unity, with zero uncertainty. Similarly, it is assumed that the Ottawa sand used to construct the pads contains negligible moisture; hence, the moisture correction factor is also assumed to be unity, with zero uncertainty.

Table 1-4. Correction Factors Derived During This Study for the Calibration Pads (continued)

Pad	Correction Factor[a]	
	Radon-222 Exhalation	Moisture Content[b]
RPT	1.368 ± 0.309	1.071 ± 0.008
RPB	1.000 ± 0.000[c]	1.000 ± 0.000[c]
SPK	1.368 ± 0.886	1.071 ± 0.008
SPL	1.508 ± 0.119	1.092 ± 0.010
SPH	1.406 ± 0.081	1.085 ± 0.010
SPT	1.368 ± 0.298	1.079 ± 0.009
SPB	1.000 ± 0.000[c]	1.000 ± 0.000[c]
CE2	1.238 ± 0.107	1.080 ± 0.009
CE4	1.268 ± 0.074	1.097 ± 0.011
CPK	1.368 ± 0.781	1.074 ± 0.008
CPL	1.477 ± 0.117	1.086 ± 0.010
CPH	1.307 ± 0.078	1.088 ± 0.010
CPT	1.368 ± 0.316	1.092 ± 0.010
CPB	1.000 ± 0.000[c]	1.000 ± 0.000[c]

[a]Uncertainties are one sigma (68 percent confidence level). See Sections 4.2 and 4.3 for further details on these factors.

[b]The moisture correction factors cited here are those for Ra-226. Correction factors for Th-232 and K-40 are nearly, but not exactly, the same (see Section 4.2).

[c]It is assumed that the barren pads contain no measurable radium; hence, no radon would be produced and the exhalation correction factor is assumed to be unity, with zero uncertainty. Similarly, it is assumed that the Ottawa sand used to construct the pads contains negligible moisture; hence, the moisture correction factor is also assumed to be unity, with zero uncertainty.

2.0 BACKGROUND AND METHODOLOGY

2.1 CONCEPTS AND LIMITATIONS

For the purpose of assigning parameters to the pads, it was assumed that the pads would be used only for calibrating instruments responsive to gamma rays emanating from the pads. The specific isotopes of interest are Ra-226, where the instruments are responsive primarily to the daughters Bi-214 and Pb-214; Th-232, where the instruments are responsive primarily to the daughters Tl-208 and Ac-228; and K-40, where the instruments are responsive directly to K-40. It would be ideal if the

instruments responded linearly to the dry-weight concentrations of these isotopes; however, complicating factors modify the observed proportionality. Two main factors are moisture, which affects all three isotopes, and Rn-222 exhalation, which affects Ra-226. Moisture modifies the proportionality because it attenuates gamma-ray count rates. Radon-222 exhalation modifies the proportionality because it escapes from the pads and is a daughter between Ra-226 and Bi-214 in the Ra-226 decay chain. Another complicating factor that must be considered for certain instruments is the dead time of the measurement system.

The parameter assignments made in this study are the result of three major steps. First, physical samples collected from the pads were assayed in the laboratory to determine a 'laboratory assay' estimate of the concentrations of Ra-226, Th-232, and K-40 in each pad. Second, in-situ measurements of gamma-ray count rates at specific gamma-ray energies were made, and the observed count rates were corrected for instrument dead time, moisture content of each pad, and radon-222 exhalation from each pad. Third, the two data sets were correlated to derive a 'best estimate' of the concentrations of Ra-226, Th-232, and K-40 in each pad.

It is often suggested that these concentration assignments should be based on laboratory data only. However, experience has shown (Heistand and George, 1981; George and others, 1983) that analyzing samples from the pads does not always produce a reliable estimate of the radioelement concentrations in the pads. Experience has also shown that observed count rates obtained using a specific instrument on a specific pad can be very repeatable. Thus, the ratios of concentrations in two or more pads can be determined reasonably precisely through in-situ gamma-ray measurements, while the absolute concentrations in each pad may be relatively uncertain if they are determined from laboratory measurements only. The method used in this study is therefore justified by the fact that the assigned concentrations satisfy two important criteria: they are consistent by virtue of the in-situ data collected and traceable to standards as a result of the correlation between in-situ and laboratory data.

The method used in this study to assign concentrations does impose certain limitations on the results. First, the assignments are for calibration of gamma-ray measurements only, the objective of the study being to assign concentrations for the three isotopes of interest in terms of their (equivalent) gamma-ray intensities. Second and third, the assignments reflect a specific state of moisture content and Rn-222 exhalation in the pads. Corrections were made for these conditions with a view to

making the assignments independent of them; however, this requires that similar corrections be applied by a user to reflect the state of these conditions at the time of routine calibrations. Unless the user has the capability to make moisture and exhalation measurements, he must assume some representative values. It is well known that apparent concentrations of the Walker Field pads vary with meteorologic conditions (Stromswold, 1978; Novak, 1985); however, the magnitude of this effect is not presently known for the rest of the pads. The Walker Field pads are exposed to rain, snow, and ice, whereas all other pads considered in this study are kept covered and dry. Because they are kept dry, we expect variations in moisture and exhalation to be smaller.

2.2 METHOD USED TO MAKE ASSIGNMENTS

2.2.1 Fundamental Relationships

The fundamental relationships between the count rates (in cps) observed using the high-resolution detector and the dry-weight concentrations (in pCi/g) of the isotopes of interest are the following:

- For Ra-226:
$$C_{Ra} = k_{Ra} F_e F_m(1765) [R_{db}(1765)] \quad (2\text{-}1)$$
- For Th-232:
$$C_{Th} = k_{Th} F_m(2615) [R_{db}(2615)] \quad (2\text{-}2)$$
- For K-40:
$$C_K = k_K F_m(1461) [R_{db}(1461) - S_{Th}] \quad (2\text{-}3)$$

where

$$R_{db}(E) = F_d R_o(E) - F_{dB} B_o(E) \quad (2\text{-}4)$$

and where C_{Ra}, C_{Th}, and C_K are dry-weight concentrations of Ra-226, Th-232, and K-40, respectively; k_{Ra}, k_{Th}, and k_K are proportionality constants for the isotope indicated; F_e is the correction factor for Rn-222 exhalation; $F_m(E)$ is the moisture correction factor for the gamma-ray energy indicated; $R_{db}(E)$ is the observed count rate corrected for dead time and ambient background for the energy indicated; F_d is the correction for dead time of the measurement system; F_{dB} is the correction for dead time of the PB pad measurement at a given site; $R_o(E)$ is the observed

count rate at the gamma-ray energy indicated; and $B_o(E)$ is the observed background count rate at the energy indicated. Background was determined from measurements on the barren pad at each site. The variable S_{Th} is used to correct the count rate observed in the 1461-keV photopeak from K-40 for interference from the 1459-keV photopeak from Ac-228, a thorium daughter.

Measurements and data analyses leading to evaluations of each of the above-mentioned factors are detailed in subsequent sections of this report. A brief description of the procedures used to evaluate each of these factors and to ultimately determine the parameter assignments is provided in the following subsection.

2.2.2 Summary of Procedure

The following step-by-step procedure was used to derive the parameter assignments:

1. Prior to commencing measurements on the calibration pads, proper functioning of the detector and electronic equipment was verified and system performance was quantified. Measurements were made to assess detector resolution and efficiency, system linearity with energy, system dead time, and system sensitivity to a specific gamma-ray source held in a specific repeatable geometry. Measurements of detector resolution and system sensitivity to the specific source were repeated routinely during the course of the study to monitor and verify continued adequate performance of the system.

2. Measurements were made of the gamma-ray intensities on each calibration pad. The detector was collimated, and a 4096-channel spectrum for each pad was stored on magnetic tape.

3. Net photopeak areas were extracted from each spectrum for a few specific photopeaks, using an algorithm described by Murri and others (1983); these results were designated the observed count rates. The photopeaks extracted for the parameter assignments were 1765 keV, 2615 keV, and 1461 keV from Ra-226, Th-232, and K-40, respectively. One other photopeak, 1001 keV from Pa-234m, was extracted for pads containing more than 'barren' amounts of radium in order to determine the correction for Rn-222 exhalation.

4. Moisture was measured in each of the pads using a commercially available 'moisture gauge' which measures the partial density of water. The dry bulk density of each pad was determined in the laboratory from samples of concrete from the models. These two values were combined with the gamma-ray mass attenuation coefficients for dry concrete and for water at the specific energies of interest to calculate the moisture correction factor for each pad. This factor is the ratio of the wet to dry linear attenuation coefficients (Wilson and Stromswold, 1981).

5. Radon-222 exhalation was measured for each of the pads containing significant radium by measuring the intensity of the Pa-234m photopeak. Protactinium-234m is a short-lived daughter of U-238 and is therefore a direct measure of U-238. Radium-226 concentration can be inferred from U-238 concentration if the U-238/Ra-226 equilibrium ratio is known. In this case, the equilibrium ratio for the uranium ore used to construct the pads is known to be close to unity. The apparent U-238/Bi-214 equilibrium ratio was then determined through relative comparison of U-238/Bi-214 concentrations. This equilibrium ratio is the desired exhalation correction factor.

6. Laboratory measurements were conducted to determine radium, thorium, and potassium concentrations. Both radiometric and wet-chemical methods were used, but the main emphasis was placed on the former. The assays were made on physical samples that were collected from the models while they were being constructed. The samples were prepared for assaying by crushing and drying, then packing in aluminum cans which were sealed and set aside to permit secular equilibrium to occur. The radiometric assays were made using a high-resolution gamma-ray spectroscopy system calibrated with uranium and thorium standards (the 100A Series) from New Brunswick Laboratory (Trahey and others, 1982) and a potassium standard of K_2CO_3. Wet-chemical methods were used to determine U-238 concentrations and to check potassium concentrations.

7. The resulting data sets (Steps 3 through 6) were combined by means of a regression analysis to derive the best estimates of concentrations for each of the pads. These results are the parameter assignments for the pads.

8. An analysis was performed to estimate the uncertainty in each of the concentration assignments.

2.3 METHOD USED TO VERIFY ASSIGNMENTS

2.3.1 Fundamental Relationships

Measurements were made with a sodium iodide detector to verify the parameter assignments. The detector, 4 inches in diameter by 4 inches in length, is part of a system known as the Calibration Facilities Monitoring System (CFMS). The CFMS was used to collect gamma-ray count-rate data in the 'standard KUT' spectral windows (Wilson and Stromswold, 1981). For purposes of this study, it was assumed that gamma-ray flux from K-40 affects only the count rate in the potassium window, while flux from both radium (uranium) and thorium affects the count rates in all three windows. This assumption neglects pileup effects and therefore assumes reasonably low count rates; however, the assumption is consistent with what is expected theoretically and observed in practice.

The fundamental relationships between the observed count rates (in cps) and the in-situ concentrations (in pCi/g) of the three isotopes of interest are the following:

$$R_{db}(W_K)F_m(W_K) = a_{11}C_K + a_{12}C_{Ra}/F_e + a_{13}C_{Th} \qquad (2\text{-}5)$$

$$R_{db}(W_{Ra})F_m(W_{Ra}) = a_{22}C_{Ra}/F_e + a_{23}C_{Th} \qquad (2\text{-}6)$$

$$R_{db}(W_{Th})F_m(W_{Th}) = a_{32}C_{Ra}/F_e + a_{33}C_{Th} \qquad (2\text{-}7)$$

where

$$R_{db}(W) = F_d[R_o(W)]R_o(W) - F_d[B_o(W)]B_o(W) \qquad (2\text{-}8)$$

and where C_K, C_{Ra}, C_{Th}, $F_m(W)$, F_e, $F_d[R]$, $R_o(W)$, and $B_o(W)$ are as defined for equations (2-1) through (2-4) except that W indicates a relatively wide spectral window W rather than a specific energy E; and a_{11}, a_{12}, a_{13}, a_{22}, a_{23}, a_{32}, and a_{33} are constants, related to other constants commonly called sensitivity factors and stripping ratios.

2.3.2 Summary of Procedure

The following step-by-step procedure was used to verify the parameter assignments:

1. Dead time for the CFMS was determined using the two-source method described by Kohman (1949).

2. Detector sensitivity, linearity, and resolution were monitored routinely using specific gamma-ray sources in a repeatable geometry.

3. The observed count rate was measured for each pad following a standard setup procedure.

4. An 'overdetermined' calibration factor for the CFMS was derived by performing a regression analysis on all corrected data from all of the pads. The regression was based on the set of equations (2-5) through (2-8). Correction factors for moisture and exhalation were the same ones used to assign the parameters to the pads, derived from data acquired with the high-purity germanium detector.

5. Using the calculated calibration coefficients and the assigned parameters for each pad, the 'expected' count rates for each window on each pad were calculated. These 'expected' count rates were compared with the observed count rates in an attempt to verify the assigned parameters for each pad.

3.0 FIELD MEASUREMENTS FOR PARAMETER ASSIGNMENT

3.1 COLLECTION OF GAMMA-RAY DATA

3.1.1 Equipment Description and Performance

The high-resolution gamma-ray spectroscopy system used for the field measurements consists of an intrinsic germanium detector with a charge-sensitive preamplifier, an ORTEC Model 572 amplifier, a Tracor Northern TN-1213 (200-MHz) analog-to-digital converter (ADC) stabilized by a Tracor Northern NS-454 digital stabilizer, a Tracor Northern TN-1710 multichannel analyzer (MCA), and various peripheral equipment as shown in Figure 3-1

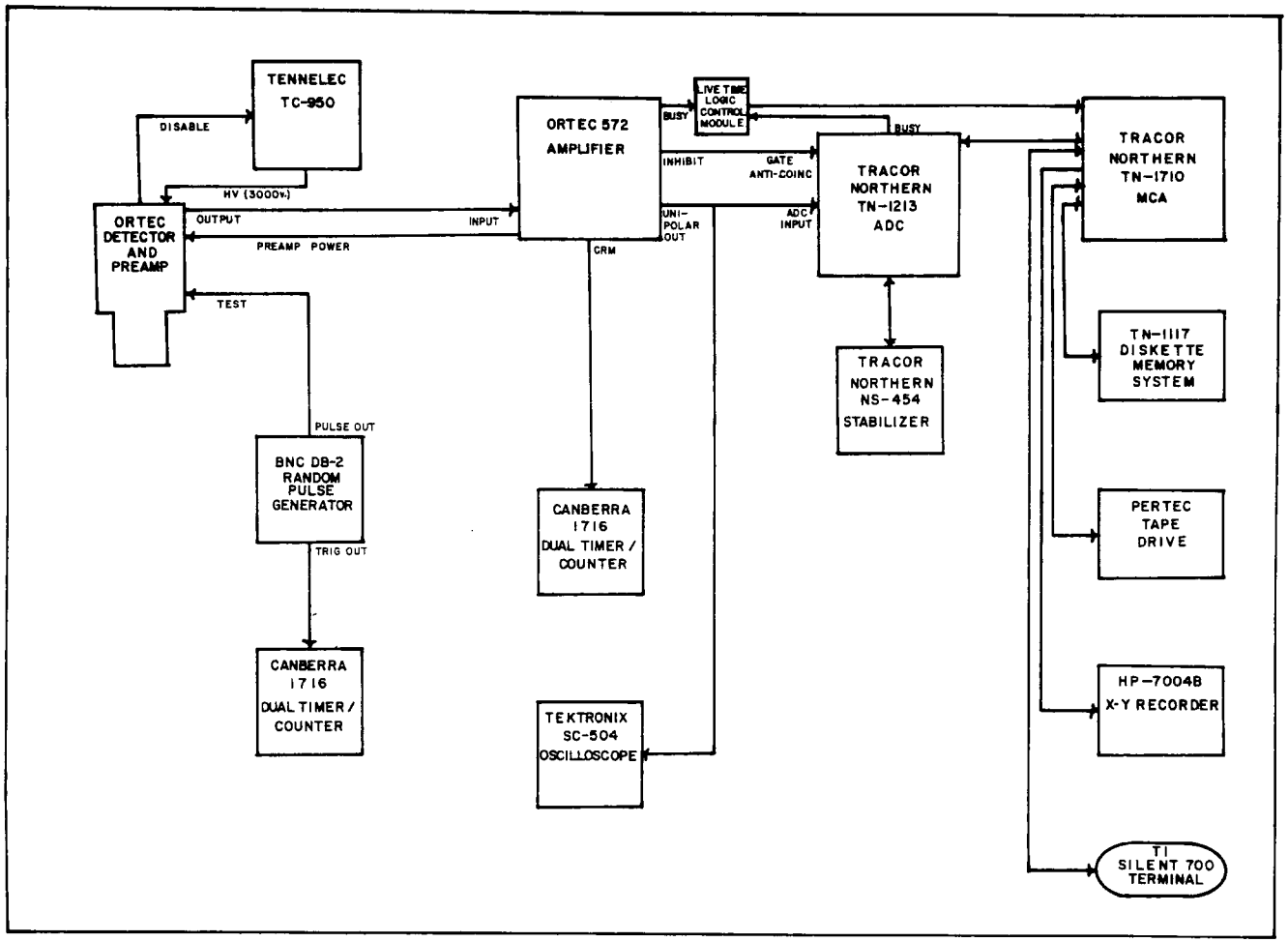

Figure 3-1. Block Diagram of Mobile Gamma-Ray Spectroscopy System with ORTEC HPGe Portable Germanium Detector

(Murri and others, 1983). Data acquired using this system are stored on magnetic tape and subsequently transferred to a local computer for reduction.

The detector is an ORTEC Gamma Gage with supporting storage/fill dewar. Specifications and measured characteristics of the particular detector used are listed in Table 3-1.

Table 3-1. Characteristics of the Germanium Detector

Parameter	Specified	Measured
Diameter (cm)	5.57	[a]
Length (cm)	6.64	[a]
Active Volume (cm^3)	148.4	[a]
Resolution (keV at 1333 keV)	2.10	1.97
Efficiency at 1333 keV [in percent relative to a 3 in. x 3 in. NaI(Tl) detector]	30.0	33.8
Peak-to-Compton Ratio	52:1	70.4:1

[a]Not measured by Bendix.

To ensure that the field measurements would reliably represent the prevailing radiometric conditions of the calibration pads, proper functioning of the gamma-ray spectroscopy system was verified both prior to and during the course of data acquisition on the pads. This frequent monitoring ensured that the system was operating properly at the start of data collection and remained stable throughout the data-gathering effort.

One element of this verification procedure consisted of demonstrating the validity of the pulser method, which was used for dead-time correction (Murri and others, 1983). To accomplish this verification, measurements were made using the two-source method, and each measurement was corrected for dead time on the basis of the concurrently gathered pulser data, as described in Section 4.1.1. A residual dead-time correction was then computed from these adjusted data, using the polynomial method described by Kohman (Kohman, 1949; George, 1982). If the dead-time correction provided by the pulser method were adequate, then the residual dead-time correction would be near 1.00, i.e., no correction would be needed. It was found in this study that, within counting statistics, no residual correction was needed, i.e., that the pulser method alone was adequate. These data and results are presented in Table 3-2 and Figure 3-2.

Table 3-2. Pulser Dead-Time Verification Data and Results

Observed Count Rate, R_o (cps)

Source 1	Source 2	Sources 1 and 2	Background
413.00	1039.14	1230.41	199.49
452.30	1203.56	1447.13	
509.21	1413.96	1732.32	
719.95	2302.16	2794.51	
929.81	3172.80	3871.49	

Corrected Count Rate, R_c (cps)[a]

Source 1	Source 2	Sources 1 and 2	Background
409.40	1059.86	1260.47	199.49
451.35	1206.32	1461.80	
513.66	1429.50	1753.80	
721.62	2333.46	2850.03	
928.88	3241.36	3966.56	

Residual Dead-Time Correction Factor, F_{dr}

$$F_{dr} = 1 - (3.104363 \times 10^{-6})R_c + (6.989682 \times 10^{-10})R_c^2$$

R_c	F_{dr}
1260.47	0.99720
1461.80	0.99696
1753.80	0.99671
2850.03	0.99683
3966.56	0.99868

[a] $R_c = F_d R_o$, where F_d was determined from pulser measurements.

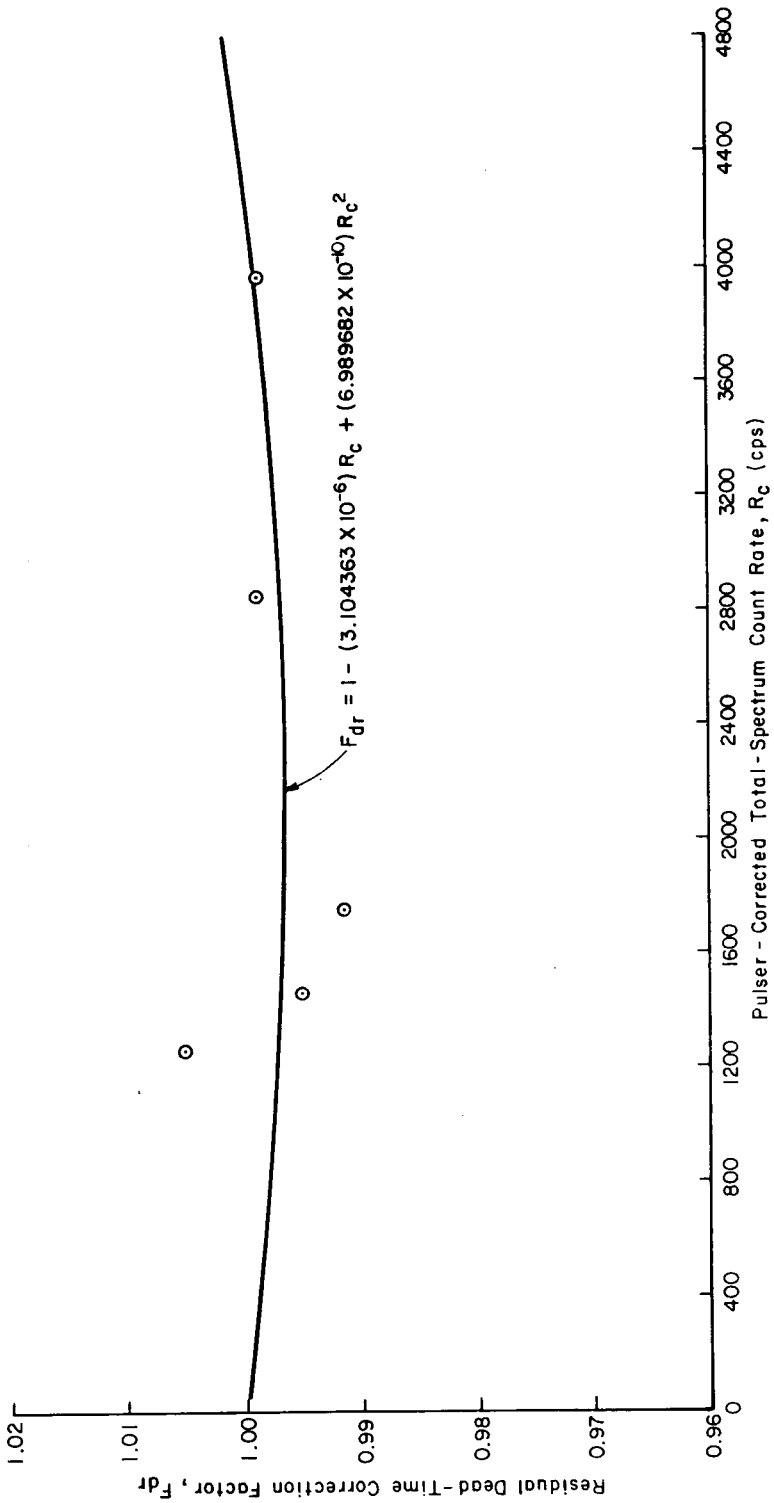

Figure 3-2. Pulser Dead-Time Verification

Two indicators of proper hardware functioning are system resolution and sensitivity. Resolution was monitored using the 1333-keV gamma ray of Co-60, as described in Section 3.1.2. The results of repeated measurements are plotted as a function of the measurement sequence number in Figure 3-3, where the sequence number is a rough indicator of time. The mean value of 2.59 $\pm$ 0.09 keV at 1333 keV is greater than the value of 1.97 keV cited in Table 3-1, because the amplifier pulse-shaping time constant was adjusted to improve performance at high count rates, thereby degrading observed resolution. Nevertheless, the resolution obtained in the field was quite adequate for the desired application. Stability of the system was good, as evidenced by the small fluctuations in resolution measurements (Figure 3-3). In fact, the maximum fluctuations correspond to less than 0.5 channel in the MCA.

Sensitivity is a measure of detector photopeak efficiency, i.e., counts registered in the photopeak per corresponding gamma ray incident on the detector. This measured value was monitored using the 1765-keV photopeak of Bi-214 in equilibrium with its parent Ra-226 in a sealed 'button' source. The net area (counts) in this photopeak, corrected for system dead time, is plotted versus its measurement sequence number in Figure 3-4. As can be seen, 68 percent of the measured values lie within their one-sigma uncertainties of the mean value of 7843.5 counts, as expected from Poisson statistics.

On the basis of the results described above, it was concluded that the high-resolution gamma-ray spectroscopy system was functioning properly throughout the period of data acquisition on the pads, and that, as a consequence, there appear to be no significant systematic errors that would invalidate these data.

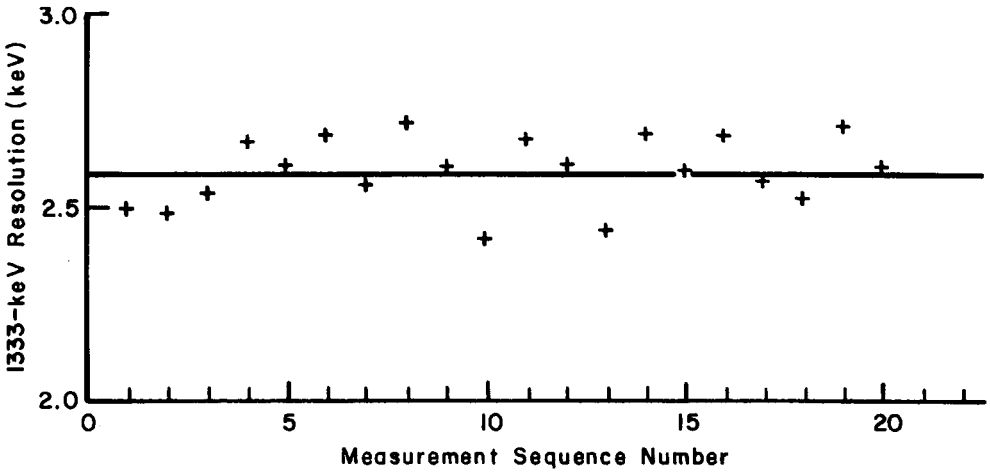

Figure 3-3. Resolution of the HPGe Gamma-Ray Spectroscopy System Using a Co-60 Source

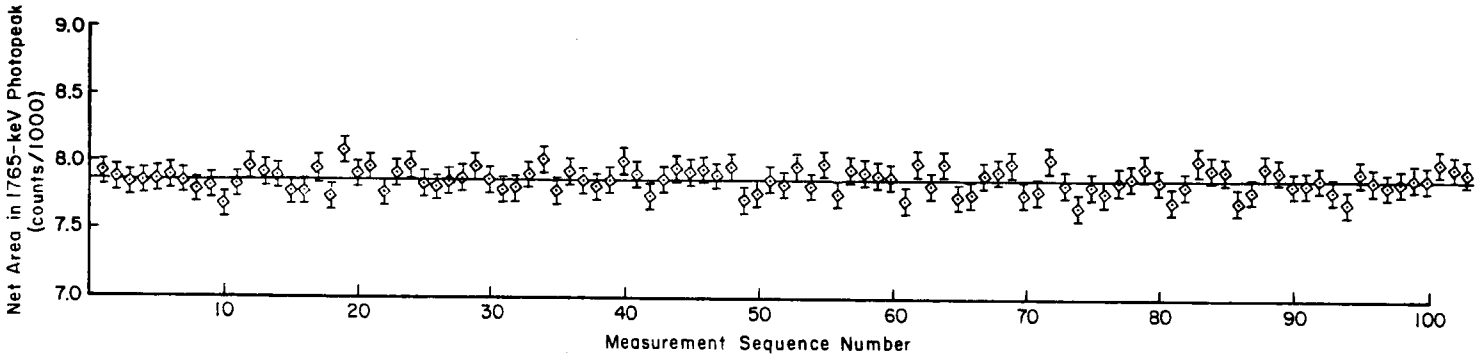

Figure 3-4. Sensitivity of the Germanium Detector to a 1-μCi Ra-226 Source

3.1.2 Data-Collection Procedures and Spectrum Reduction

In order to make the measurements as repeatable as possible, a specific procedure for data collection was followed. In the event that the spectroscopy system had been powered down after its previous use, the system was powered up and allowed to equilibrate electronically for at least 1 hour prior to starting data acquisition each day. Following this equilibration period, adjustments of amplifier DC level and pole zero were made in accord with procedures given in the manufacturer's operating manual. The amplifier gain and ADC zero level were then adjusted, if necessary, to obtain specific, predetermined, energy-per-channel and energy-of-channel-zero values for energy calibration of the MCA. After performing these adjustments, the DC level and pole zero were rechecked and 'fine tuned' if necessary.

Spectral measurements were then made on both Co-60 and Ra-226 standard ('button') reference sources to ensure that the system was operating within its warranted characteristics and that the results were statistically consistent with previous measurements of the same sources. To eliminate the potential for errors that might occur as a result of variable reference-source positioning, a plastic jig was used to maintain the reference sources in a repeatable measurement geometry relative to the detector.

Once the verification measurements were completed, the detector, attached to its storage/fill dewar and supporting stand, was positioned above the center of the pad to be measured. The lower surface of the detector was maintained at a height of 7.6 cm above the pad surface. In order to reduce interference from other radioactive sources and to eliminate field-of-view effects due to differing pad radii, the detector was shielded by lead in the form of a cylindrical annulus, 5.1 cm in radial thickness by 10.5 cm in vertical (axial) thickness. These dimensions are adequate to exclude from 90 percent (in the case of the 2615-keV radiation) to 95 percent (1461 keV) of the ambient background radiation, and to effectively collimate the radiation from each pad into a beam of constant cross-sectional area.

The mean repetition frequency of the random pulser was then adjusted to a suitable value, based on the gross count rate observed on the pad (Murri and others, 1983); the amplitude of the pulser signal was adjusted to place the peak centroid in a preselected channel of the MCA. Spectral data from each pad were then acquired for 5000 seconds of MCA live time in a 4096-channel analyzer. The resulting spectra were written onto nine-track magnetic tape for subsequent computer processing.

Following data acquisition on each pad, the Ra-226 standard source was remeasured to ascertain whether any significant change in system characteristics had occurred during pad measurement. If such a change was detected, the gain, zero-level, DC-level, and pole-zero adjustments were made as necessary, and the pad measurement was repeated.

After each spectral measurement of a pad, the interstitial moisture in the concrete was measured using a commercially available moisture gauge, as described in Section 3.2. This measurement was always deferred until the spectral measurement was completed to avoid introducing spurious gamma radiation into the spectra due to neutron activation of the pad material by the moisture gauge.

Spectrum reduction was accomplished by searching predefined regions of interest to determine the presence and net area of spectral peaks. The energies and corresponding channel regions are listed in Table 3-3. The regions are defined in such a way that at least ten channels of Compton background occur on each side of the peak.

Table 3-3. Peaks and Spectral Regions for Analysis

Nuclide	Energy (keV)	Peak Centroid Channel	Spectral Region	
			First Channel	Last Channel
Bi-214[a]	609.3	932	910	960
Pa-234m[b]	1001.2	1532	1505	1560
Bi-214[a]	1120.3	1714	1685	1740
Co-60[c]	1332.5	2038	2015	2065
K-40[b]	1460.8	2235	2206	2266
Bi-214[a,b,c]	1764.5	2699	2671	2731
Pulser	1980.7	3030	3000	3060
Bi-214[a]	2204.2	3372	3343	3403
Bi-214[a]	2447.8	3745	3716	3776
Tl-208[b]	2614.5	4000	3972	4032

[a]Peaks used for determination of detector photopeak efficiency.

[b]Peaks used for determination of concentration assignments in this study.

[c]Peaks used for monitoring system performance.

The data in each region were first 'smoothed' using a five-point, binomial smoothing algorithm (Murri and others, 1983). Next, first differences were computed from the smoothed data using a four-point, central-difference algorithm. The first-difference array was then checked point by point to determine the boundaries of the peak. Because of the criteria used to define these boundaries (cf. Murri and others, 1983), the data-reduction software effectively imposes minimum detection limits on each peak in the spectrum. These limits depend primarily on the shape of the peak and of the spectrum in the vicinity of the peak, as well as the peak-to-Compton ratio. Thus, a peak that may appear 'detectable' to an operator viewing the spectrum on the MCA display screen might not be 'found' by the software if it is not sufficiently prominent above the Compton continuum or if the smoothed data in the lower energy half of the peak do not increase monotonically with channel number. Peaks which were so 'missed' are designated in the various tables in this report as being 'below detection limit.' Since this limit depends in part on the spectral shape, no absolute limits of radioelement concentration (minimum detectable activities) corresponding to the software 'detection limits' have been computed.

Once the boundaries of the peak were determined, the width was checked to ensure that it was a real peak and not just a broad excursion in the spectrum, such as a Compton edge. Six channels on each side of the peak were then averaged to determine the high-energy and low-energy Compton backgrounds. The background under the peak was calculated using an algorithm described by Gunnink (1979); this value was then subtracted from the number of gross counts in the peak to yield the net area. The net area must exceed a predetermined value (arbitrarily set as ten counts for this analysis) in order for the peak to be designated as 'detectable.' Uncertainties in the background and net area were also computed, on the basis of standard error-propagation techniques (Bevington, 1969).

The resulting data set for each pad (Table 3-4) contains the following components: the net area in each radioelement photopeak of interest used in this study (1001 keV, 1461 keV, 1765 keV, and 2615 keV) together with its uncertainty as computed by the algorithm described above; the net area observed in the pulser 'photopeak' and its uncertainty; the pulser 'trigger out' count (the number of pulses input during the MCA live-time interval), as recorded on a scaler; the dry bulk density of the concrete matrix, determined from laboratory measurements; and the partial density of interstitial water, as measured by the moisture gauge. In addition, the ambient background in each photopeak of interest was measured at each field calibration site; these data are

presented in Table 3-5. It was assumed that background activity at each site was well represented by the spectrum obtained on the PB (barren) pad at that site.

Table 3-4. Net-Area, Dead-Time-Correction, Density, and Moisture Data

Pad	Net Area (counts)[a] K-40 (1461 keV)	Bi-214('Ra-226') (1765 keV)	Tl-208('Th-232') (2615 keV)	Pa-234m (1001 keV)	Pulser	Pulser Input[b] (counts)	Dry Bulk Density[c] (g/cc)	Moisture[d] (g/cc)
E1	2548.1 ± 62.0	4615.2 ± 72.2	453.0 ± 22.0	356.4 ± 43.5	11823.2 ± 110.4	11828	1.89	0.116
E2	2570.8 ± 83.6	17016.5 ± 137.6	427.2 ± 21.9	1115.4 ± 83.9	30198.1 ± 177.9	30291	1.84	0.123
E4	2074.6 ± 128.8	83492.8 ± 309.3	358.1 ± 22.7	5268.3 ± 194.1	92837.4 ± 319.7	95160	1.84	0.143
E5	2605.2 ± 190.1	192349.6 ± 471.1	380.1 ± 25.6	12011.0 ± 327.7	88765.4 ± 332.5	94123	1.94	0.114
H1	2061.8 ± 48.1	243.9 ± 17.9	384.8 ± 20.1	[e]	18495.1 ± 136.4	18498	1.86	0.185
H2	9682.5 ± 100.7	240.7 ± 18.0	99.0 ± 11.1	[e]	44879.2 ± 212.1	44879	1.87	0.142
H3	4335.7 ± 142.8[f]	70766.1 ± 285.3[f]	860.0 ± 31.5[f]	4291.6 ± 180.7[f]	99830.2 ± 324.2[f]	101278[f]	1.89	0.181
H4	2901.6 ± 91.0	2685.9 ± 81.3	35590.7 ± 191.2	[e]	59993.1 ± 256.5	60407	1.92	0.099
H5	7086.4 ± 124.1	23095.1 ± 165.1	9965.3 ± 101.2	1291.1 ± 104.6	73822.9 ± 278.3	74340	1.93	0.143
PK	9386.5 ± 98.9	169.8 ± 15.2	85.0 ± 10.9[g]	[e]	21457.9 ± 146.7	21466	1.94	0.145
PL	3039.3 ± 84.9	16252.5 ± 134.2	380.4 ± 20.5	1138.2 ± 79.2	43399.4 ± 210.4	43589	1.90	0.180
PH	2995.3 ± 132.9	72524.6 ± 288.8	365.3 ± 21.6	5311.4 ± 185.0	94483.2 ± 320.5	96607	1.92	0.180
PT	3439.4 ± 80.2	1242.6 ± 54.4	16661.5 ± 130.8	[e]	22820.1 ± 158.8	22835	1.90	0.162
W1	2294.9 ± 50.6	250.5 ± 18.0	387.8 ± 21.2	[e]	2676.8 ± 53.5	2683	1.91	0.256
W2	7995.8 ± 91.9	471.9 ± 25.1	500.1 ± 22.9	[e]	2312.4 ± 49.3	2327	1.99	0.260
W3	3208.1 ± 62.4	407.5 ± 26.8	2617.5 ± 52.3	[e]	7341.8 ± 90.8	7397	1.92	0.208
W4	3161.0 ± 64.3	2376.4 ± 52.7	554.9 ± 24.2	157.0 ± 35.0[g]	27133.5 ± 165.7	28218	1.91	0.247
W5	6361.4 ± 85.8	1825.4 ± 46.6	1011.6 ± 32.6	[e]	38389.2 ± 196.9	38407	1.97	0.244
NPL	2056.5 ± 56.3	2855.1 ± 57.3	359.8 ± 19.9	235.3 ± 33.9	1483.7 ± 42.0	1493	1.94	0.176
PPL	2042.9 ± 54.2	2991.4 ± 58.3	384.7 ± 20.9	209.2 ± 31.2	17637.7 ± 134.0	17610	1.95	0.176
NPH	2124.2 ± 66.8	8789.2 ± 99.2	408.4 ± 21.5	603.4 ± 58.1	17267.2 ± 134.6	17330	1.95	0.191
PPH	2061.7 ± 67.8	8693.4 ± 99.0	393.7 ± 20.8	724.9 ± 62.5	25229.8 ± 160.8	25322	1.95	0.199
GE2	2392.6 ± 82.4	16947.7 ± 137.9	410.6 ± 21.7	1127.6 ± 84.2	28351.5 ± 179.2	28633	1.85	0.237
GE4	2217.8 ± 128.0	81451.4 ± 305.6	429.4 ± 23.8	5660.8 ± 203.1	121392.9 ± 357.3	123873	1.84	0.148
GPK	9561.6 ± 99.6	225.5 ± 17.2	83.0 ± 11.0[g]	[e]	7632.4 ± 87.7	7628	1.96	0.127
GPL	2999.4 ± 84.4	15191.0 ± 130.9	334.7 ± 19.8	1208.9 ± 82.1	26033.2 ± 164.7	26180	1.90	0.165

[a]Data are results from 5000-sec (live time) spectrum, unless otherwise noted. Uncertainties are one sigma (68 percent confidence interval).

[b]Pulser 'trigger out' count is the number of pulses input during the MCA live-time interval.

[c]Laboratory measurement of dry bulk density in samples from the pads (see Appendix B).

[d]Partial density of interstitial water in the pad (see Section 3.2).

[e]Below detection limit.

[f]10000 sec (live time).

[g]Read directly from the MCA (TN1710 peak search module).

[h]5233 sec (live time).

Table 3-4. Net-Area, Dead-Time-Correction, Density, and Moisture Data (continued)

Pad	Net Area (counts)[a] K-40 (1461 keV)	Bi-214('Ra-226') (1765 keV)	Tl-208('Th-232') (2615 keV)	Pa-234m (1001 keV)	Pulser	Pulser Input[b] (counts)	Dry Bulk Density[c] (g/cc)	Moisture[d] (g/cc)
GPH	3122.7 ± 138.1	69899.4 ± 280.0	380.3 ± 22.0	5307.8 ± 180.2	120460.6 ± 356.9	122790	1.91	0.142
GPT	3246.3 ± 75.9	1346.1 ± 54.5	16199.6 ± 128.9	[e]	16728.6 ± 137.7	16777	1.89	0.146
TE2	2519.0 ± 82.2	16586.1 ± 136.1	402.1 ± 20.9	1198.6 ± 83.6	33336.0 ± 186.2	33532	1.83	0.177
TE4	2125.3 ± 129.6	75122.1 ± 293.3	316.2 ± 20.8	5349.0 ± 196.6	142088.2 ± 386.8	145072	1.86	0.223
TPK	10458.0 ± 103.9[h]	201.6 ± 16.4[h]	65.9 ± 9.5[h]	[e]	45585.8 ± 213.6[h]	45547[h]	1.95	0.131
TPL	2947.9 ± 82.7	14992.1 ± 130.0	329.9 ± 19.2	1177.8 ± 82.5	49693.0 ± 225.3	49876	1.88	0.157
TPH	2834.5 ± 126.8	66686.1 ± 275.4	323.7 ± 20.5	5579.5 ± 186.3	142687.3 ± 386.8	145138	1.90	0.158
TPT	3394.4 ± 77.5	1181.7 ± 53.6	16635.7 ± 130.7	[e]	42989.4 ± 212.4	43074	1.90	0.155
MPK	9842.1 ± 101.3	211.4 ± 16.1	89.6 ± 10.3	[e]	31521.0 ± 170.6	31523	1.90	0.124
MPL	3090.6 ± 84.8	15958.5 ± 134.3	377.3 ± 20.5	1275.3 ± 78.9	50712.7 ± 229.0	51000	1.90	0.147
MPH	3016.9 ± 130.5	70049.8 ± 283.0	338.5 ± 21.1	5542.0 ± 192.6	154435.9 ± 401.2	157338	1.89	0.126
MPT	3550.8 ± 77.8	1428.0 ± 55.7	16916.1 ± 131.6	[e]	38236.0 ± 196.1[g]	38403	1.86	0.125
RPK	9590.8 ± 100.0	183.2 ± 15.3	116.2 ± 11.7	[e]	33488.0 ± 183.4	33515	1.92	0.161
RPL	3134.1 ± 85.0	15693.4 ± 132.4	386.8 ± 20.9	1122.0 ± 82.2	29452.4 ± 174.6	29521	1.90	0.147
RPH	3106.3 ± 128.9	68181.1 ± 280.0	390.4 ± 22.0	5286.2 ± 188.1	134429.5 ± 375.3	137198	1.89	0.144
RPT	3657.7 ± 79.4	1258.5 ± 54.8	17026.6 ± 132.3	[e]	35368.0 ± 194.0	35453	1.88	0.121
SPK	9630.5 ± 99.7	175.2 ± 15.0	95.8 ± 10.8	[e]	4373.4 ± 66.5	4377	1.90	0.123
SPL	3043.9 ± 84.7	15556.2 ± 132.5	373.9 ± 20.1	1340.6 ± 83.2	39779.7 ± 203.3	39980	1.89	0.157
SPH	2776.8 ± 127.5	67086.0 ± 279.2	347.7 ± 21.4	5391.1 ± 188.3	168381.9 ± 422.4	172021	1.89	0.145
SPT	3285.6 ± 75.0	1365.4 ± 53.5	16520.3 ± 130.3	[e]	23465.0 ± 161.1[g]	23518	1.89	0.136
CE2	2661.0 ± 83.6	16611.8 ± 136.2	465.6 ± 22.9	1170.6 ± 84.6	27344.5 ± 169.4	27447	1.85	0.135
CE4	2255.1 ± 135.7	79685.4 ± 301.4	376.7 ± 22.2	5769.3 ± 202.7	137213.2 ± 388.6	139830	1.84	0.162
CPK	9615.4 ± 99.8	209.5 ± 17.0	104.0 ± 11.4[g]	[e]	10189.9 ± 101.3	10216	1.94	0.130
CPL	2988.8 ± 84.1	15826.5 ± 132.9	372.8 ± 20.6	1332.0 ± 82.9	39362.4 ± 205.5	39569	1.89	0.148
CPH	2937.2 ± 132.5	65791.2 ± 274.2	356.3 ± 21.1	4911.4 ± 184.6	142634.3 ± 392.4	145348	1.91	0.153
CPT	3087.9 ± 74.4	1178.0 ± 51.1	15515.5 ± 126.6	[e]	24630.5 ± 162.8	24663	1.89	0.157

[a] Data are results from 5000-sec (live time) spectrum, unless otherwise noted. Uncertainties are one sigma (68 percent confidence interval).

[b] Pulser 'trigger out' count is the number of pulses input during the MCA live-time interval.

[c] Laboratory measurement of dry bulk density in samples from the pads (see Appendix B).

[d] Partial density of interstitial water in the pad (see Section 3.2).

[e] Below detection limit.

[f] 10000 sec (live time).

[g] Read directly from the MCA (TN1710 peak search module).

[h] 5233 sec (live time).

Table 3-5. Ambient Background Activity Observed on the PB Pad at Each Site[a]

Pad	Net Area (counts)[b]			
	K-40 (1461 keV)	Bi-214('Ra-226') (1765 keV)	Tl-208('Th-232') (2615 keV)	Pa-234m (1001 keV)
PB	89.1 ± 12.4	62.2 ± 9.6	59.0 ± 8.8[c]	d
GPB	105.3 ± 13.6	117.7 ± 13.7	81.6 ± 10.4	d
TPB	69.0 ± 10.2[c]	70.7 ± 9.5	63.0 ± 7.9[c]	d
MPB	54.8 ± 10.1	167.5 ± 14.8	78.0 ± 9.6[c]	d
RPB	152.9 ± 14.2	60.2 ± 9.9	94.0 ± 9.7[c]	d
SPB	144.9 ± 13.7	66.0 ± 9.5[c]	88.7 ± 10.2	d
CPB	118.7 ± 13.8	70.6 ± 10.6	84.0 ± 9.2[c]	d

[a]NPL, NPH, PPL, and PPH pads were measured while they were physically located at the DOE Grand Junction Projects Office (background pad PB).

[b]Uncertainties are one sigma (68 percent confidence interval).

[c]Read directly from the MCA (TN-1710) peak-search module.

[d]Below detection limit.

3.2 COLLECTION OF MOISTURE DATA

3.2.1 Equipment Description

Interstitial moisture contained in the pads was determined from data collected with a Model 3411-B Surface Moisture-Density Gauge manufactured by Troxler Electronic Laboratories, Inc. The instrument measures the count rate of those neutrons, emitted by an americium-beryllium neutron source contained in the instrument, that have been reduced to thermal energies by collision with hydrogen nuclei in the material being measured and backscattered into the instrument's detector. These count-rate data are then input to a microprocessor, also contained in the instrument, to calculate the amount of moisture (partial density of water) in the material under investigation. The microprocessor compares the observed neutron count rate with the count rate obtained when the instrument is mounted on a factory-supplied reference block. The block permits calibration against a standard of known hydrogen content.

Initial calibration of the instrument was performed by the manufacturer. This calibration was verified by measuring the moisture content in the upper barren zone of the KW model and

comparing the results with previous moisture measurements obtained for this model (Koizumi, 1981). The KW model is a borehole calibration model located in Grand Junction; the outside surface of a portion of its upper barren zone is accessible.

The moisture-density gauge may be operated in either a 'backscatter' or a 'direct transmission' mode. As mentioned above, the former was used in measurements on the concrete pads. The large size of the pads makes them appear 'infinite' to the instrument, so no correction for the effect of finite pad size is needed. The depth of investigation (98 percent signal) for 0.25 g/cc of interstitial water is 8 inches (Troxler Electronic Laboratories, Inc., 1980). The manufacturer cautions that a surface error must be considered when making measurements on surfaces that are not flat. This error is stated to be -0.017 g/cc at 0.25 g/cc of water if the detector is positioned 1.25 mm (0.050 in.) above the surface while measuring in the backscatter mode. Since the surfaces of the calibration pads are only approximately flat, care was taken with each measurement to obtain maximum pad-to-detector contact. The effect of detector elevation was tested, and it was determined that no correction need be applied to the moisture measurements to compensate for the 'rough' surfaces of the pads.

The moisture-density gauge also contains a Cs-137 gamma-ray source and a detector for use in determining the dry bulk density of the material under investigation. Since most of the pads are significantly enriched with radium, thorium, or potassium, however, the density response of the instrument was erroneous due to the high gamma-ray activity of the enriched concrete. As a consequence, the density readings obtained with this instrument were not used in this study and hence are not reported. Instead, all of the dry-bulk-density data reported herein are the results of laboratory measurements made on samples that were collected when the pads were being constructed.

3.2.2 Data-Collection Procedures

Moisture data were collected on the pads according to procedures described in the manufacturer's instruction manual. After turning the instrument on and allowing it to stabilize for several minutes, a measurement was made on the reference block. Measurements were then made on one or more of the concrete pads. A 'slow' acquisition time of 4 minutes was used for all readings. Table 3-6 presents the moisture data acquired on each of the calibration pads.

The observed count rate measured by the instrument on the reference standard was very consistent over the course of the measurements; for all repeat measurements on the reference block, the coefficient of variation in the observed count rates was 0.71 percent, which is well within the manufacturer's stated tolerance limit of 1 percent. In addition, the hydrogen content of the reference standard is warranted by the manufacturer to an accuracy of 4 percent. These two uncertainties, when combined in quadrature with the counting uncertainties associated with measurements made on the pads, result in an overall uncertainty in the measured moisture values of approximately 11 percent.

Table 3-6. Results of Neutron Moisture Measurements Made Using the Troxler Model 3411-B Moisture-Density Gauge

Pad	Date of Measurement	Observed Counts	Moisture[a] (g/cc)
E1	02/02/83	94	0.118
	04/11/83	91	0.113
E2	02/02/83	99	0.126
	04/11/83	96	0.120
E4	02/02/83	110	0.142
	04/11/83	112	0.144
E5	02/02/83	90	0.112
	04/11/83	93	0.116
CE2	09/12/83	104	0.135
CE4	09/12/83	122	0.162
GE2	06/09/83	173	0.238
	06/09/83	172	0.236
GE4	06/09/83	115	0.150
	06/09/83	112	0.145
TE2	06/15/83	136	0.183
	06/16/83	128	0.171
TE4	06/15/83	163	0.225
	06/16/83	160	0.220
H1	02/02/83	139	0.186
	04/06/83	138	0.184
H2	02/02/83	112	0.145
	04/06/83	108	0.139

[a]Computed by the instrument (Model 3411-B) according to the manufacturer's calibration results and data collected on the factory-supplied reference block.

Table 3-6. Results of Neutron Moisture Measurements Made Using the Troxler Model 3411-B Moisture-Density Gauge (continued)

Pad	Date of Measurement	Observed Counts	Moisture[a] (g/cc)
H3	02/02/83	137	0.183
	02/18/83	136	0.182
	03/11/83	134	0.177
H4	02/02/83	84	0.103
	04/06/83	79	0.095
H5	02/02/83	107	0.138
	04/06/83	114	0.148
W1	03/02/83	194	0.256
W2	03/02/83	197	0.260
W3	03/02/83	158	0.208
W4	03/02/83	187	0.247
W5	03/02/83	185	0.244
PK	02/02/83	100	0.127
	04/06/83	122	0.160
	04/11/83	115	0.149
CPK	09/12/83	101	0.130
GPK	06/09/83	99	0.126
	06/09/83	100	0.127
TPK	06/15/83	100	0.129
	06/16/83	102	0.132
SPK	09/07/83	97	0.123
RPK	08/27/83	120	0.161
MPK	08/08/83	96	0.122
	08/09/83	98	0.126
PL	02/02/83	126	0.167
	04/06/83	141	0.188
	04/11/83	139	0.185
CPL	09/12/83	113	0.148
GPL	06/09/83	125	0.165
	06/09/83	124	0.164
TPL	06/15/83	118	0.156
	06/16/83	119	0.158
SPL	09/07/83	119	0.157
RPL	08/27/83	111	0.147

[a]Computed by the instrument (Model 3411-B) according to the manufacturer's calibration results and data collected on the factory-supplied reference block.

Table 3-6. Results of Neutron Moisture Measurements Made Using the Troxler Model 3411-B Moisture-Density Gauge (continued)

Pad	Date of Measurement	Observed Counts	Moisture[a] (g/cc)
MPL	08/08/83	111	0.146
	08/09/83	112	0.147
PH	02/02/83	126	0.167
	04/06/83	143	0.191
	04/11/83	137	0.182
CPH	09/12/83	116	0.153
GPH	06/09/83	110	0.142
	06/09/83	109	0.141
TPH	06/15/83	119	0.157
	06/16/83	119	0.158
SPH	09/07/83	111	0.145
RPH	08/27/83	109	0.144
MPH	08/08/83	99	0.128
	08/09/83	97	0.124
PT	02/02/83	116	0.151
	04/06/83	129	0.170
	04/11/83	125	0.164
CPT	09/12/83	119	0.157
GPT	06/09/83	114	0.148
	06/09/83	111	0.144
TPT	06/15/83	119	0.157
	06/16/83	116	0.153
SPT	09/07/83	105	0.136
RPT	08/27/83	94	0.121
MPT	08/08/83	96	0.123
	08/09/83	99	0.127
NPL	05/03/83	132	0.176
PPL	05/03/83	132	0.176
NPH	05/03/83	142	0.191
PPH	05/03/83	147	0.199

[a]Computed by the instrument (Model 3411-B) according to the manufacturer's calibration results and data collected on the factory-supplied reference block.

4.0 REDUCTION OF FIELD DATA FOR PARAMETER ASSIGNMENT

In order to relate the measurements made on the pads to their corresponding radiometric concentrations, as described by equations (2-1) through (2-3), the data presented in Table 3-4 must first be converted to count rates by dividing the counts and their uncertainties by the MCA acquisition live time. These count rates must then be corrected for system dead time and the presence of ambient background radiation, then for attenuation by moisture, and, finally, for Bi-214/Ra-226 disequilibrium if necessary.

4.1 CORRECTION FOR DEAD TIME AND BACKGROUND

4.1.1 Method

The dead-time correction factor, F_d, is computed by dividing the pulser 'trigger out' count by the observed pulser 'photopeak' area,

$$F_d = C_T/A_p \qquad (4\text{-}1)$$

Uncertainty in F_d is calculated using the relationship

$$\sigma(F_d) = \sqrt{\sigma^2(A_p)/A_p^2 - 1/C_T} \qquad (4\text{-}2)$$

where A_p and $\sigma(A_p)$ are the net area and its uncertainty, respectively, as determined from the peak-area extraction algorithm described in Section 3.1.2, and C_T is the 'trigger out' count. The covariance term reflecting the correlation between A_p and C_T has been included. It is assumed that $\sigma^2(C_T) = C_T$, i.e., that the pulser 'trigger out' signal is described by Poisson statistics.

The presence of an ambient background count rate in the photopeak of interest, due to naturally occurring potassium, uranium, and thorium in the environment, also requires application of a correction. Thus, the dead-time and background-corrected count rate in the photopeak of energy E is

$$R'(E) = F_d R_o(E) - F_{dB} B_o(E) \qquad (4\text{-}3)$$

where F_d is its applicable dead-time correction factor, $R_o(E)$ is the count rate observed in the photopeak of energy E, F_{dB} is the dead-time correction factor applicable to the PB pad measurement, and $B_o(E)$ is the count rate observed in the photopeak of energy E on the PB pad at the applicable site. The uncertainty in the

dead-time and background-corrected count rate, $\sigma[R'(E)]$, is calculated using the equation

$$\sigma[R'(E)] = \left\{R_o^2(E)\sigma^2(F_d) + F_d^2\sigma^2[R_o(E)] + B_o^2(E)\sigma^2(F_{dB}) + F_{dB}^2\sigma^2[B_o(E)]\right\}^{1/2} \quad (4\text{-}4)$$

4.1.2 Results

The dead-time correction factors and their uncertainties, as computed using equations (4-1) and (4-2), are presented in Table 4-1. The background/dead-time correction factors, F_{dB}, and the background count rates, B_o, observed at each site are presented in Tables 4-2 and 4-3, respectively.

Table 4-1. Dead-Time Correction Factors, F_d

Pad	F_d[a]	Pad	F_d[a]
E1	1.000 ± 0.002	GE4	1.020 ± 0.001
E2	1.003 ± 0.001	GPK	0.999 ± 0.001
E4	1.025 ± 0.001	GPL	1.006 ± 0.001
E5	1.060 ± 0.002	GPH	1.019 ± 0.001
H1	1.000 ± 0.001	GPT	1.003 ± 0.003
H2	1.000 ± 0.000	TE2	1.006 ± 0.001
H3	1.015 ± 0.001	TE4	1.021 ± 0.001
H4	1.007 ± 0.001	TPK	0.999 ± 0.000
H5	1.007 ± 0.001	TPL	1.004 ± 0.001
PK	1.000 ± 0.000	TPH	1.017 ± 0.001
PL	1.004 ± 0.001	TPT	1.002 ± 0.001
PH	1.022 ± 0.001	MPK	1.000 ± 0.000
PT	1.001 ± 0.002	MPL	1.006 ± 0.001
W1	1.002 ± 0.005	MPH	1.019 ± 0.001
W2	1.006 ± 0.005	MPT	1.004 ± 0.001
W3	1.008 ± 0.004	RPK	1.001 ± 0.000
W4	1.040 ± 0.001	RPL	1.002 ± 0.001
W5	1.000 ± 0.001	RPH	1.021 ± 0.001
NPL	1.006 ± 0.012	RPT	1.002 ± 0.001
PPL	0.998 ± 0.001	SPK	1.001 ± 0.002
NPH	1.004 ± 0.002	SPL	1.005 ± 0.001
PPH	1.004 ± 0.001	SPH	1.022 ± 0.001
GE2	1.010 ± 0.002	SPT	1.002 ± 0.002

[a]Uncertainties are one sigma (68 percent confidence interval).

Table 4-1. Dead-Time Correction Factors, F_d (continued)

Pad	F_d[a]	Pad	F_d[a]
CE2	1.004 ± 0.001	CPL	1.005 ± 0.001
CE4	1.019 ± 0.001	CPH	1.019 ± 0.001
CPK	1.003 ± 0.001	CPT	1.001 ± 0.002

[a]Uncertainties are one sigma (68 percent confidence interval).

Table 4-2. Background/Dead-Time Correction Factors, F_{dB}

Calibration Site	F_{dB}[a]
Grand Junction, Colorado	1.0002 ± 0.0003
Grants, New Mexico	0.9921 ± 0.0006
George West, Texas	0.9997 ± 0.0003
Morgantown, West Virginia	1.0006 ± 0.0005
Reno, Nevada	1.0084 ± 0.0003
Spokane, Washington	0.9982 ± 0.0006
Casper, Wyoming	0.9999 ± 0.0012

[a]Uncertainties are one sigma (68 percent confidence interval).

Table 4-3. Observed Background Count Rates in Photopeaks of Energies of Interest, $B_o(E)$

Calibration Site	Count Rate (cps)[a]		
	$B_o(1461)$	$B_o(1765)$	$B_o(2615)$
Grand Junction, Colorado	0.018 ± 0.002	0.012 ± 0.002	0.012 ± 0.002
Grants, New Mexico	0.021 ± 0.003	0.024 ± 0.003	0.016 ± 0.002
George West, Texas	0.014 ± 0.002	0.014 ± 0.002	0.013 ± 0.002
Morgantown, West Virginia	0.011 ± 0.002	0.034 ± 0.003	0.016 ± 0.002
Reno, Nevada	0.031 ± 0.003	0.012 ± 0.002	0.019 ± 0.002
Spokane, Washington	0.029 ± 0.003	0.013 ± 0.002	0.018 ± 0.002
Casper, Wyoming	0.024 ± 0.003	0.014 ± 0.002	0.017 ± 0.002

[a]MCA live time = 5000 sec. Uncertainties are one sigma (68 percent confidence interval).

Examination of the data presented in Table 4-1 reveals that the dead-time correction factors for the pads enriched in only potassium or thorium are essentially unity, within their uncertainties, except for the MPT and CPK pads. The reason for the slightly higher correction required for these pads is not known; however, as is demonstrated in Section 6 of this report, the effect of these higher correction factors on the final radioelement concentrations is insignificant.

In the case of the radium-enriched pads, the dead-time correction factor tends to increase as the observed count rate increases, which is the expected result. Two exceptions are the W4 and NPL pads; the reasons for the relatively large correction for W4 and the large uncertainty in the correction for NPL are not presently known.

4.2 CORRECTION FOR MOISTURE

4.2.1 Method

The moisture correction factor, $F_m(E)$, compensates for attenuation of gamma radiation by water in the pore spaces of the concrete. Application of this correction factor to the observed count rates yields count rates that would be expected from a dry source. The source material itself attenuates gamma radiation, and it is assumed here that the ratio of 'dry' to 'moist' count rates is inversely proportional to the ratio of the 'dry' to 'moist' linear attenuation coefficients (Wilson and Stromswold, 1981), i.e.,

$$F_m(E) = \frac{R'_d(E)}{R'_m(E)}$$

$$= \frac{\mu_m(E)}{\mu_d(E)} = \frac{\mu_{Mc}(E)\rho_c + \mu_{Mw}(E)\rho_w}{\mu_{Mc}(E)\rho_c}$$

$$= 1 + \frac{\mu_{Mw}(E)\rho_w}{\mu_{Mc}(E)\rho_c} \qquad (4\text{-}5)$$

where R'_d and R'_m are the dead-time and background-corrected 'dry' and 'moist' count rates, respectively, as computed from equation (4-3); $\mu_{Mc}(E)$ and $\mu_{Mw}(E)$ are the mass attenuation coefficients for gamma rays of energy E in dry concrete and water, respec-

tively; and ρ_c and ρ_w are the densities of dry concrete and water, respectively, in the bulk material.

The uncertainty in $F_m(E)$ is calculated using the relationship

$$\sigma[F_m(E)] = [F_m(E) - 1] \left\{ \frac{\sigma^2[\mu_{Mw}(E)]}{\mu^2_{Mw}(E)} + \frac{\sigma^2[\mu_{Mc}(E)]}{\mu^2_{Mc}(E)} + \frac{\sigma^2(\rho_w)}{\rho^2_w} + \frac{\sigma^2(\rho_c)}{\rho^2_c} \right\}^{1/2} \quad (4\text{-}6)$$

The values used for $\mu_{Mw}(E)$ and $\mu_{Mc}(E)$ are presented in Table 4-4. Relative uncertainties, $\sigma[\mu_{Mw}(E)]/\mu_{Mw}(E)$ and $\sigma[\mu_{Mc}(E)]/\mu_{Mc}(E)$, were assumed to be 2 percent (Siegbahn, 1968). The relative uncertainty in the dry bulk density of the source matrix, $\sigma(\rho_c)/\rho_c$, was taken to be 1 percent on the basis of the reported laboratory measurements, whereas the relative uncertainty in the moisture, $\sigma(\rho_w)/\rho_w$, was taken to be 11 percent, as discussed in Section 3.2. Thus,

$$\sigma[F_m(E)] \approx 0.114[F_m(E) - 1] \quad (4\text{-}7)$$

Table 4-4. Mass Attenuation Coefficients for Gamma-Ray Energies of Interest[a]

Energy (keV)	Mass Attenuation Coefficient (cm^2/g)	
	Concrete	Water
609	0.0805	0.0890
1001	0.0637	0.0707
1120	0.0600	0.0667
1461	0.0524	0.0583
1765	0.0477	0.0526
2204	0.0426	0.0470
2448	0.0404	0.0443
2615	0.0392	0.0424

[a]Mass attenuation coefficients taken from Radiological Health Handbook, revised edition, January 1970, U.S. Department of Health, Education, and Welfare.

4.2.2 Results

The values obtained for $F_m(E)$ are presented in Table 4-5. As the data demonstrate, F_m for any given pad is not a strong function of gamma-ray energy in the range 1461 to 2615 keV (Wilson and Stromswold, 1981). Consequently, little error would result if the value for $F_m(1765)$ were used to correct the 'potassium' and 'thorium' count rates as well. In the interest of precision, however, the values computed for $F_m(1461)$ and $F_m(2615)$ were used in the present analyses.

Table 4-5. Moisture Correction Factors for Photopeaks of Energies of Interest, $F_m(E)$

Pad	$F_m(1461)$[a]	$F_m(1765)$[a]	$F_m(2615)$[a]
E1	1.068 ± 0.008	1.068 ± 0.008	1.066 ± 0.008
E2	1.074 ± 0.008	1.074 ± 0.008	1.072 ± 0.008
E4	1.086 ± 0.010	1.086 ± 0.010	1.084 ± 0.010
E5	1.065 ± 0.007	1.065 ± 0.007	1.064 ± 0.007
H1	1.111 ± 0.013	1.110 ± 0.013	1.108 ± 0.012
H2	1.084 ± 0.010	1.084 ± 0.010	1.082 ± 0.009
H3	1.107 ± 0.012	1.106 ± 0.012	1.104 ± 0.012
H4	1.057 ± 0.007	1.057 ± 0.006	1.056 ± 0.006
H5	1.082 ± 0.009	1.082 ± 0.009	1.080 ± 0.009
PK	1.083 ± 0.009	1.082 ± 0.009	1.081 ± 0.009
PL	1.105 ± 0.012	1.104 ± 0.012	1.102 ± 0.012
PH	1.104 ± 0.012	1.103 ± 0.012	1.101 ± 0.012
PT	1.095 ± 0.011	1.094 ± 0.011	1.092 ± 0.011
W1	1.149 ± 0.017	1.148 ± 0.017	1.145 ± 0.017
W2	1.145 ± 0.017	1.144 ± 0.016	1.141 ± 0.016
W3	1.121 ± 0.014	1.119 ± 0.014	1.117 ± 0.013
W4	1.144 ± 0.016	1.143 ± 0.016	1.140 ± 0.016
W5	1.138 ± 0.016	1.137 ± 0.016	1.134 ± 0.015
NPL	1.101 ± 0.012	1.100 ± 0.011	1.098 ± 0.011
PPL	1.100 ± 0.011	1.100 ± 0.011	1.098 ± 0.011
NPH	1.109 ± 0.012	1.108 ± 0.012	1.106 ± 0.012
PPH	1.114 ± 0.013	1.113 ± 0.013	1.110 ± 0.013
GE2	1.143 ± 0.016	1.141 ± 0.016	1.139 ± 0.016
GE4	1.089 ± 0.010	1.089 ± 0.010	1.087 ± 0.010
GPK	1.072 ± 0.008	1.071 ± 0.008	1.070 ± 0.008
GPL	1.097 ± 0.011	1.096 ± 0.011	1.094 ± 0.011
GPH	1.083 ± 0.009	1.082 ± 0.009	1.080 ± 0.009

[a]Uncertainties are one sigma (68 percent confidence interval).

Table 4-5. Moisture Correction Factors for Photopeaks of Energies of Interest, $F_m(E)$ (continued)

Pad	$F_m(1461)$[a]	$F_m(1765)$[a]	$F_m(2615)$[a]
GPT	1.086 ± 0.010	1.085 ± 0.010	1.084 ± 0.010
TE2	1.111 ± 0.013	1.110 ± 0.013	1.108 ± 0.012
TE4	1.135 ± 0.015	1.133 ± 0.015	1.131 ± 0.015
TPK	1.074 ± 0.008	1.073 ± 0.008	1.072 ± 0.008
TPL	1.092 ± 0.011	1.092 ± 0.010	1.090 ± 0.010
TPH	1.092 ± 0.010	1.091 ± 0.010	1.089 ± 0.010
TPT	1.092 ± 0.010	1.091 ± 0.010	1.089 ± 0.010
MPK	1.073 ± 0.008	1.072 ± 0.008	1.071 ± 0.008
MPL	1.086 ± 0.010	1.085 ± 0.010	1.084 ± 0.010
MPH	1.074 ± 0.008	1.074 ± 0.008	1.072 ± 0.008
MPT	1.075 ± 0.009	1.074 ± 0.008	1.073 ± 0.008
RPK	1.093 ± 0.011	1.092 ± 0.011	1.091 ± 0.010
RPL	1.086 ± 0.010	1.085 ± 0.010	1.084 ± 0.010
RPH	1.085 ± 0.010	1.084 ± 0.010	1.082 ± 0.009
RPT	1.072 ± 0.008	1.071 ± 0.008	1.070 ± 0.008
SPK	1.072 ± 0.008	1.071 ± 0.008	1.070 ± 0.008
SPL	1.092 ± 0.011	1.092 ± 0.010	1.090 ± 0.010
SPH	1.085 ± 0.010	1.085 ± 0.010	1.083 ± 0.009
SPT	1.080 ± 0.009	1.079 ± 0.009	1.078 ± 0.009
CE2	1.081 ± 0.009	1.080 ± 0.009	1.079 ± 0.009
CE4	1.098 ± 0.011	1.097 ± 0.011	1.095 ± 0.011
CPK	1.075 ± 0.008	1.074 ± 0.008	1.072 ± 0.008
CPL	1.087 ± 0.010	1.086 ± 0.010	1.085 ± 0.010
CPH	1.089 ± 0.010	1.088 ± 0.010	1.087 ± 0.010
CPT	1.092 ± 0.011	1.092 ± 0.010	1.090 ± 0.010

[a]Uncertainties are one sigma (68 percent confidence interval).

Also apparent from the data is the fact that the moisture correction factors for the W pads are noticeably higher than those for most of the other pads, largely because the W pads are exposed to precipitation whereas the other pads are normally kept covered. Three exceptions are the GE2, TE2, and TE4 pads, which were found uncovered by the field crew upon their arrival at the Grants and George West sites. In addition, the somewhat higher values for the NPL, NPH, PPL, and PPH pads are probably a reflection of their being less than 1 year old when measured, and hence not 'cured' to the extent of the other P pads.

4.3 CORRECTION FOR RADON-222 EXHALATION

4.3.1 Method

In order to relate Bi-214 count rates to Ra-226 concentrations, corrections must be applied to compensate for any radiometric disequilibrium that exists between Bi-214 and its parents prior to production of Rn-222 in the decay chain. To determine the appropriate correction factors, measurements were made to characterize the radium-enriched calibration pads at Grand Junction and at the field calibration sites in terms of Bi-214/Ra-226 disequilibrium, which is a measure of radon exhalation. As used here, the term 'exhalation' refers to the escape of radon from the bulk material, and not to the 'emanation' or recoil of newly formed radon atoms into the pore spaces between mineral grains in the host matrix.

The approach involved calculating the activity of Pa-234m relative to that of Bi-214 from measurements of the 1001-keV and 1765-keV gamma rays, respectively. Strictly speaking, this method yields a measurement of the amount of Bi-214/U-238 equilibrium only. However, results of laboratory measurements, some of which have been published, demonstrate that the ores used to construct the pads are characterized by high degrees of Ra-226/U-238 equilibrium (Ward, 1978). The gamma-ray measurements made for this study are therefore also representative of the degrees of Bi-214/Ra-226 equilibrium contained in the pads. It must be noted, however, that radon exhalation is known to be influenced by meteorologic conditions. Since the results reported herein are based only on single measurements made over a relatively short time span, they may not be representative of a long-term or annual average.

The calculated results are quite sensitive to the values used for the absolute intensities of the 1001-keV and 1765-keV gamma rays. Although there is reasonably good agreement among the values reported in the literature for the latter gamma ray, there is considerable disparity with respect to the former. As a consequence, measurements were performed by the Bendix Analytical Chemistry Laboratory on sealed, New Brunswick Laboratory (NBL) standard samples (Series 100A) for which Bi-214/U-238 equilibrium states were known, and a value was determined for the 1001-keV gamma-ray intensity in the following manner. First, the count rates observed in the most prominent Pb-214 and Bi-214 gamma-ray peaks (295 keV, 352 keV, 609 keV, 1120 keV, 1765 keV, and 2204 keV) were divided by their respective absolute intensities, given in Table 4-6. The logarithms of these quantities were then plotted against the logarithms of their energies, yielding a very

linear graph. Linearity results because the normalized count rates are proportional to the absolute photopeak efficiencies of the detector, and the logarithm of this efficiency is a linear function of the logarithm of the gamma-ray energy, in the energy range of interest. A straight line was fitted through the plotted points using the least-squares method, and the normalized count rate that should be observed in the 1001-keV photopeak, assuming secular equilibrium between Bi-214 and U-238, was calculated. This value was compared with the count rate actually observed in this peak, adjusted for Ra-226/U-238 disequilibrium in the standard, and the required intensity was then computed. This value, 861 $\pm$ 16 gamma rays per 10^5 decays of the parent isotope, was used in the calculation of the radon-exhalation correction factor, F_e.

Table 4-6. Absolute Intensities of Gamma Rays Used for Detector Efficiency Determination[a]

Decay	Energy (keV)	Intensity[b]
Pb-214 ⟶ Bi-214	295.2	0.189 $\pm$ 0.020
	352.0	0.367 $\pm$ 0.040
Bi-214 ⟶ Po-214	609.3	0.461 $\pm$ 0.012
	1120.3	0.150 $\pm$ 0.004
	1764.5	0.158 $\pm$ 0.005
	2204.2	0.0499 $\pm$ 0.0016
	2447.8	0.0154 $\pm$ 0.0004

[a]Gamma rays per decay of parent isotope. Data taken from Lederer and Shirley, 1978.

[b]Uncertainties are one sigma (68 percent confidence interval).

The count rates observed for the 1001-keV and 1765-keV gamma rays on each pad (Table 3-4) were corrected for differences in attenuation by assuming, as discussed in Section 4.2.1, that relative attenuations are inversely proportional to the relative linear attenuation coefficients. Since the radon-exhalation correction is applied after the moisture correction, the ratio of linear attenuation coefficients is just the ratio of the mass attenuation coefficients for the dry source matrix material (Table 4-4), assuming that both count rates have already been corrected for moisture.

The difference in detector response to the two energies of interest was compensated for by determining the detector's relative photopeak efficiency as a function of energy, based on spectral gamma-ray data acquired on the eight Grand Junction pads having the highest radium concentrations (H3, H5, PL, PH, and the four E pads). It was assumed that the count rate observed in a gamma-ray photopeak of energy E, $R_o(E)$, corrected for system dead time and ambient background, is related to the activity of the source, A, by the relationship

$$R_o(E) = AI(E)f_g f_a(E)\varepsilon(E) \qquad (4\text{-}8)$$

where I(E) is the absolute intensity of the gamma ray of interest, f_g is the fraction of the 4π solid angle subtended by the detector at the source, $f_a(E)$ is the fraction of the gamma rays unattenuated by absorbers between the source and the detector, and $\varepsilon(E)$ is the absolute photopeak efficiency of the detector for the gamma radiation of interest. It is apparent that if a single radioisotope emits gamma rays of more than one energy in each disintegration, the relative count rates of gamma ray i and gamma ray j will be of the form

$$\frac{R_o(E_i)}{R_o(E_j)} = \left[\frac{I(E_i)}{I(E_j)}\right]\left[\frac{f_a(E_i)}{f_a(E_j)}\right]\left[\frac{\varepsilon(E_i)}{\varepsilon(E_j)}\right] \qquad (4\text{-}9)$$

Thus, the relative photopeak efficiency of the detector is of the form

$$\begin{aligned}\frac{\varepsilon(E_i)}{\varepsilon(E_j)} &= \left[\frac{I(E_j)}{I(E_i)}\right]\left[\frac{f_a(E_j)}{f_a(E_i)}\right]\left[\frac{R_o(E_i)}{R_o(E_j)}\right] \\ &= \left[\frac{\mu(E_i)}{\mu(E_j)}\right]\left[\frac{R_o(E_i)/I(E_i)}{R_o(E_j)/I(E_j)}\right]\end{aligned} \qquad (4\text{-}10)$$

If the radioisotope is Bi-214, we may assume that gamma ray j corresponds to the 1765-keV gamma ray, yielding the relationship

$$\frac{\varepsilon(E_i)}{\varepsilon(1765)} = \left[\frac{\mu(E_i)}{\mu(1765)}\right]\left[\frac{R_o(E_i)/I(E_i)}{R_o(1765)/I(1765)}\right] \qquad (4\text{-}11)$$

Assuming that gamma ray i corresponds successively to the 609-keV, 1120-keV, 2204-keV, and 2448-keV gamma rays, the right-hand side of equation (4-11) could be evaluated using the spectral

gamma-ray, moisture, and density data observed for each pad, together with the values of absolute gamma-ray intensity given in Table 4-6. The average value, $\varepsilon(E_i)/\varepsilon(1765)$, was then computed. As was mentioned above, a plot of log $[\varepsilon(E_i)/\varepsilon(1765)]$ is very nearly linear, and the equation of this line, as determined from the least-squares method, has the form

$$\overline{\log[\varepsilon(E_i)/\varepsilon(1765)]} = -0.62448 \log E_i + 2.02016 \qquad (4\text{-}12)$$

Thus, the relative photopeak efficiency sought is

$$\frac{\varepsilon(1001)}{\varepsilon(1765)} = 1.4010 \pm 0.0171$$

The uncertainty quoted in the relative efficiency is the square root of the variance in $\varepsilon(1001)/\varepsilon(1765)$, as computed from the eight individual estimates.

In summary, the radon-exhalation correction factor was calculated in the following manner:

$$F_e = \frac{R_o(1001)\varepsilon(1765)\mu(1001)I(1765)}{R_o(1765)\varepsilon(1001)\mu(1765)I(1001)} \qquad (4\text{-}13)$$

where $R_o(E)$ is the count rate observed for gamma rays of energy E, $\varepsilon(1001)/\varepsilon(1765)$ is the relative photopeak efficiency of the detector, $\mu(1001)/\mu(1765)$ is the relative attenuation factor, and I(E) is the absolute intensity for gamma rays of energy E. Uncertainty in F_e was calculated according to the relationship

$$\sigma(F_e) = F_e \left\{ \frac{\sigma^2[R_o(1001)]}{R_o^2(1001)} + \frac{\sigma^2[R_o(1765)]}{R_o^2(1765)} + \frac{\sigma^2[I(1001)]}{I^2(1001)} + \frac{\sigma^2[I(1765)]}{I^2(1765)} + \frac{\sigma^2[\mu(1001)]}{\mu^2(1001)} + \frac{\sigma^2[\mu(1765)]}{\mu^2(1765)} + \frac{\sigma^2(\varepsilon)}{\varepsilon^2} \right\}^{1/2} \qquad (4\text{-}14)$$

where $\sigma[R(E)]/R(E)$ is the relative uncertainty in count rate R(E), $\sigma[I(E)]/I(E)$ is the relative uncertainty in gamma-ray intensity I(E), $\sigma[\mu(E)]/\mu(E)$ is the relative uncertainty in the

mass attenuation coefficient (assumed to be 2 percent; cf. Section 4.2.1), and $\sigma(\varepsilon)/\varepsilon$ is the uncertainty in the relative efficiency of the detector.

4.3.2 Results

The correction factors for radon-222 exhalation from the calibration pads are presented in Table 4-7. Pads for which the intensity of the 1001-keV gamma ray was below detection limit were arbitrarily assigned an exhalation factor equal to the average, $\bar{F}_e$, of the factors determined for the other pads of the same type. The uncertainty in this average value was derived by first calculating the count rate of the 1001-keV gamma ray that would yield this correction factor ($\bar{F}_e$) using equation (4-13). The uncertainty expected in the calculated count rate was then determined by performing a log-log regression of observed count rates of 1001-keV gamma rays versus their uncertainties. Finally, these calculated values for $R_o(1001)$ and $\sigma[R_o(1001)]$ were inserted into equation (4-14) to compute $\sigma(\bar{F}_e)$.

These calculations were required for those pads commonly referred to as the K pads, Th pads, and barren pads. Although some fraction of the radon-222 produced in these pads is probably exhaled, the low concentrations of radium-226 contained in the pads most likely render these losses negligible relative to their effect on the apparent concentrations.

Examination of the data presented in Table 4-7 reveals that relative uncertainties in the value of F_e are rather large, the lowest being approximately 5 percent for the E5 pad. Smaller uncertainties could have been achieved with longer data-acquisition times, but practical constraints limited the degree of precision obtainable. For example, doubling the acquisition time would have decreased the relative uncertainty to some 3.5 percent in the case of the E5 pad, but the W5 pad would still have had an uncertainty of approximately 14 percent as compared with the 20 percent uncertainty cited in the table. These uncertainties will propagate through the calculations and ultimately manifest themselves as relatively large uncertainties in the assigned radium concentrations of the radium-enriched pads. To achieve a precision of approximately 1 percent in these concentrations, however, would have required data-acquisition times on the order of 500,000 seconds, which would have been prohibitively long.

Table 4-7. Radon-222 Exhalation Correction Factors, F_e

Pad	F_e[a]	Pad	F_e[a]
E1	1.364 ± 0.185	GPH	1.332 ± 0.076
E2	1.151 ± 0.102	GPT	1.368 ± 0.306[b]
E4	1.105 ± 0.065	TE2	1.272 ± 0.108
E5	1.093 ± 0.058	TE4	1.248 ± 0.075
H1	1.022 ± 0.574[b]	TPK	1.368 ± 0.819[b]
H2	1.022 ± 0.591[b]	TPL	1.384 ± 0.119
H3	1.063 ± 0.067	TPH	1.466 ± 0.083
H4	1.022 ± 0.188[b]	TPT	1.368 ± 0.317[b]
H5	0.980 ± 0.092	MPK	1.368 ± 1.499[b]
PK	1.368 ± 0.863[b]	MPL	1.413 ± 0.110
PL	1.232 ± 0.104	MPH	1.387 ± 0.080
PH	1.282 ± 0.074	MPT	1.368 ± 0.302[b]
PT	1.368 ± 0.310[b]	RPK	1.368 ± 0.819[b]
W1	1.171 ± 0.601[b]	RPL	1.254 ± 0.107
W2	1.171 ± 0.431[b]	RPH	1.358 ± 0.079
W3	1.171 ± 0.466[b]	RPT	1.368 ± 0.309[b]
W4	1.171 ± 0.272	SPK	1.368 ± 0.886[b]
W5	1.171 ± 0.233[b]	SPL	1.508 ± 0.119
NPL	1.471 ± 0.233	SPH	1.406 ± 0.081
PPL	1.254 ± 0.190	SPT	1.368 ± 0.298[b]
NPH	1.213 ± 0.134	CE2	1.238 ± 0.107
PPH	1.470 ± 0.150	CE4	1.268 ± 0.074
GE2	1.175 ± 0.105	CPK	1.368 ± 0.781[b]
GE4	1.218 ± 0.071	CPL	1.477 ± 0.117
GPK	1.368 ± 0.904[b]	CPH	1.307 ± 0.078
GPL	1.405 ± 0.114	CPT	1.368 ± 0.316[b]

[a]Uncertainties are one sigma (68 percent confidence interval).

[b]Intensity of 1001-keV gamma ray of Pa-234m is below detection limit (see discussion in Section 4.3.2).

4.4 CORRECTION FOR INTERFERENCE OF ACTINIUM-228 WITH POTASSIUM-40

As mentioned in Section 4.1.1, the count rate observed in the 1461-keV photopeak, due primarily to K-40, requires an additional correction due to the interference of 1459-keV radiation from Ac-228, a daughter of Th-232. In order to determine this correction factor, it was assumed, as discussed in Section 4.3.1, that

the count rate observed in a gamma-ray photopeak of energy E, $R_o(E)$, corrected for system dead time and background, is related to the activity of the source, A, by the relationship

$$R_o(E) = AI(E)f_g f_a(E)\varepsilon(E) \qquad (4\text{-}8)$$

where I(E) is the absolute intensity (gammas per disintegration of parent) of the gamma ray of interest, f_g is the fraction of the 4π solid angle subtended by the detector at the source, $f_a(E)$ is the fraction of the gamma rays unattenuated by absorbers between the source and the detector, and $\varepsilon(E)$ is the absolute photopeak efficiency of the detector for the gamma radiation of interest. Applying equation (4-8) to the decays of Ac-228 and Tl-208, respectively, yields the equations

$$R_o(1459) = A_{228}I(1459)f_g f_a(1459)\varepsilon(1459) \qquad (4\text{-}15)$$

$$R_o(2615) = A_{208}I(2615)f_g f_a(2615)\varepsilon(2615) \qquad (4\text{-}16)$$

Dividing equation (4-15) by equation (4-16) gives the relationship

$$\frac{R_o(1459)}{R_o(2615)} = \left[\frac{A_{228}}{A_{208}}\right]\left[\frac{I(1459)}{I(2615)}\right]\left[\frac{f_a(1459)}{f_a(2615)}\right]\left[\frac{\varepsilon(1459)}{\varepsilon(2615)}\right] \qquad (4\text{-}17)$$

In addition, it was assumed that Bi-212 is in secular equilibrium with Ac-228, and that 36 percent (B_α) of the decays of Bi-212 produce Tl-208. Finally, it was assumed that 99.79 percent of the decays of Tl-208 result in emission of the 2615-keV gamma radiation, whereas only 0.9315 percent of the decays of Ac-228 result in emission of 1459-keV gamma rays (Lederer and Shirley, 1978).

Thus, $A_{208} = 0.360A_{228}$ and we may write equation (4-17) as

$$\frac{R_o(1459)}{R_o(2615)} = \left[\frac{1}{0.360}\right]\left[\frac{0.009315}{0.9979}\right]\left[\frac{f_a(1459)}{f_a(2615)}\right]\left[\frac{\varepsilon(1459)}{\varepsilon(2615)}\right] \qquad (4\text{-}18)$$

Again, it is assumed that relative attenuations are inversely proportional to the linear attenuation coefficients, yielding the relationship

$$\frac{f_a(1459)}{f_a(2615)} = \frac{\mu(2615)}{\mu(1459)} \tag{4-19}$$

where the linear attenuation coefficient is of the form

$$\mu(E) = \mu_{Mc}(E)\rho_c + \mu_{Mw}(E)\rho_w \tag{4-20}$$

where $\mu_{Mc}(E)$ and $\mu_{Mw}(E)$ are the mass attenuation coefficients of the source matrix material and water, respectively, and ρ_c and ρ_w are the densities of the dry source matrix and interstitial water, respectively. The relative attenuation factor will therefore vary from pad to pad, depending on the dry bulk density of the concrete and on the amount of interstitial moisture. Hence, we may write equation (4-18) as

$$\frac{R_o(1459)}{R_o(2615)} = 0.02593 \left[\frac{\mu_{Mc}(2615)\rho_c + \mu_{Mw}(2615)\rho_w}{\mu_{Mc}(1459)\rho_c + \mu_{Mw}(1459)\rho_w}\right] \left[\frac{\varepsilon(1459)}{\varepsilon(2615)}\right] \tag{4-21}$$

The relative photopeak efficiency of the detector, $\varepsilon(1459)/\varepsilon(2615)$, was determined experimentally, as discussed in Section 4.3.1. From equation (4-12), the relative photopeak efficiency sought was computed to be

$$\frac{\varepsilon(1459)}{\varepsilon(2615)} = \frac{\varepsilon(1459)/\varepsilon(1765)}{\varepsilon(2615)/\varepsilon(1765)} = 1.4395 \pm 0.0159$$

The uncertainty quoted in the relative efficiency is the square root of the variance in $\varepsilon(1459)/\varepsilon(2615)$, as computed from the eight individual estimates. Inserting this value for the relative efficiency into equation (4-21) yields the relationship

$$\begin{aligned} R_o(1459) &= 0.03733\left[\frac{\mu_{Mc}(2615)\rho_c + \mu_{Mw}(2615)\rho_w}{\mu_{Mc}(1459)\rho_c + \mu_{Mw}(1459)\rho_w}\right] R_o(2615) \\ &= s(2615)R_o(2615) \end{aligned} \tag{4-22}$$

Since the dry bulk density does not differ greatly from one pad to another, and since the partial density of interstitial water is only about one-tenth the density of the dry concrete, s(2615) in equation (4-22) effectively reduces to

$$s(2615) = 0.0278 \pm 0.0028 \qquad (4\text{-}23)$$

This quantity, multiplied by $R_o(2615)$, must be subtracted from the count rate observed in the 1461-keV photopeak to yield the count rate due to K-40.

The uncertainty in s(2615) was calculated using the equation

$$\sigma[s(2615)] = s(2615)\left\{\left[\frac{\sigma(B_\alpha)}{B_\alpha}\right]^2 + \left[\frac{\sigma[I(1459)]}{I(1459)}\right]^2 + \left[\frac{\sigma[I(2615)]}{I(2615)}\right]^2 + \left[\frac{\sigma[\mu(1459)]}{\mu(1459)}\right]^2 + \left[\frac{\sigma[\mu(2615)]}{\mu(2615)}\right]^2 + \left[\frac{\sigma(\varepsilon)}{\varepsilon}\right]^2\right\}^{1/2} \qquad (4\text{-}24)$$

where $\varepsilon = \varepsilon(1459)/\varepsilon(2615)$ and

$$\sigma[\mu(E)] = \left\{\rho_c^2\sigma^2[\mu_{Mc}(E)] + \mu_{Mc}^2(E)\sigma^2(\rho_c) + \rho_w^2\sigma^2[\mu_{Mw}(E)] + \mu_{Mw}^2(E)\sigma^2(\rho_w)\right\}^{1/2} \qquad (4\text{-}25)$$

The following values are taken from Lederer and Shirley (1978):

$$B_\alpha = 0.3600 \pm 0.0003$$

$$I(1459) = 0.009315 \pm 0.000466$$

$$I(2615) = 0.9979 \pm 0.0001$$

Values for $\mu_{Mc}(E)$ and $\mu_{Mw}(E)$ are those given in Table 4-4, assuming relative uncertainties of 2 percent in those values. Values for the density of the dry concrete matrix and of the interstitial water are assumed to have relative uncertainties of 1 percent and 11 percent, respectively. Inserting all of these values and their associated uncertainties into equation (4-24) yields $\sigma(\mu)/\mu \approx 2$ percent. From the data used to compute the relative photopeak efficiency of the detector, it was found that $\sigma(E)/\varepsilon \approx$ 1 percent; thus, $\sigma[s(2615)]/s(2615) \approx 10$ percent.

4.5 RESULTS

Using the data presented in Tables 3-4 and 3-5, the correction factors required to reduce the field data were determined as described above. These correction factors [cf. Tables 4-1, 4-2, 4-3, 4-5, and 4-7 and equation (4-23)] were applied to the observed data in the following manner to yield corrected count rates, $R_c(E)$:

- Potassium

$$R_c(1461) = F_m(1461)\left\{F_d[R_o(1461) - s(2615)R_o(2615)] - F_{dB}[B_o(1461) - s(2615)B_o(2615)]\right\} \quad (4\text{-}26)$$

- Radium

$$R_c(1765) = F_e F_m(1765)[F_d R_o(1765) - F_{dB} B_o(1765)] \quad (4\text{-}27)$$

- Thorium

$$R_c(2615) = F_m(2615)[F_d R_o(2615) - F_{dB} B_o(2615)] \quad (4\text{-}28)$$

Uncertainties in the corrected count rates, $\sigma[R_c(E)]$, were calculated using the equations

$$\sigma[R_c(1461)] = R_c(1461)\left\{\left[\frac{\sigma[F_m(1461)]}{F_m(1461)}\right]^2 + \frac{\sigma^2[R'(1461)]}{[R'(1461) - s(2615)R'(2615)]^2} + \frac{s^2(2615)\sigma^2[R'(2615)]}{[R'(1461) - s(2615)R'(2615)]^2} + \frac{R'^2(2615)\sigma^2[s(2615)]}{[R'(1461) - s(2615)R'(2615)]^2}\right\}^{1/2} \quad (4\text{-}29)$$

$$\sigma[R_c(1765)] = R_c(1765)\left\{\left[\frac{\sigma(F_e)}{F_e}\right]^2 + \left[\frac{\sigma[F_m(1765)]}{F_m(1765)}\right]^2 - \left[\frac{\sigma[R'(1765)]}{R'(1765)}\right]^2\right\}^{1/2} \quad (4\text{-}30)$$

$$\sigma[R_c(2615)] = R_c(2615)\left\{\left[\frac{\sigma[F_m(2615)]}{F_m(2615)}\right]^2 + \left[\frac{\sigma[R'(2615)]}{R'(2615)}\right]^2\right\}^{1/2} \quad (4\text{-}31)$$

where $R'(E)$ and $\sigma[R'(E)]$ are given by equations (4-3) and (4-4). The covariance term reflecting the correlation between F_e and $R'_c(1765)$ has been included in equation (4-30). The corrected count rates for the gamma rays of interest, together with their associated one-sigma uncertainties, are presented in Table 4-8.

Table 4-8. Corrected Count Rates for Photopeaks of Energies of Interest, $R_c(E)$

Pad	Corrected Count Rate (cps)[a]		
	$R_c(1461)$	$R_c(1765)$	$R_c(2615)$
E1	0.523 ± 0.014	1.327 ± 0.178	0.084 ± 0.005
E2	0.532 ± 0.019	4.203 ± 0.372	0.079 ± 0.005
E4	0.441 ± 0.029	20.527 ± 1.205	0.067 ± 0.006
E5	0.567 ± 0.043	47.456 ± 2.496	0.073 ± 0.006
H1	0.436 ± 0.012	0.042 ± 0.024	0.072 ± 0.005
H2	2.081 ± 0.029	0.040 ± 0.024	0.009 ± 0.003
H3	0.465 ± 0.017	8.422 ± 0.527	0.083 ± 0.004
H4	0.388 ± 0.029	0.571 ± 0.107	7.554 ± 0.062
H5	1.465 ± 0.031	4.918 ± 0.458	2.155 ± 0.029
PK	2.014 ± 0.028	0.033 ± 0.021	0.005 ± 0.003
PL	0.653 ± 0.020	4.427 ± 0.372	0.071 ± 0.005
PH	0.655 ± 0.031	20.970 ± 1.215	0.069 ± 0.005
PT	0.633 ± 0.021	0.354 ± 0.082	3.629 ± 0.046
W1	0.506 ± 0.014	0.052 ± 0.027	0.076 ± 0.005

[a]MCA live time = 5000 sec. Uncertainties are one sigma (68 percent confidence interval).

Table 4-8. Corrected Count Rates for Photopeaks of Energies of Interest, $R_c(E)$ (continued)

Pad	Corrected Count Rate (cps)[a]		
	$R_c(1461)$	$R_c(1765)$	$R_c(2615)$
W2	1.820 ± 0.035	0.110 ± 0.041	0.101 ± 0.006
W3	0.689 ± 0.016	0.093 ± 0.037	0.576 ± 0.014
W4	0.728 ± 0.019	0.645 ± 0.151	0.118 ± 0.007
W5	1.421 ± 0.028	0.470 ± 0.094	0.216 ± 0.009
NPL	0.434 ± 0.014	0.911 ± 0.142	0.066 ± 0.005
PPL	0.428 ± 0.013	0.807 ± 0.121	0.071 ± 0.005
NPH	0.451 ± 0.016	2.355 ± 0.258	0.078 ± 0.005
PPH	0.438 ± 0.017	2.834 ± 0.286	0.075 ± 0.005
GE2	0.527 ± 0.020	4.560 ± 0.407	0.076 ± 0.005
GE4	0.469 ± 0.029	22.009 ± 1.283	0.078 ± 0.006
GPK	2.026 ± 0.027	0.031 ± 0.022	0.001 ± 0.003
GPL	0.637 ± 0.020	4.667 ± 0.376	0.056 ± 0.005
GPH	0.665 ± 0.032	20.498 ± 1.161	0.067 ± 0.005
GPT	0.587 ± 0.020	0.365 ± 0.084	3.504 ± 0.043
TE2	0.546 ± 0.019	4.691 ± 0.398	0.075 ± 0.005
TE4	0.475 ± 0.031	21.675 ± 1.301	0.058 ± 0.005
TPK	2.128 ± 0.027	0.037 ± 0.023	0.000 ± 0.003
TPL	0.630 ± 0.020	4.525 ± 0.386	0.058 ± 0.005
TPH	0.613 ± 0.028	21.677 ± 1.225	0.058 ± 0.005
TPT	0.627 ± 0.021	0.332 ± 0.079	3.617 ± 0.044
MPK	2.099 ± 0.027	0.012 ± 0.015	0.002 ± 0.003
MPL	0.661 ± 0.020	4.871 ± 0.378	0.064 ± 0.005
MPH	0.646 ± 0.029	21.206 ± 1.213	0.057 ± 0.005
MPT	0.653 ± 0.021	0.372 ± 0.084	3.628 ± 0.040
RPK	2.064 ± 0.030	0.037 ± 0.023	0.004 ± 0.003
RPL	0.647 ± 0.020	4.264 ± 0.361	0.063 ± 0.005
RPH	0.652 ± 0.030	20.465 ± 1.186	0.065 ± 0.005
RPT	0.652 ± 0.021	0.353 ± 0.081	3.630 ± 0.039
SPK	2.035 ± 0.027	0.031 ± 0.021	0.001 ± 0.003
SPL	0.635 ± 0.020	5.146 ± 0.403	0.063 ± 0.005
SPH	0.582 ± 0.029	20.904 ± 1.203	0.058 ± 0.005
SPT	0.581 ± 0.020	0.384 ± 0.085	3.550 ± 0.041
CE2	0.549 ± 0.019	4.441 ± 0.380	0.082 ± 0.006
CE4	0.476 ± 0.031	22.580 ± 1.313	0.065 ± 0.005
CPK	2.046 ± 0.027	0.041 ± 0.024	0.004 ± 0.003
CPL	0.626 ± 0.020	5.084 ± 0.399	0.063 ± 0.005
CPH	0.624 ± 0.031	19.060 ± 1.128	0.060 ± 0.005
CPT	0.556 ± 0.020	0.332 ± 0.078	3.368 ± 0.042

[a]MCA live time = 5000 sec. Uncertainties are one sigma (68 percent confidence interval).

5.0 LABORATORY MEASUREMENTS

5.1 METHODS

5.1.1 Sample Collection and Preparation

Samples of the enriched concrete were collected at the time the pads were constructed. In certain cases as few as three samples were collected, but for most of the pads a statistically adequate number was acquired. The samples were collected by simply 'catching' a container full of the wet concrete mix as the concrete was being poured into the forms for the pads.

The samples were collected in 1.89-liter, cylindrical, ice-cream cartons and allowed to air dry. Each sample was sawed in half along its axis, and the two halves prepared for different analyses. In order to drive off free moisture, one half was dried at 110°C, until negligible weight loss resulted from further drying. The dry bulk density was measured, then this half of the sample was archived. The other half was prepared for radiometric and chemical analysis using the following procedure:

1. Crush to pebbles approximately 1 cm in diameter.

2. Dry at 110°C, to drive off free moisture, until negligible weight loss results from further drying.

3. Grind to minus-28 mesh (grains approximately 0.64 mm in diameter).

4. Blend.

5. Pack a portion (about 600 grams) into aluminum cans, 10.2 cm in diameter by 5.7 cm in height, for radiometric analysis.

6. Pulverize a portion (about 100 grams) to minus-100 mesh (grains approximately 0.15 mm in diameter) for chemical analysis.

7. Archive remaining portion.

5.1.2 Radiometric Analysis

A canned sample was shelved for at least 20 days to establish equilibrium between radium and its daughters. Concentrations of equivalent radium-226 (and equivalent uranium), equivalent thorium-232, and potassium-40 were then determined by comparing

measurements of gamma-ray intensities from the sample with those from certified standards.* Standards used by the Bendix Analytical Chemistry Laboratory for radium-226 (uranium) and thorium-232 were the 100A Series supplied by New Brunswick Laboratory (Trahey and others, 1982). The calibration standard for potassium was not certified, but was obtained from reagent-grade potassium carbonate.

High-resolution gamma-ray spectroscopy using a Ge(Li) detector system (Dechant and Donivan, 1984) was the method used by the laboratory to perform radiometric analysis of the samples. The spectral photopeaks used in the assays were the 1765-keV line from Bi-214 (radium), the 2615-keV line from Tl-208 (thorium), and the 1461-keV line from K-40. As with the field data, the measurement for K-40 at 1461 keV was corrected for interference from a Th-232 daughter (see Section 4.4). All laboratory measurements were also corrected for ambient background radiation, for differences in sample density (or weight) relative to the density of the standards, and for disequilibrium between uranium and radium in the standards (Dechant and Donivan, 1984; George and others, 1983).

At the time these measurements were made, the Bendix Analytical Chemistry Laboratory reported assays for Bi-214 (the 1765-keV photopeak) in units of weight-ppm of equivalent uranium. Since the desired unit for this study was mass-normalized activity of Ra-226, a conversion was required. The calculated relationship between Ra-226 and naturally occurring uranium in secular equilibrium (George and Knight, 1982) is

$$1 \text{ wt-ppm(eU)} = 0.3337 \text{ pCi(eRa-226)/g}$$

Similarly, at the time these measurements were made, the laboratory reported measurements for Tl-208 in units of weight-ppm of equivalent thorium and measurements for K-40 in units of weight-

*The term 'equivalent,' as used herein, refers to the fact that the concentration of a daughter element is measured directly, and then the 'equivalent' concentration of the parent is inferred, assuming secular equilibrium between daughter and parent. Furthermore, in the case of naturally occurring elements (uranium and potassium, in particular), isotopes are assumed to be present in naturally occurring ratios.

percent potassium (in natural isotopic abundance). Conversion factors used for these isotopes (George and Knight, 1982) are the following:

$$1 \text{ wt-ppm(eTh)} = 0.1092 \text{ pCi(eTh-232)/g}$$

$$1 \text{ wt-\%(K)} = 8.372 \text{ pCi(K-40)/g}$$

The laboratory also calculated an uncertainty for each assay, based on counting statistics only. The result was reported as a relative uncertainty, expressed as a percentage of the assay value at the two-sigma (95 percent confidence) level (i.e., twice the coefficient of variation).

5.1.3 Chemical Analysis

Certain chemical analyses were performed on some of the samples. In the case of uranium, the analytical technique used to determine concentration depended on the approximate uranium content of the sample. A fluorometric analysis was performed on samples containing less than approximately 500 ppm uranium, whereas a colorimetric method was used on samples having higher concentrations. The potassium concentrations were determined using atomic absorption spectrometry, and thorium concentrations were determined by means of x-ray fluorescence spectrometry.

5.2 RESULTS

5.2.1 Radiometric Analysis

Complete results of the radiometric assays are presented in Appendix A. The laboratory occasionally reported results based on conditions different from those just described (denoted by the symbols '!', '<', and '?' in Appendix A), but none of these results were used for this study. Furthermore, many of the samples from the E pads, and some samples from other pads, were solid concrete--they were collected by pouring the wet concrete mix directly into aluminum cans. Results from these samples were also omitted from the calculations, since removal of free moisture was not complete, resulting in apparently decreased radiometric assays.

The laboratory-assay results are summarized in Table 5-1. The mean value reported for each pad (M in Table 5-1) was calculated by simple (unweighted) averaging of the assays of all samples

from that pad, except for the exclusions mentioned above. Also presented in Table 5-1 is an estimate of the standard deviation about the mean (2S) for the samples from each pad; the value tabulated is twice the coefficient of variation, as described in Section 5.1.2. This estimate is admittedly poor when there are few samples (i.e., fewer than 10).

The uncertainties reported by the laboratory are not explicitly included in the tabulated assay uncertainties, because they are included implicitly (i.e., if all samples were identical, then the sample-to-sample observed uncertainty should be about the same as the reported uncertainty). The reported uncertainty is based on counting statistics only, however, and past experience with samples from the total-count logging models has shown much larger deviations from sample to sample than can be explained only on the basis of counting uncertainties in the assay results (George and others, 1983). Consequently, the uncertainties cited in Table 5-1 are those determined from the sample variances about their means.

5.2.2 Chemical Analysis

Complete results of all chemical analyses are presented in Appendix B; these results are summarized in Table 5-2. The estimated standard deviation of the samples from each pad was calculated as described for the radiometric analyses. The chemical data were not used in this study other than for 'eye-ball' comparisons of results for radium and potassium. However, the data are reported herein to ensure a permanent record of them.

Table 5-1. Summary of Results of Laboratory Radiometric Analysis of Construction Samples from the Pads[a]

Pad	Net Weight[b]			Potassium-40			Radium-226			Thorium-232		
	N	M (g)	2S (%)	N	M (pCi/g)	2S (%)	N	M (pCi/g)	2S (%)	N	M (pCi/g)	2S (%)
E1	5	536.5	12.5	5	13.4	9.2	5	25.7	16.5	4	0.6	41.3
E2	5	583.8	1.4	5	14.2	8.7	5	82.5	2.7	4	1.0	21.8
E4	4	562.2	1.4	4	11.7	21.0	4	409.8	1.1	1	0.7	13.9
E5	3	578.5	3.3	3	14.2	27.0	3	860.0	1.5	1	1.0	8.9
CE2	3	590.1	3.5	3	13.4	10.8	3	80.3	4.6	2	0.9	12.0
CE4	3	551.3	1.6	2	12.6	18.9	3	399.8	2.1	1	0.7	14.1
GE2	4	603.1	0.9	3	12.6	13.3	4	81.4	4.9	1	0.7	13.3
GE4	4	568.9	2.8	2	12.6	14.6	4	383.9	4.5	1	0.9	10.6
TE2	3	566.3	6.6	2	12.6	24.4	3	79.8	2.7	c		
TE4	3	547.0	5.7	1	10.9	11.6	3	394.2	1.7	c		
W1	10	511.3	2.2	10	12.6	5.8	1	0.7	25.9	c		
W2	10	515.0	6.0	10	45.2	4.6	6	1.8	12.9	4	0.9	27.0
W3	10	577.6	1.7	10	16.7	3.6	5	1.7	14.9	10	4.7	7.6
W4	10	587.3	3.1	10	16.7	6.4	10	12.2	16.7	c		
W5	10	608.4	2.3	10	33.5	3.5	10	8.0	13.5	c		
H1	10	686.5	2.5	10	10.9	4.4	6	0.9	22.9	6	0.7	13.7
H2	8	578.0	2.5	8	56.1	3.7	5	0.6	30.2	c		
H3	7	605.2	3.4	7	10.9	8.8	7	167.0	3.4	2	0.6	22.5
H4	10	694.5	3.0	10	11.7	11.5	10	11.5	5.1	10	75.3	3.2
H5	9	612.4	5.0	9	38.5	3.9	9	113.7	3.4	9	21.8	4.0
PK	6	629.6	5.8	6	51.1	2.5	2	1.7	12.2	c		
CPK	6	679.3	1.3	6	51.1	1.8	c			c		
GPK	6	688.5	1.2	6	51.9	4.0	c			c		
TPK	8	681.5	1.0	8	51.9	2.6	c			c		
SPK	7	677.2	1.5	7	51.9	1.8	c			c		
RPK	7	681.3	1.0	7	51.9	2.5	c			c		
MPK	6	687.0	0.8	6	51.9	2.1	c			c		
PL	6	690.8	0.8	6	15.1	5.3	6	89.1	1.3	1	0.7	12.8
CPL	6	699.2	1.5	6	15.1	6.6	6	89.0	3.7	2	0.5	27.1
GPL	6	696.4	1.4	6	15.1	9.3	6	88.7	3.4	1	0.6	14.9
TPL	6	675.5	3.0	6	15.1	9.6	6	89.9	10.3	3	0.6	13.8
SPL	6	688.1	0.7	6	15.9	11.5	6	91.6	1.8	1	0.6	13.4
RPL	6	695.1	1.2	6	15.9	5.3	6	90.7	2.1	2	0.7	18.0

[a]N = the number of samples analyzed for which the photopeak was detected; M = the mean value of N samples; 2S = twice the coefficient of variation for N samples.

[b]Data on sample weight are included to indicate the relative densities and uniformity of the individual sets of samples.

[c]The photopeak for this isotope was below the laboratory detection limit for all of the samples.

Table 5-1. Summary of Results of Laboratory Radiometric Analysis of Construction Samples from the Pads[a] (continued)

Pad	Net Weight[b]			Potassium-40			Radium-226			Thorium-232		
	N	M (g)	2S (%)	N	M (pCi/g)	2S (%)	N	M (pCi/g)	2S (%)	N	M (pCi/g)	2S (%)
MPL	6	700.8	0.5	6	15.1	11.2	6	89.1	2.0	2	0.6	15.5
PH	6	669.5	2.9	6	15.1	9.2	6	358.6	2.8	1	0.6	15.2
CPH	6	654.8	0.7	6	14.2	9.2	6	366.7	1.7	3	0.6	17.6
GPH	6	661.2	1.0	6	15.1	16.5	6	370.1	1.2	2	0.6	14.0
TPH	6	669.1	1.7	6	14.2	12.3	6	367.4	1.8	1	0.4	21.3
SPH	6	682.8	1.0	6	15.1	15.2	6	359.7	1.2	1	0.6	13.2
RPH	6	672.9	3.8	6	15.1	9.1	6	367.2	1.1	2	0.5	19.6
MPH	6	698.4	0.9	6	15.9	8.8	6	373.9	2.0	c		
PT	6	691.8	1.4	6	13.4	11.6	6	6.7	15.8	6	30.2	2.6
CPT	6	675.5	1.4	6	14.2	3.8	6	6.0	6.7	6	30.6	2.1
GPT	6	696.1	1.6	6	15.1	6.0	6	6.3	10.6	6	28.3	15.4
TPT	6	685.2	0.8	6	14.2	4.7	6	5.7	13.1	6	29.7	3.5
SPT	6	680.9	2.3	6	14.2	3.8	6	6.2	16.2	6	30.2	2.2
RPT	6	689.1	2.3	6	14.2	6.0	6	6.2	10.0	6	31.1	3.2
MPT	6	678.4	3.3	6	15.1	8.1	5	7.1	10.4	6	32.0	3.2
NPL	6	668.6	1.9	6	10.9	4.8	6	14.7	3.4	2	0.7	12.6
PPL	6	660.0	3.1	6	10.9	7.5	6	15.2	9.0	3	0.6	41.4
NPH	6	667.4	1.6	6	10.9	10.9	6	44.6	7.2	2	0.8	11.4
PPH	6	650.0	2.3	6	10.9	5.9	6	46.0	4.5	2	0.6	14.7
PB	5	711.0	1.2	c			c			c		

[a]N = the number of samples analyzed for which the photopeak was detected; M = the mean value of N samples; 2S = twice the coefficient of variation for N samples.

[b]Data on sample weight are included to indicate the relative densities and uniformity of the individual sets of samples.

[c]The photopeak for this isotope was below the laboratory detection limit for all of the samples.

Table 5-2. Summary of Results of Laboratory Chemical Analysis of Construction Samples from the Pads[a]

Pad	N	Potassium		Uranium		Thorium	
		M (wt-%)	2S (%)	M (wt-ppm)	2S (%)	M (wt-ppm)	2S (%)
E1	3	1.2	25.0	63.6	8.1		
E1	11			60.9	7.4		
E2	3	0.7	23.0	234.5	2.1		
E4	3	0.5	76.0	1164.0	2.6		
E5	3	1.3	22.0	2537.0	2.5		
CE2	3	1.2	25.0	262.7	3.2		
CE4	3	1.0	0.0	1155.0	2.1		
GE2	3	1.5	33.0	274.0	3.6		
GE4	3	0.7	43.0	1201.0	0.4		
TE2	3	0.6	17.0	274.0	1.8		
TE4	3	0.5	0.0	1235.0	3.5		
W1	30	1.6	3.4	2.5	22.0	14.3	17.0
W2	30	5.1	5.1	5.8	35.0	14.5	35.0
W3	30	2.2	3.2	4.4	29.0	47.2	14.0
W4	30	2.2	2.5	35.3	24.0	15.0	30.0
W5	30	4.3	2.8	24.3	33.0	22.1	28.0
H1	19	1.3	2.3	1.6	91.0	5.6	20.0
H2	19	5.9	3.2	2.1	64.0	2.8	64.0
H3	19	1.3	2.4	435.6	7.0	23.1	6.9
H4	19	1.3	5.3	23.3	9.5	586.8	6.2
H5	19	4.4	2.5	351.7	6.3	192.2	4.8
PK	5	5.9	1.1	2.5	24.0		
CPK	5	6.1	0.9	1.4	34.0		
GPK	5	6.1	0.8	3.2	12.0		
TPK	5	6.1	1.2	2.2	58.0		
SPK	5	6.1	1.7	2.4	30.0		
RPK	5	6.0	1.5	2.9	26.0		
MPK	5	6.0	1.9	2.9	16.0		
PL	5	1.8	2.5	261.9	16.0		
CPL	5	1.8	0.6	261.9	9.0		
GPL	5	1.9	3.3	255.1	8.0		
TPL	5	1.8	6.8	246.6	7.0		
SPL	5	1.9	1.1	235.6	8.0		
RPL	5	1.8	1.4	242.4	5.0		
MPL	5	1.9	1.5	250.8	6.0		
PH	5	1.8	1.1	1088.0	3.5		
CPH	5	1.8	1.1	1114.0	2.1		

[a]N = the number of samples analyzed; M = the mean value of N samples; 2S = twice the coefficient of variation for N samples.

Table 5-2. Summary of Results of Laboratory Chemical Analysis of Construction Samples from the Pads[a] (continued)

Pad	N	Potassium		Uranium		Thorium	
		M (wt-%)	2S (%)	M (wt-ppm)	2S (%)	M (wt-ppm)	2S (%)
GPL	5	1.8	0.8	1096.0	3.7		
TPH	5	1.8	2.0	1122.0	4.3		
SPH	5	1.8	2.3	1103.0	3.9		
RPH	5	1.9	1.6	1112.0	4.0		
MPH	5	1.9	1.2	1154.0	1.8		
PT	5	1.8	2.4	21.3	22.0		
CPT	5	1.9	3.1	19.7	11.0		
GPT	5	1.8	6.0	19.2	9.0		
TPT	5	1.8	1.6	19.8	20.0		
SPT	5	1.8	1.0	18.1	15.0		
RPT	5	1.8	2.4	19.3	11.0		
MPT	5	1.9	1.3	19.2	12.0		
NPL	5	1.3	3.0	41.1	13.0		
PPL	5	1.3	1.4	55.3	6.6		
NPH	5	1.3	2.3	146.9	2.2		
PPH	5	1.2	2.6	139.3	7.3		
xPB	35	<0.01		1.0	24.0		

[a]N = the number of samples analyzed; M = the mean value of N samples; 2S = twice the coefficient of variation for N samples.

6.0 DATA ANALYSIS FOR PARAMETER ASSIGNMENT

6.1 METHOD

6.1.1 Best-Fit Procedure

As described thus far, two data sets were generated for purposes of parameter assignment, one comprising corrected count rates and the other, laboratory assays. The next step involved determining a best-fit regression for these data sets, the results of which would be used to estimate actual concentrations for each pad.

Selection of the methods for making the best-fit regression and best estimates of radioelement concentrations is somewhat arbitrary. The typical approach when performing instrument calibration is to designate the properties of the calibration

standard (e.g., radioelement concentrations) as the independent variables and the responses of the measurement system (e.g., count rates) as the dependent variables. For purposes of this study, the opposite approach was taken--corrected count rate is the abscissa (usually 'independent') variable and laboratory assay is the ordinate (usually 'dependent') variable.

It was assumed that corrections, especially background subtractions, were performed properly, such that a pad having zero activity would yield a corrected count rate of zero. As a consequence, the best-fit regression was constrained to pass through the origin. Furthermore, the minimization procedure used was based on the sum of the squared fractional residuals, rather than the more commonly used linear-least-squares fit which minimizes the sum of the squared absolute residuals. Finally, the best estimate of radioelement concentration was determined to be the point on the regression line that is nearest, in perpendicular distance, to the measured data point, and also consistent with counting statistics in the corrected count rates.

Stated mathematically, the foregoing is equivalent to assuming that the radiometric concentration, G_i, of radioelement i (i corresponds to K, Ra, and Th) is related to the corrected count rate, $R_c(E_i)$, at energy E_i by

$$G_i = k_i R_c(E_i) \qquad (6\text{-}1)$$

where the slope, k_i, is the system sensitivity factor for radioelement i (concentration/cps). This factor was determined by minimizing the sum of the squares of the relative errors in the concentrations, S_i, with respect to k_i, using the equation

$$S_i = \sum_{j=1}^{N} [C_j(i) - k_i R_{cj}(E_i)]^2 / [k_i R_{cj}(E_i)]^2 \qquad (6\text{-}2)$$

where $C_j(i)$ is the laboratory assay for radioelement i in pad j, $R_{cj}(E_i)$ is the corrected count rate for energy E_i from pad j, and N is the number of pads used to determine the fit. Justification for this approach is discussed in George (1982) and George and others (1983).

In determining the best fit for each radioelement, only those data points corresponding to pads enriched in that particular radioelement were used; this approach avoided excessive weighting of the fit by the low-concentration points, since the fit was already being forced through the origin. Also, laboratory-assay

values were not reported for several of the low-concentration points.

Uncertainties in the sensitivity factors were calculated from the equation

$$\sigma^2(k_i) = \sum_{j=1}^{N} [\partial k_i / \partial R_{cj}(E_i)]^2 \sigma^2[R_{cj}(E_i)] \qquad (6\text{-}3)$$

Having thus determined the slope of the best-fit line through the data points, an attempt was made to reconcile, as much as possible, the values of the 'fitted' concentrations, $k_i R_c(E_i)$, with the laboratory assays, C(i). To accomplish this reconciliation, 'adjusted' count rates, $R_a(E_i)$, were determined in the following manner. The point on the best-fit line closest to each data point was calculated using the equation

$$R_a(E_i) = \frac{C(i) + k_i R_c(E_i)}{2k_i} \qquad (6\text{-}4)$$

If $|R_c(E_i) - R_a(E_i)| \leq 2\sigma[R_c(E_i)]$, then the adjusted count rate was taken to be R_a as just calculated, and the concentration assigned to this measurement was determined from the equation

$$G_i = k_i R_a(E_i) \qquad (6\text{-}5)$$

On the other hand, if $|R_c(E_i) - R_a(E_i)| > 2\sigma[R_c(E_i)]$, then the adjusted count rate was taken to be

$$R_a(E_i) = R_c(E_i) - 2\sigma[R_c(E_i)]\,\mathrm{sgn}[R_c(E_i) - R_a(E_i)] \qquad (6\text{-}6)$$

where $\mathrm{sgn}(x) = +1$ if $x \geq 0$, and $\mathrm{sgn}(x) = -1$ if $x < 0$. The assigned concentration was still determined using equation (6-5). The uncertainty in $R_a(E_i)$ was assumed to be the same as that in $R_c(E_i)$ because, from a statistical standpoint, a repeated measurement of the pad could easily yield a corrected count rate equal to $R_a(E_i)$, but the computed uncertainty would still be approximately equal to $\sigma[R_c(E_i)]$. By adjusting the data in this manner, the derived concentrations are both statistically consistent with the (presumed repeatable) in-situ measurements (within a 95 percent confidence interval) and more in agreement with the standard-traceable laboratory assays. In those cases where laboratory assays were not reported, the assigned concentrations were determined from equation (6-1), i.e., $R_a(E_i) = R_c(E_i)$ and $G_i = k_i R_c(E_i)$.

6.1.2 Analysis for Uncertainty

The uncertainties in the assigned concentrations, as determined from equation (6-5), were computed using the equation

$$\sigma(G_i) = \left\{ R_a^2(E_i)\sigma^2(k_i) + k_i^2\sigma^2[R_a(E_i)] \right\}^{1/2} \qquad (6\text{-}7)$$

where the parameters are defined in Section 6.1.1. We acknowledge that equation (6-7) is not rigorously correct, since the system sensitivity factors, k_i, and the 'adjusted' count rates, $R_a(E_i)$, are functions of the corrected count rates, $R_c(E_i)$. The quantities k_i and $R_a(E_i)$ are therefore not independent, and equation (6-7) neglects this correlation. However, due to the fact that the fractional differences between the laboratory assays and the fitted concentrations were minimized in the determination of k_i, each point influences the fit to the same extent as every other point. Furthermore, because the number of points used to determine k_i (11, 35, and 10 for k_K, k_{Ra}, and k_{Th}, respectively) is fairly large, a small change in one of the corrected count rates would have a negligible effect on the computed value of k. Consequently, the covariance term ignored in equation (6-7) is small. Moreover, since an increase in one of the corrected count rates would tend to decrease the calculated value of k for a given laboratory-assay value, the sign of this covariance term would be negative. Equation (6-7) therefore represents an upper limit on the propagated uncertainty in the computed concentrations, resulting from uncertainties associated with each of the factors involved. Calculation of each of these component uncertainties was detailed throughout Section 4.

6.2 RESULTS

Values for the system sensitivity factors, k_i, determined from the line-fitting process, are presented below:

$$k_K = 25.245 \pm 0.119 \text{ pCi(K-40)/g-cps}$$

$$k_{Ra} = 18.604 \pm 0.324 \text{ pCi(eRa-226)/g-cps}$$

$$k_{Th} = 8.843 \pm 0.037 \text{ pCi(eTh-232)/g-cps}$$

Plots of C(i) versus $R_c(E_i)$, together with the best-fit lines, are provided in Figures 6-1 through 6-3. The values of $R_c(E_i)$ and $R_a(E_i)$ are presented in Table 6-1. Table 6-2 lists the resulting concentrations and their uncertainties, together with the laboratory assays for purposes of comparison. Examination of the data in Table 6-2 reveals that the radiometric concentrations

computed from the slope of the best-fit line through the data points, using the 'adjusted' count rates (count rates statistically consistent with the 'corrected' count rates), are in good agreement with the laboratory-assay results, in most cases.

6.3 DISCUSSION

For all of the pads, the K-40 concentrations determined using the in-situ data are within two standard deviations of the laboratory-assay concentrations (i.e., overlapping 'error bars'), and, in most cases, have precisions as great as, or greater than, the laboratory precision. With respect to the radium concentrations, the agreement is also within two standard deviations in most cases. However, as described in Section 4.3.2, the relatively large uncertainties in the concentrations inferred from the in-situ measurements are apparent, due to the relatively large uncertainties in the radon-exhalation factor, F_e. The laboratory assays do not suffer from this problem, since those samples were stored in sealed cans and given sufficient time prior to analysis to permit establishment of Bi-214/Ra-226 equilibrium. However, large sampling variances in the laboratory assays are apparent in many cases (e.g., E1, H1, H2, W1, W4, and the xPT pads). Some disparity between the laboratory assays and the in-situ results is also evident in the Th-232 data; however, due to the relatively large uncertainties in the laboratory values, the 'error bars' again overlap in most cases.

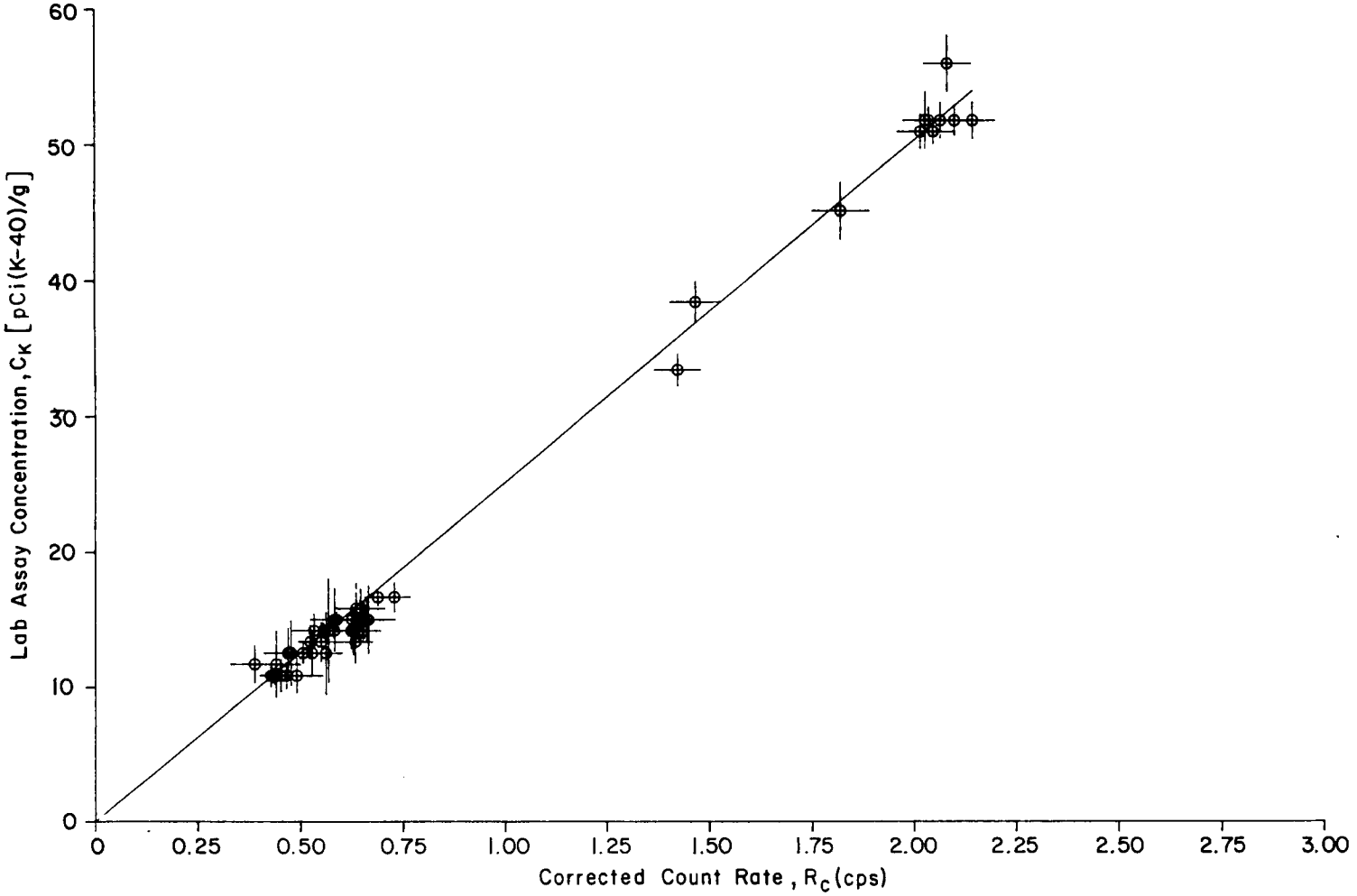

Figure 6-1. Regression of Corrected Count Rate Versus Laboratory Assay Concentration for Potassium

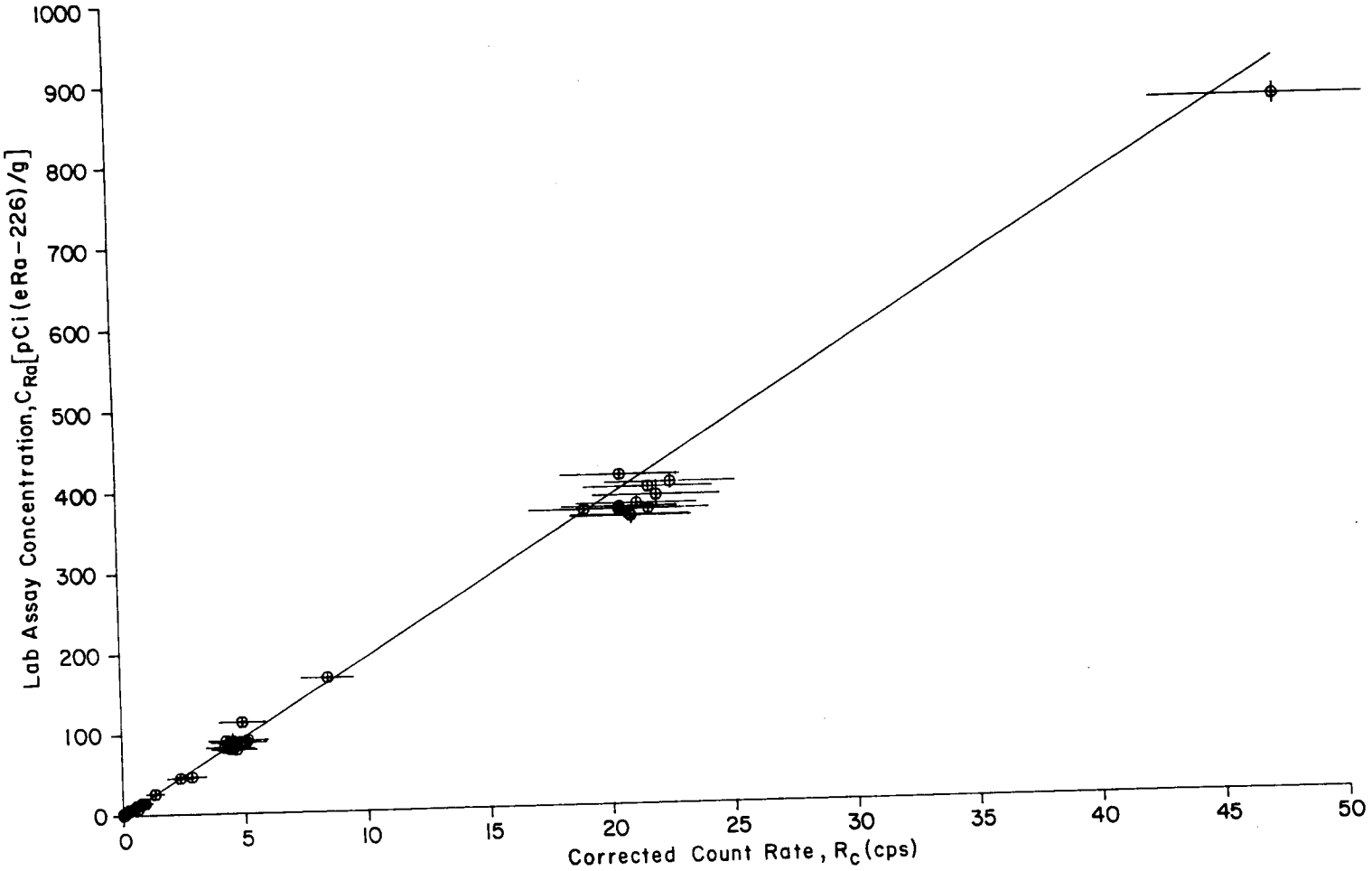

Figure 6-2. Regression of Corrected Count Rate Versus Laboratory Assay Concentration for Radium

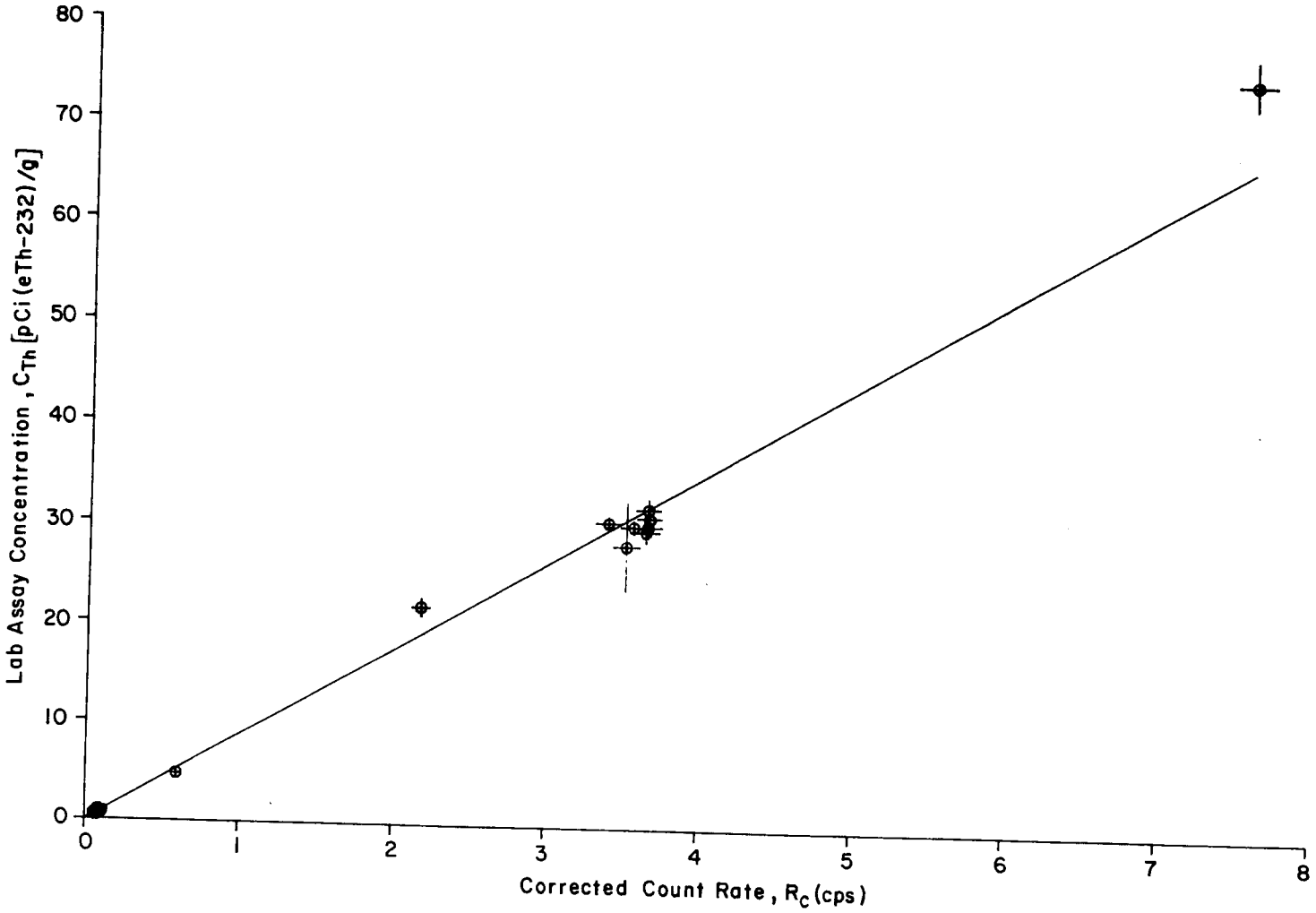

Figure 6-3. Regression of Corrected Count Rate Versus Laboratory Assay Concentration for Thorium

Table 6-1. Comparison of Corrected In-Situ Count Rates with 'Adjusted' Count Rates

Pad	Count Rate (cps)[a]					
	R_c(1461)	R_a(1461)	R_c(1765)	R_a(1765)	R_c(2615)	R_a(2615)
E1	0.523 ± 0.014	0.527 ± 0.014	1.327 ± 0.178	1.355 ± 0.178	0.084 ± 0.005	0.076 ± 0.005
E2	0.532 ± 0.019	0.548 ± 0.019	4.203 ± 0.372	4.318 ± 0.372	0.079 ± 0.005	0.089 ± 0.005
E4	0.441 ± 0.029	0.453 ± 0.029	20.527 ± 1.205	21.277 ± 1.205	0.067 ± 0.006	0.074 ± 0.006
E5	0.567 ± 0.043	0.565 ± 0.043	47.456 ± 2.496	46.841 ± 2.496	0.073 ± 0.006	0.085 ± 0.006
H1	0.436 ± 0.012	0.434 ± 0.012	0.042 ± 0.024	0.045 ± 0.024	0.072 ± 0.005	0.076 ± 0.005
H2	2.081 ± 0.029	2.139 ± 0.029	0.040 ± 0.024	0.036 ± 0.024	0.009 ± 0.003	0.009 ± 0.003
H3	0.465 ± 0.017	0.448 ± 0.017	8.422 ± 0.527	8.699 ± 0.527	0.083 ± 0.004	0.075 ± 0.004
H4	0.388 ± 0.029	0.426 ± 0.029	0.571 ± 0.107	0.593 ± 0.107	7.554 ± 0.062	7.678 ± 0.062
H5	1.465 ± 0.031	1.495 ± 0.031	4.918 ± 0.458	5.515 ± 0.458	2.155 ± 0.029	2.213 ± 0.029
PK	2.014 ± 0.028	2.018 ± 0.028	0.033 ± 0.021	0.062 ± 0.021	0.005 ± 0.003	0.005 ± 0.003
PL	0.653 ± 0.020	0.625 ± 0.020	4.427 ± 0.372	4.607 ± 0.372	0.071 ± 0.005	0.073 ± 0.005
PH	0.655 ± 0.031	0.626 ± 0.031	20.970 ± 1.215	20.122 ± 1.215	0.069 ± 0.005	0.068 ± 0.005
PT	0.633 ± 0.021	0.591 ± 0.021	0.354 ± 0.082	0.356 ± 0.082	3.629 ± 0.046	3.537 ± 0.046
W1	0.506 ± 0.014	0.502 ± 0.014	0.052 ± 0.027	0.044 ± 0.027	0.076 ± 0.005	0.076 ± 0.005
W2	1.820 ± 0.035	1.805 ± 0.035	0.110 ± 0.041	0.103 ± 0.041	0.101 ± 0.006	0.099 ± 0.006
W3	0.689 ± 0.016	0.676 ± 0.016	0.093 ± 0.037	0.091 ± 0.037	0.576 ± 0.014	0.556 ± 0.014
W4	0.728 ± 0.019	0.696 ± 0.019	0.645 ± 0.151	0.649 ± 0.151	0.118 ± 0.007	0.118 ± 0.007
W5	1.421 ± 0.028	1.374 ± 0.028	0.470 ± 0.094	0.449 ± 0.094	0.216 ± 0.009	0.216 ± 0.009
NPL	0.434 ± 0.014	0.433 ± 0.014	0.911 ± 0.142	0.851 ± 0.142	0.066 ± 0.005	0.073 ± 0.005
NPH	0.451 ± 0.016	0.441 ± 0.016	2.355 ± 0.258	2.376 ± 0.258	0.078 ± 0.005	0.082 ± 0.005
PPL	0.428 ± 0.013	0.430 ± 0.013	0.807 ± 0.121	0.811 ± 0.121	0.071 ± 0.005	0.070 ± 0.005
PPH	0.438 ± 0.017	0.435 ± 0.017	2.834 ± 0.286	2.652 ± 0.286	0.075 ± 0.005	0.071 ± 0.005
GE2	0.527 ± 0.020	0.512 ± 0.020	4.560 ± 0.407	4.468 ± 0.407	0.076 ± 0.005	0.079 ± 0.005
GE4	0.469 ± 0.029	0.483 ± 0.029	22.009 ± 1.283	21.321 ± 1.283	0.078 ± 0.006	0.090 ± 0.006
GPK	2.026 ± 0.027	2.041 ± 0.027	0.031 ± 0.022	0.031 ± 0.022	0.001 ± 0.003	0.001 ± 0.003
GPL	0.637 ± 0.020	0.617 ± 0.020	4.667 ± 0.376	4.718 ± 0.376	0.056 ± 0.005	0.059 ± 0.005
GPH	0.665 ± 0.032	0.631 ± 0.032	20.498 ± 1.161	20.197 ± 1.161	0.067 ± 0.005	0.069 ± 0.005
GPT	0.587 ± 0.020	0.592 ± 0.020	0.365 ± 0.084	0.353 ± 0.084	3.504 ± 0.043	3.418 ± 0.043

[a]Uncertainties are one sigma (68 percent confidence interval).

Table 6-1. Comparison of Corrected In-Situ Count Rates with 'Adjusted' Count Rates (continued)

Pad	Count Rate (cps)[a]					
	R_c(1461)	R_a(1461)	R_c(1765)	R_a(1765)	R_c(2615)	R_a(2615)
TE2	0.546 ± 0.019	0.522 ± 0.019	4.691 ± 0.398	4.490 ± 0.398	0.075 ± 0.005	0.075 ± 0.005
TE4	0.475 ± 0.031	0.453 ± 0.031	21.675 ± 1.301	21.433 ± 1.301	0.058 ± 0.005	0.058 ± 0.005
TPK	2.128 ± 0.027	2.092 ± 0.027	0.037 ± 0.023	0.037 ± 0.023	0.000 ± 0.003	0.000 ± 0.003
TPL	0.630 ± 0.020	0.613 ± 0.020	4.525 ± 0.386	4.678 ± 0.386	0.058 ± 0.005	0.064 ± 0.005
TPH	0.613 ± 0.028	0.588 ± 0.028	21.677 ± 1.225	20.714 ± 1.225	0.058 ± 0.005	0.051 ± 0.005
TPT	0.627 ± 0.021	0.595 ± 0.021	0.332 ± 0.079	0.320 ± 0.079	3.617 ± 0.044	3.529 ± 0.044
MPK	2.099 ± 0.027	2.078 ± 0.027	0.012 ± 0.015	0.012 ± 0.015	0.002 ± 0.003	0.002 ± 0.003
MPL	0.661 ± 0.020	0.629 ± 0.020	4.871 ± 0.378	4.831 ± 0.378	0.064 ± 0.005	0.063 ± 0.005
MPH	0.646 ± 0.029	0.638 ± 0.029	21.206 ± 1.213	20.653 ± 1.213	0.057 ± 0.005	0.057 ± 0.005
MPT	0.653 ± 0.021	0.625 ± 0.021	0.372 ± 0.084	0.377 ± 0.084	3.628 ± 0.040	3.622 ± 0.040
RPK	2.064 ± 0.030	2.060 ± 0.030	0.037 ± 0.023	0.037 ± 0.023	0.004 ± 0.003	0.004 ± 0.003
RPL	0.647 ± 0.020	0.639 ± 0.020	4.264 ± 0.361	4.570 ± 0.361	0.063 ± 0.005	0.070 ± 0.005
RPH	0.652 ± 0.030	0.624 ± 0.030	20.465 ± 1.186	20.101 ± 1.186	0.065 ± 0.005	0.060 ± 0.005
RPT	0.652 ± 0.021	0.610 ± 0.021	0.353 ± 0.081	0.344 ± 0.081	3.630 ± 0.039	3.573 ± 0.039
SPK	2.035 ± 0.027	2.046 ± 0.027	0.031 ± 0.021	0.031 ± 0.021	0.001 ± 0.003	0.001 ± 0.003
SPL	0.635 ± 0.020	0.633 ± 0.020	5.146 ± 0.403	5.035 ± 0.403	0.063 ± 0.005	0.067 ± 0.005
SPH	0.582 ± 0.029	0.589 ± 0.029	20.904 ± 1.203	20.118 ± 1.203	0.058 ± 0.005	0.065 ± 0.005
SPT	0.581 ± 0.020	0.572 ± 0.020	0.384 ± 0.085	0.359 ± 0.085	3.550 ± 0.041	3.483 ± 0.041
CE2	0.549 ± 0.019	0.540 ± 0.019	4.441 ± 0.380	4.378 ± 0.380	0.082 ± 0.006	0.089 ± 0.006
CE4	0.476 ± 0.031	0.487 ± 0.031	22.580 ± 1.313	22.034 ± 1.313	0.065 ± 0.005	0.074 ± 0.005
CPK	2.046 ± 0.027	2.034 ± 0.027	0.041 ± 0.024	0.041 ± 0.024	0.004 ± 0.003	0.004 ± 0.003
CPL	0.626 ± 0.020	0.611 ± 0.020	5.084 ± 0.399	4.933 ± 0.399	0.063 ± 0.005	0.061 ± 0.005
CPH	0.624 ± 0.031	0.594 ± 0.031	19.060 ± 1.128	19.385 ± 1.128	0.060 ± 0.005	0.062 ± 0.005
CPT	0.556 ± 0.020	0.560 ± 0.020	0.332 ± 0.078	0.327 ± 0.078	3.368 ± 0.042	3.413 ± 0.042

[a]Uncertainties are one sigma (68 percent confidence interval).

Table 6-2. Comparison of Laboratory Assays with 'Best-Fit' Concentrations[a]

Pad	Concentration (pCi/g)[b]					
	C_K	G_K	C_{Ra}	G_{Ra}	C_{Th}	G_{Th}
E1	13.4 ± 1.2	13.3 ± 0.7	25.7 ± 4.3	25.2 ± 6.7	0.6 ± 0.3	0.7 ± 0.1
E2	14.2 ± 1.2	13.8 ± 1.0	82.5 ± 2.2	80.3 ± 14.1	1.0 ± 0.2	0.8 ± 0.1
E4	11.7 ± 2.5	11.4 ± 1.5	409.8 ± 4.5	395.8 ± 46.9	0.7 ± 0.1	0.7 ± 0.1
E5	14.2 ± 3.8	14.3 ± 2.2	860.0 ± 12.9	871.5 ± 97.7	1.0 ± 0.1	0.8 ± 0.1
H1	10.9 ± 0.5	11.0 ± 0.6	0.9 ± 0.2	0.8 ± 0.9	0.7 ± 0.1	0.7 ± 0.1
H2	56.1 ± 2.1	54.0 ± 1.6	0.6 ± 0.2	0.7 ± 0.9	c	0.1 ± 0.1
H3	10.9 ± 1.0	11.3 ± 0.9	167.0 ± 5.7	161.8 ± 20.4	0.6 ± 0.1	0.7 ± 0.1
H4	11.7 ± 1.4	10.8 ± 1.5	11.5 ± 0.6	11.0 ± 4.0	75.3 ± 2.4	67.9 ± 1.2
H5	38.5 ± 1.5	37.8 ± 1.6	113.7 ± 3.9	102.6 ± 17.4	21.8 ± 0.9	19.6 ± 0.5
PK	51.1 ± 1.3	51.0 ± 1.5	1.7 ± 0.2	1.2 ± 0.8	c	0.0 ± 0.1
PL	15.1 ± 0.8	15.8 ± 1.0	89.1 ± 1.2	85.7 ± 14.2	0.7 ± 0.1	0.6 ± 0.1
PH	15.1 ± 1.4	15.8 ± 1.6	358.6 ± 10.0	374.4 ± 47.1	0.6 ± 0.1	0.6 ± 0.1
PT	13.4 ± 1.6	14.9 ± 1.1	6.7 ± 1.1	6.6 ± 3.1	30.2 ± 0.8	31.3 ± 0.9
W1	12.6 ± 0.7	12.7 ± 0.7	0.7 ± 0.2	0.8 ± 1.0	c	0.7 ± 0.1
W2	45.2 ± 2.1	45.6 ± 1.8	1.8 ± 0.2	1.9 ± 1.5	0.9 ± 0.2	0.9 ± 0.1
W3	16.7 ± 0.6	17.1 ± 0.8	1.7 ± 0.3	1.7 ± 1.4	4.7 ± 0.4	4.9 ± 0.3
W4	16.7 ± 1.1	17.6 ± 1.0	12.2 ± 2.0	12.1 ± 5.6	c	1.0 ± 0.1
W5	33.5 ± 1.2	34.7 ± 1.5	8.0 ± 1.1	8.4 ± 3.5	c	1.9 ± 0.2
NPL	10.9 ± 0.5	10.9 ± 0.7	14.7 ± 0.5	15.8 ± 5.3	0.7 ± 0.1	0.6 ± 0.1
NPH	10.9 ± 1.2	11.1 ± 0.8	44.6 ± 3.2	44.2 ± 9.7	0.8 ± 0.1	0.7 ± 0.1
PPL	10.9 ± 0.8	10.8 ± 0.7	15.2 ± 1.4	15.1 ± 5.5	0.6 ± 0.3	0.6 ± 0.1
PPH	10.9 ± 0.6	11.0 ± 0.9	46.0 ± 2.1	49.3 ± 10.8	0.6 ± 0.1	0.6 ± 0.1
GE2	12.6 ± 1.7	12.9 ± 1.0	81.4 ± 4.0	83.1 ± 15.4	0.7 ± 0.1	0.7 ± 0.1
GE4	12.6 ± 1.8	12.2 ± 1.5	383.9 ± 17.3	396.7 ± 49.7	0.9 ± 0.1	0.8 ± 0.1
GPK	51.9 ± 2.1	51.5 ± 1.5	c	0.6 ± 0.8	c	0.0 ± 0.1
GPL	15.1 ± 1.4	15.6 ± 1.0	88.7 ± 3.0	87.8 ± 14.3	0.6 ± 0.1	0.5 ± 0.1
GPH	15.1 ± 2.5	15.9 ± 1.6	370.1 ± 4.4	375.7 ± 45.1	0.6 ± 0.1	0.6 ± 0.1
GPT	15.1 ± 0.9	14.9 ± 1.0	6.3 ± 0.7	6.6 ± 3.1	28.3 ± 4.4	30.2 ± 0.8
TE2	12.6 ± 3.1	13.2 ± 1.0	79.8 ± 2.2	83.5 ± 15.1	c	0.7 ± 0.1
TE4	10.9 ± 1.3	11.4 ± 1.6	394.2 ± 6.7	398.7 ± 50.4	c	0.5 ± 0.1
TPK	51.9 ± 1.4	52.8 ± 1.5	c	0.7 ± 0.9	c	0.0 ± 0.1
TPL	15.1 ± 1.5	15.5 ± 1.0	89.9 ± 9.3	87.0 ± 14.7	0.6 ± 0.1	0.6 ± 0.1
TPH	14.2 ± 1.8	14.9 ± 1.4	367.4 ± 6.6	385.4 ± 47.5	0.4 ± 0.1	0.5 ± 0.1
TPT	14.2 ± 0.7	15.0 ± 1.1	5.7 ± 0.8	6.0 ± 3.0	29.7 ± 1.0	31.2 ± 0.8
MPK	51.9 ± 1.1	52.5 ± 1.5	c	0.2 ± 0.6	c	0.0 ± 0.1
MPL	15.1 ± 1.7	15.9 ± 1.0	89.1 ± 1.8	89.9 ± 14.4	0.6 ± 0.1	0.6 ± 0.1
MPH	15.9 ± 1.4	16.1 ± 1.5	373.9 ± 7.5	384.2 ± 47.1	c	0.5 ± 0.1
MPT	15.1 ± 1.2	15.8 ± 1.1	7.1 ± 0.7	7.0 ± 3.1	32.0 ± 1.0	32.0 ± 0.8
RPK	51.9 ± 1.3	52.0 ± 1.6	c	0.7 ± 0.9	c	0.0 ± 0.1
RPL	15.9 ± 0.8	16.1 ± 1.0	90.7 ± 1.9	85.0 ± 7.8	0.7 ± 0.1	0.6 ± 0.1
RPH	15.1 ± 1.4	15.8 ± 1.5	367.2 ± 4.0	374.0 ± 46.0	0.5 ± 0.1	0.5 ± 0.1
RPT	14.2 ± 0.9	15.4 ± 1.1	6.2 ± 0.6	6.4 ± 3.0	31.1 ± 1.0	31.6 ± 0.7
SPK	51.9 ± 0.9	51.6 ± 1.5	c	0.6 ± 0.8	c	0.0 ± 0.1
SPL	15.9 ± 1.8	16.0 ± 1.0	91.6 ± 1.7	93.7 ± 15.4	0.6 ± 0.1	0.6 ± 0.1

[a] C = laboratory assay; G = best-fit concentration.
[b] Uncertainties are two sigmas (95 percent confidence interval).
[c] Below detection limit.

Table 6-2. Comparison of Laboratory Assays with 'Best-Fit' Concentrations[a] (continued)

Pad	Concentration (pCi/g)[b]					
	C_K	G_K	C_{Ra}	G_{Ra}	C_{Th}	G_{Th}
SPH	15.1 ± 2.3	14.9 ± 1.5	359.7 ± 4.3	374.3 ± 46.6	0.6 ± 0.1	0.6 ± 0.1
SPT	14.2 ± 0.5	14.5 ± 1.0	6.2 ± 1.0	6.7 ± 3.2	30.2 ± 0.7	30.8 ± 0.8
CE2	13.4 ± 1.5	13.6 ± 1.0	80.3 ± 3.7	81.5 ± 14.4	0.9 ± 0.1	0.8 ± 0.1
CE4	12.6 ± 2.4	12.3 ± 1.6	399.8 ± 8.4	409.9 ± 50.9	0.7 ± 0.1	0.7 ± 0.1
CPK	51.1 ± 0.9	51.4 ± 1.5	[c]	0.8 ± 0.9	[c]	0.0 ± 0.1
CPL	15.1 ± 1.0	15.4 ± 1.0	89.0 ± 3.3	91.8 ± 15.2	0.5 ± 0.1	0.5 ± 0.1
CPH	14.2 ± 1.3	15.0 ± 1.6	366.7 ± 6.2	360.6 ± 43.8	0.6 ± 0.1	0.6 ± 0.1
CPT	14.2 ± 0.5	14.1 ± 1.0	6.0 ± 0.4	6.1 ± 2.9	30.6 ± 0.6	30.2 ± 0.8

[a] C = laboratory assay; G = best-fit concentration.
[b] Uncertainties are two sigmas (95 percent confidence interval).
[c] Below detection limit.

7.0 MEASUREMENTS FOR PARAMETER VERIFICATION

7.1 EQUIPMENT CONFIGURATION AND PERFORMANCE

7.1.1 Configuration

The Calibration Facilities Monitoring System (CFMS), mentioned in Section 2.3.1, was specially designed for use in characterizing and monitoring both surface and subsurface calibration models. Figure 7-1 is a block diagram showing the configuration of the system as it was used in this study. Pulses from a specially constructed pad-monitoring detector are transmitted over a few hundred feet of four-conductor armored logging cable to an ORTEC 450 Research Amplifier. Amplified and shaped pulses are then fed into a Nuclear Data, ND660, Multichannel Analyzer (MCA) controlled by an LSI-11 microprocessor; several standard peripherals are interfaced to the microprocessor. Selected hardware characteristics, physical characteristics, and settings for the system are presented in Table 7-1. The system is more fully described in George and others (1983).

The NaI(Tl) detector, 4 inches in diameter by 4 inches in height, is lightly shielded with a graded filter and integrally coupled to a photomultiplier tube (see Figure 7-2). Measurements were made using a collimator, depicted in cutaway view in Figure 7-2 and described in Table 7-1.

For purposes of this study, the system collected data in a repetitive mode wherein the microprocessor controlled the MCA, on-line data processing and reduction, and data storage. A typical measurement sequence for a given pad involved collection of approximately ten spectra, each for 200 to 500 seconds of live time. After collecting each spectrum, the microprocessor calculated the position of a preselected peak, recalculated channel number versus energy calibration coefficients to compensate for gain drift, integrated the count rates for certain regions of interest (ROI) as specified in Table 7-2, and stored on disk the complete spectrum as well as the calculated results for the ROIs.

Performance of the system was routinely monitored, using button sources placed in a repeatable geometry with respect to the detector. The sources were positioned in a jig which slipped under the detector, and which was equipped with a 1/2-inch-thick sheet of lead to shield the detector from below (see Figure 7-2). For the performance measurements, the detector and its collimating shield were placed on the deck of the CFMS truck, away from any pad.

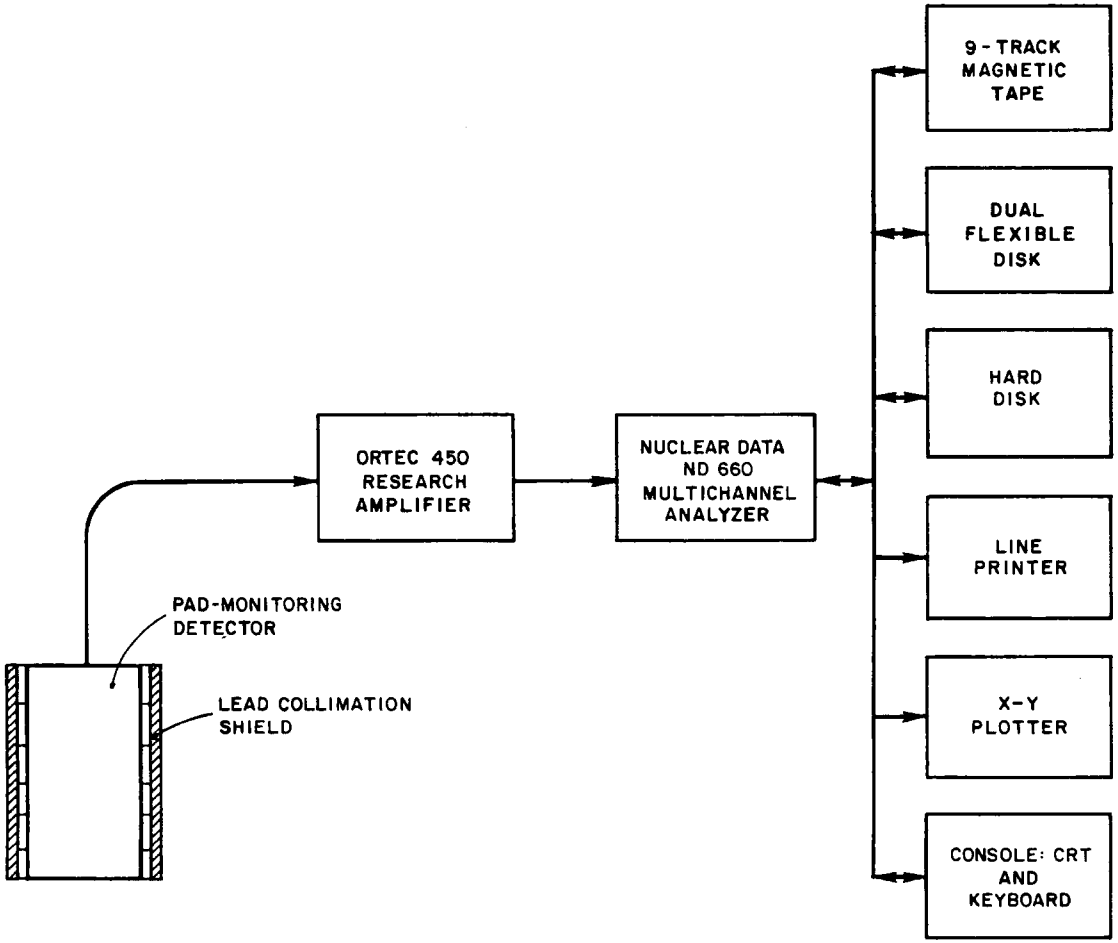

Figure 7-1. Block Diagram of CFMS Pad-Monitoring Detector System

Table 7-1. Selected Hardware, Physical Characteristics, and Instrument Settings for the CFMS Pad-Monitoring Detector System

Component/Parameter	Description
ORTEC 450 Research Amplifier	
Gain	10 (approx.)
Baseline Restoration	High
Pulse Shaping - Integrate	0.5 Microsecond
Pulse Shaping - Differentiate	Out
Input Mode	Bipolar, Norm. Negative
Output Connection	Unipolar, 10-Volt Positive
Output Pulse Shape	Unipolar (4.8 microseconds)
ND660 Multichannel Analyzer	
Pulse Coupling	DC
Conversion Gain	512
Number of Channels	512
Acquire Mode	Live Time
Detector	
Size	4 Inches x 4 Inches
Type	NaI(Tl)
Shell Diameter (O.D.)	8 Inches
Shell Thickness	0.08 Inch (stainless)
Graded Filter	0.125-Inch Lead, Over 0.063-Inch Cadmium, Over 0.031-Inch Copper (around sides and bottom)
Collimating Shield	2 Inches of Lead on Sides, 16 Inches in Height (no shield on top)
Detector Position Above Pad	5 Centimeters from Surface

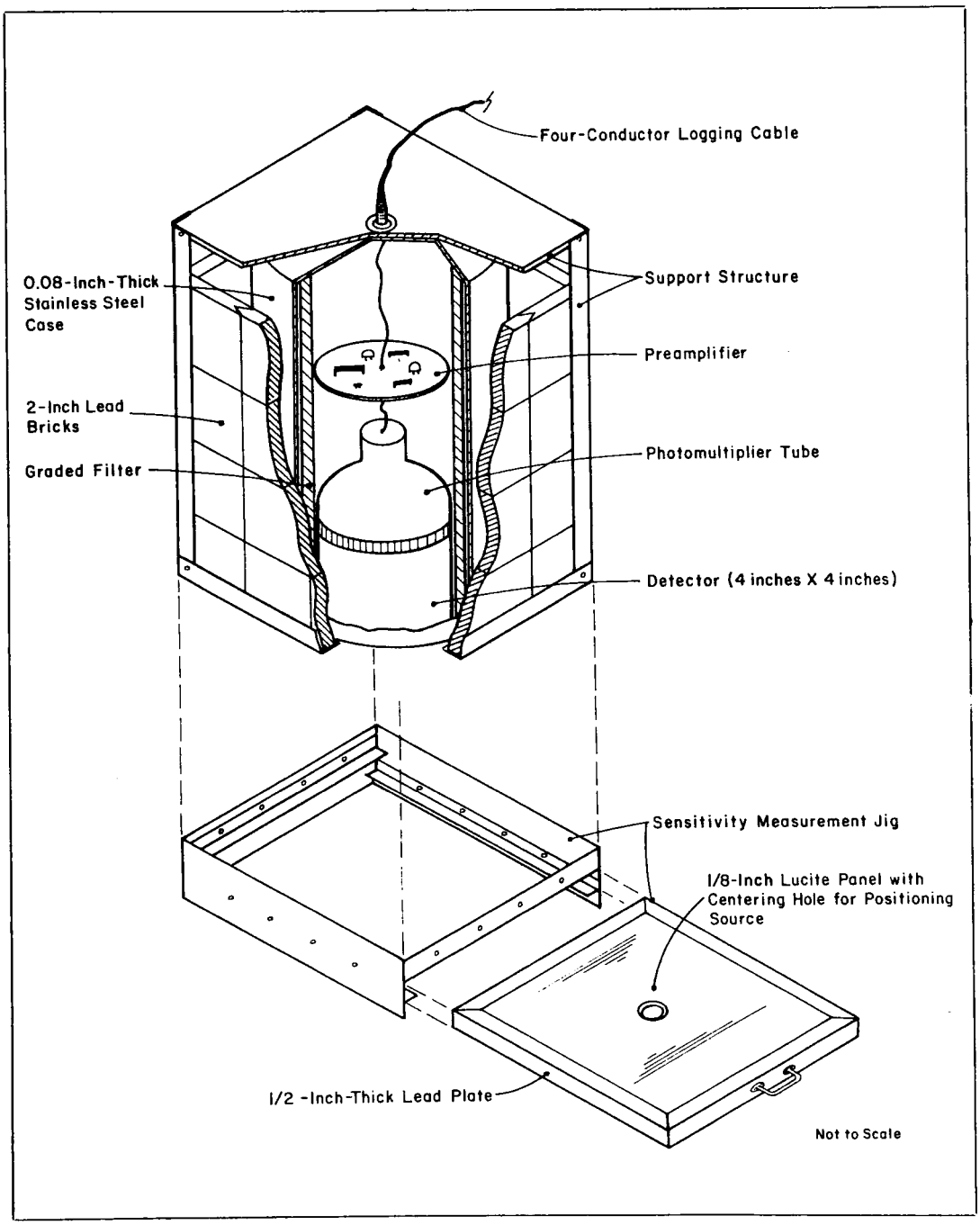

Figure 7-2. Sketch of Detector Shielding and Assembly

Table 7-2. Spectral Regions of Interest

Parameter	Principal Photopeak Energy (keV)	Region of Interest (keV)
K-40	1461	1320 - 1575
Ra-226	1765, 2204	1650 - 2390
Th-232	2615	2475 - 2765
Total Count	--	30 - 3500
High Energy	--	550 - 3500

7.1.2 Performance

Prior to initiating measurements on the pads, tests were conducted to define and document performance of the CFMS hardware. Certain tests were performed frequently during the course of the measurements to monitor dead time, linearity, resolution, and sensitivity, the last three checked using three specific sources, namely, Ra-226, Cs-137, and Th-228.

For purposes of this study, linearity refers to the relation of energy to channel number, i.e., the integral linearity of the analog-to-digital converter in the multichannel analyzer. A quadratic fit was calculated using eight photopeaks (Ra-226 - 609, 1120, 1765, and 2204 keV; Th-228 - 239, 583, and 2615 keV; Cs-137 - 661 keV). Coefficients for the quadratic equation relating channel number to gamma-ray energy were calculated and recorded routinely. Although a quadratic fit was used, the system was linear in the sense that a typical NaI/photomultiplier-based system is linear, i.e., the amplifier output pulse height is proportional to the energy of the incident gamma ray. The defining equation has the form

$$E = A_0 + A_1 C + A_2 C^2 \qquad (7\text{-}1)$$

where E is the gamma-ray energy in keV, C is the channel number in the MCA, and A_0, A_1, and A_2 are constants. Typical values for the coefficients are -26.65 for A_0, 6.623 for A_1, and 1.864×10^{-4} for A_2.

Resolution was measured routinely (approximately daily) by determining the full width at half maximum (FWHM) of the 661-keV peak of cesium-137. Results of these measurements are listed in Table 7-3 and graphically illustrated in Figure 7-3. The abscissa of

the curve in Figure 7-3 is a simple sequence number for each resolution measurement made. The data demonstrate that the detector system functioned properly during the course of the measurements.

As used herein, sensitivity refers to the observed total count rate, corrected for ambient background, due to a specific Ra-226 button source. Sensitivity checks were made at the beginning and end of each day or measurement session, and before and after each measurement on a pad. Results of the sensitivity measurements are presented in Table 7-4 and Figure 7-4; the abscissa units shown in Figure 7-4 are the sensitivity-measurement sequence numbers, analogous to those shown in Figure 7-3.

Dead time was determined using the two-source method, wherein the factor used to correct for dead time is assumed to be a third-degree polynomial (Kohman, 1949; George, 1982). The raw data for the dead-time measurements are presented in Table 7-5. A graphic representation of the polynomial correction factor, F_d, derived from the data is provided in Figure 7-5. Also indicated in Figure 7-5 is the maximum count rate encountered during this study; that rate was measured on pad E5.

Table 7-3. Resolution of the CFMS Using a Co-60 Source

Date of Measurement	Location	Resolution[a] (percent)
3/04/83	Grand Junction, Colorado	8.38
3/08/83	Grand Junction, Colorado	8.22
3/08/83	Grand Junction, Colorado	8.22
3/09/83	Grand Junction, Colorado	8.41
3/10/83	Grand Junction, Colorado	8.40
3/11/83	Grand Junction, Colorado	8.25
3/14/83	Grand Junction, Colorado	8.18
3/16/83	Grand Junction, Colorado	8.41
3/18/83	Grand Junction, Colorado	8.33
3/21/83	Grand Junction, Colorado	8.33
3/22/83	Grand Junction, Colorado	8.37
3/23/83	Grand Junction, Colorado	8.30
3/24/83	Grand Junction, Colorado	8.35
3/28/83	Grand Junction, Colorado	8.38
3/30/83	Grand Junction, Colorado	8.32
3/31/83	Grand Junction, Colorado	7.73[b]
4/11/83	Grand Junction, Colorado	8.21
4/13/83	Grand Junction, Colorado	8.37
4/27/83	Grand Junction, Colorado	8.40
5/05/83	Grand Junction, Colorado	8.26
5/11/83	Grand Junction, Colorado	8.50
5/27/83	Grand Junction, Colorado	8.37
6/07/83	Grants, New Mexico	8.23
6/09/83	Grants, New Mexico	8.24
6/12/83	George West, Texas	8.39
6/13/83	George West, Texas	8.45
8/16/83	Grand Junction, Colorado	8.30
8/19/83	Grand Junction, Colorado	8.43
8/26/83	Reno, Nevada	8.31
8/27/83	Reno, Nevada	8.37
9/01/83	Spokane, Washington	8.33
9/10/83	Casper, Wyoming	8.24
9/11/83	Casper, Wyoming	8.35
9/22/83	Grand Junction, Colorado	8.29
10/17/83	Grand Junction, Colorado	8.37
10/19/83	Grand Junction, Colorado	8.29

[a]Full width at half maximum of 661-keV photopeak from Cs-137.

[b]The cable-head connection had failed and was discovered during this measurement. It was repaired prior to taking the next measurement.

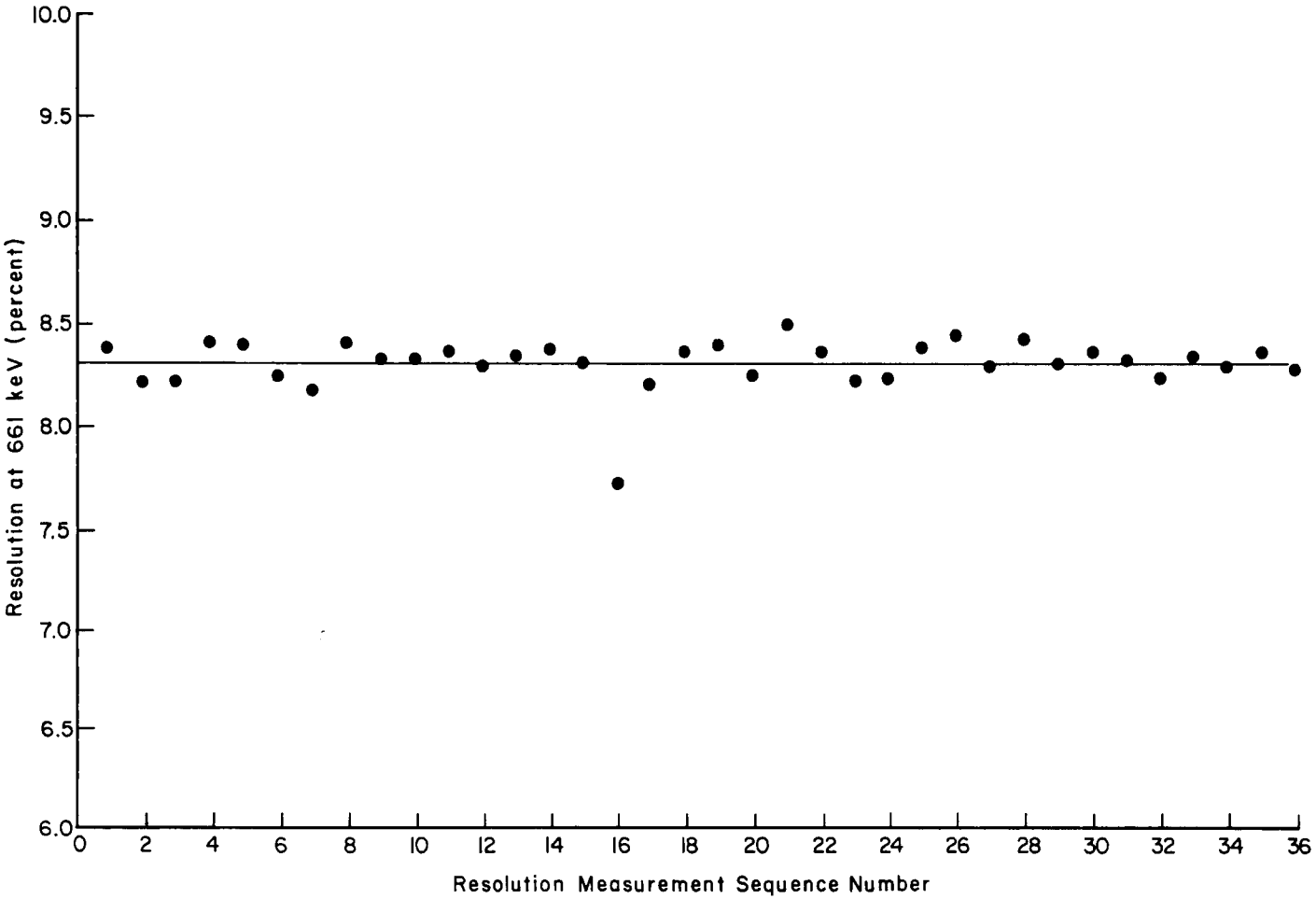

Figure 7-3. Resolution of the CFMS Using a Co-60 Source

Table 7-4. Sensitivity of the CFMS Sodium Iodide Detector to a 10-μCi Ra-226 Source

Date of Measurement	Location	Sensitivity[a] (cps)
3/04/83	Grand Junction, Colorado	21622
3/08/83	Grand Junction, Colorado	21708
3/08/83	Grand Junction, Colorado	21397
3/09/83	Grand Junction, Colorado	21683
3/09/83	Grand Junction, Colorado	21430
3/09/83	Grand Junction, Colorado	21493
3/09/83	Grand Junction, Colorado	21592
3/10/83	Grand Junction, Colorado	21584
3/10/83	Grand Junction, Colorado	21533
3/11/83	Grand Junction, Colorado	21420
3/14/83	Grand Junction, Colorado	21623
3/14/83	Grand Junction, Colorado	21573
3/14/83	Grand Junction, Colorado	21612
3/14/83	Grand Junction, Colorado	21561
3/16/83	Grand Junction, Colorado	21667
3/16/83	Grand Junction, Colorado	21760
3/16/83	Grand Junction, Colorado	21729
3/18/83	Grand Junction, Colorado	21352
3/18/83	Grand Junction, Colorado	21399
3/21/83	Grand Junction, Colorado	21754
3/21/83	Grand Junction, Colorado	21792
3/21/83	Grand Junction, Colorado	21663
3/21/83	Grand Junction, Colorado	21353
3/22/83	Grand Junction, Colorado	21649
3/22/83	Grand Junction, Colorado	21719
3/23/83	Grand Junction, Colorado	21876
3/23/83	Grand Junction, Colorado	21729
3/23/83	Grand Junction, Colorado	21723
3/24/83	Grand Junction, Colorado	21747
3/28/83	Grand Junction, Colorado	21826
3/30/83	Grand Junction, Colorado	21419
3/30/83	Grand Junction, Colorado	21642
3/30/83	Grand Junction, Colorado	21735
3/30/83	Grand Junction, Colorado	21726
3/31/83	Grand Junction, Colorado	21680
3/31/83	Grand Junction, Colorado	21779
3/31/83	Grand Junction, Colorado	21928
3/31/83	Grand Junction, Colorado	22018
3/31/83	Grand Junction, Colorado	21918

[a]Observed total count rate, corrected for ambient background.

Table 7-4. Sensitivity of the CFMS Sodium Iodide Detector to a 10-μCi Ra-226 Source (continued)

Date of Measurement	Location	Sensitivity[a] (cps)
4/11/83	Grand Junction, Colorado	21802
4/11/83	Grand Junction, Colorado	21691
4/11/83	Grand Junction, Colorado	21811
4/11/83	Grand Junction, Colorado	21772
4/11/83	Grand Junction, Colorado	21831
4/13/83	Grand Junction, Colorado	21811
4/27/83	Grand Junction, Colorado	21781
4/27/83	Grand Junction, Colorado	21785
4/27/83	Grand Junction, Colorado	21884
4/27/83	Grand Junction, Colorado	21556
4/27/83	Grand Junction, Colorado	21679
4/27/83	Grand Junction, Colorado	21698
5/05/83	Grand Junction, Colorado	21741
5/05/83	Grand Junction, Colorado	21795
5/11/83	Grand Junction, Colorado	21924
5/11/83	Grand Junction, Colorado	21582
5/27/83	Grand Junction, Colorado	21627
5/27/83	Grand Junction, Colorado	21622
6/07/83	Grants, New Mexico	21522
6/07/83	Grants, New Mexico	21573
6/07/83	Grants, New Mexico	21359
6/07/83	Grants, New Mexico	21612
6/07/83	Grants, New Mexico	22084
6/07/83	Grants, New Mexico	22100
6/09/83	Grants, New Mexico	21946
6/09/83	Grants, New Mexico	22165
6/09/83	Grants, New Mexico	22193
6/12/83	George West, Texas	22509
6/12/83	George West, Texas	22320
6/12/83	George West, Texas	22215
6/13/83	George West, Texas	22340
6/13/83	George West, Texas	22137
6/13/83	George West, Texas	22176
6/13/83	George West, Texas	22098
6/13/83	George West, Texas	22133
6/13/83	George West, Texas	22196
8/16/83	Grand Junction, Colorado	22261
8/16/83	Grand Junction, Colorado	22155

[a]Observed total count rate, corrected for ambient background.

Table 7-4. Sensitivity of the CFMS Sodium Iodide Detector to a 10-μCi Ra-226 Source (continued)

Date of Measurement	Location	Sensitivity[a] (cps)
8/16/83	Grand Junction, Colorado	22256
8/19/83	Grand Junction, Colorado	22301
8/19/83	Grand Junction, Colorado	22316
8/19/83	Grand Junction, Colorado	22341
8/19/83	Grand Junction, Colorado	21986
8/19/83	Grand Junction, Colorado	21684
8/19/83	Grand Junction, Colorado	21884
8/26/83	Reno, Nevada	22304
8/26/83	Reno, Nevada	21880
8/27/83	Reno, Nevada	21853
8/27/83	Reno, Nevada	21797
8/27/83	Reno, Nevada	21852
8/27/83	Reno, Nevada	21861
8/27/83	Reno, Nevada	21657
9/01/83	Spokane, Washington	21451
9/01/83	Spokane, Washington	21994
9/01/83	Spokane, Washington	21803
9/01/83	Spokane, Washington	21529
9/10/83	Casper, Wyoming	21602
9/10/83	Casper, Wyoming	21620
9/11/83	Casper, Wyoming	21630
9/11/83	Casper, Wyoming	21454
9/22/83	Grand Junction, Colorado	21733
10/17/83	Grand Junction, Colorado	21970
10/17/83	Grand Junction, Colorado	21949
10/19/83	Grand Junction, Colorado	21727
10/19/83	Grand Junction, Colorado	21719

[a]Observed total count rate, corrected for ambient background.

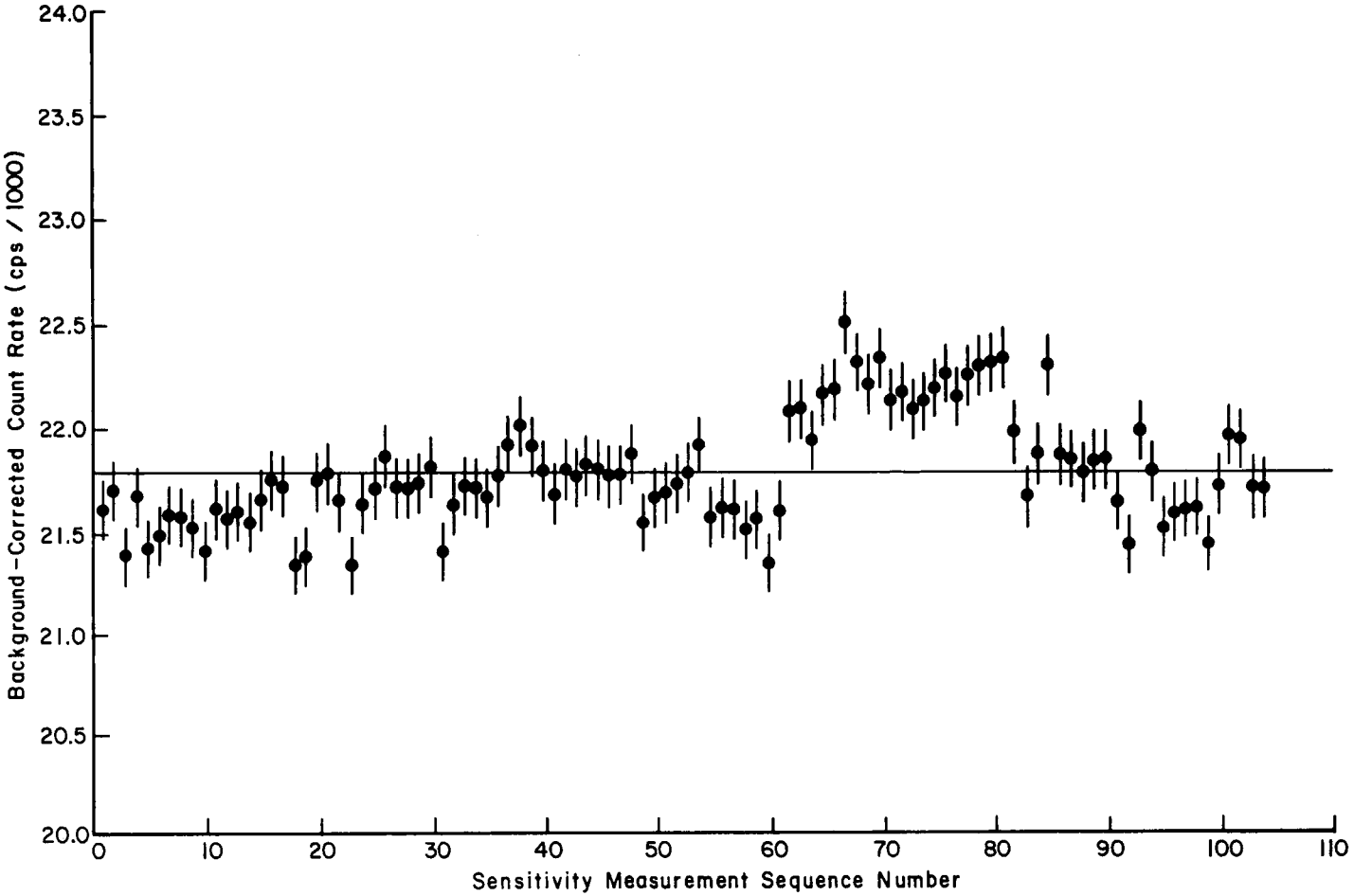

Figure 7-4. Sensitivity of the CFMS Sodium Iodide Detector to a Ra-226 Source

Table 7-5. Results of Dead-Time Measurements for the CFMS Sodium Iodide Detector Using the Two-Source Method

Date of Measurement	Acquire Time (sec)	Count Rate (cps)			
		Source 1	Source 2	Sources 1 and 2	Background
3/8/83	170	2828	2357	5084	87.0
3/8/83	150	3803	3980	7603	87.0
3/8/83	120	5322	4809	9998	87.0
3/8/83	100	6716	7262	13671	87.0
3/8/83	70	8545	8976	17059	87.3
3/8/83	60	12109	10737	22175	87.3
3/8/83	50	15848	16675	31164	86.7
3/8/83	50	21507	20343	39448	86.7
3/8/83	40	26360	24925	47482	87.0
3/8/83	40	32326	32925	58723	87.0

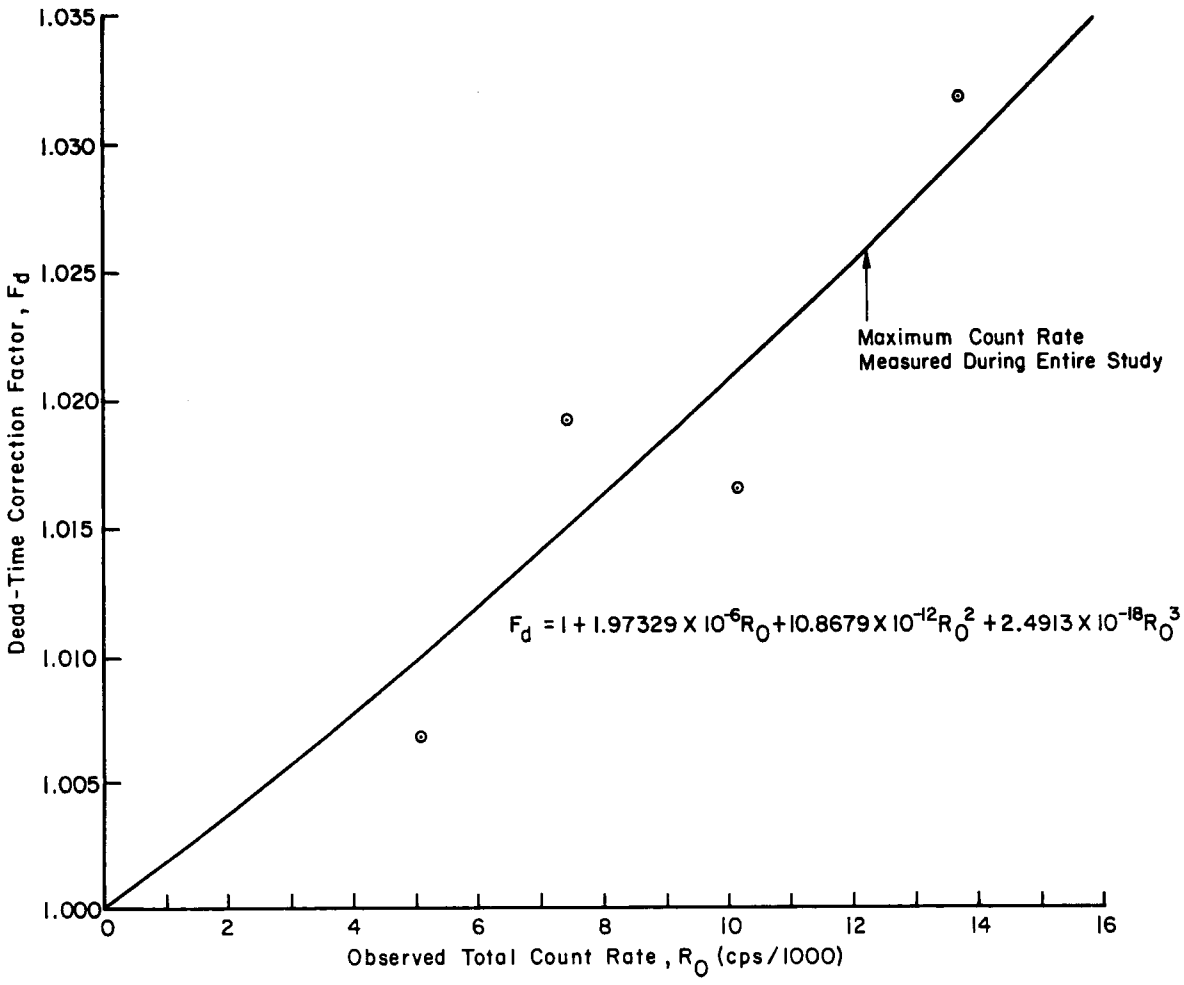

Figure 7-5. Dead-Time Correction Factor Versus Total Count Rate for the CFMS

7.2 DATA COLLECTION AND REDUCTION

7.2.1 Data Collection

The data-collection procedure used with the CFMS pad-monitoring detector system was patterned after that used to collect borehole data for total-count measurements (George and others, 1983). This procedure is outlined below.

1. Position the CFMS truck adjacent to a calibration pad.

2. Apply electrical power to the truck electronics and detector. The minimum warm-up and stabilization time is 1 hour.

3. With the detector assembly placed on the deck of the vehicle, perform the premeasurement calibration procedure as described below (George and others, 1983):

   a. Adjust the DC level (baseline) of the amplifier and the zero level of the MCA such that channel 0 in the MCA corresponds to the baseline.

   b. Using a Th-228 button source, set the amplifier gain such that the centroid of the 2615-keV photopeak of Tl-208 is positioned in channel 395 of the MCA.

   c. Measure and record the count rates from reference sources of thorium-228, radium-226, and cesium-137.

   d. Measure the ambient background.

   e. Calculate and record background-corrected sensitivity, resolution, and linearity. Detector sensitivity and resolution results were presented in Section 7.1.

4. Measure the gamma-ray activity of the calibration pad in the following manner:

   a. Move the lead collimating shield to the pad.

   b. Place the detector in the collimating shield.

   c. Collect a preliminary spectrum to set the gain-stabilization parameters at the dominant gamma-ray photopeak.

d. Measure the gamma-ray activity of the pad for approximately 3000 seconds; this typically yields 10 spectra, each characterized by 300 seconds of MCA live time. For each spectrum, counts in each region of interest (ROI) are stored in a data file on disk.

e. Return the lead collimating shield and detector to the truck platform.

5. Perform the postmeasurement calibration procedure, as described below (George and others, 1983):

   a. Readjust amplifier gain, if necessary, to position the 2615-keV gamma-ray photopeak of Tl-208 in channel 395.

   b. Measure the count rate from the Ra-226 reference source to compare postmeasurement detector sensitivity with that determined during the premeasurement calibration.

   c. Measure the ambient background.

   d. Calculate and record background-corrected sensitivity.

6. Repeat Steps 4 and 5 for each pad measured.

7. Copy the files containing ROI data for each spectrum and pad to magnetic tape.

Data relative to the CFMS measurements, including the date and time of each measurement, acquisition live time, and the number of spectra collected, are presented in Table 7-6. Measurements on the background pads (H1, PB, GPB, CPB, RPB, SPB, and TPB) were performed without using the gain-stabilization algorithm due to the lack of a prominent gamma-ray photopeak. For these measurements, the gain was assumed to be stable following the premeasurement calibration.

Table 7-6. Description of CFMS Measurements

Pad	Date of Measurement	Time of Measurement	Acquisition Time[a] (sec)	No. of Spectra Collected
E1	3/16/83	11:30	500	6
E2	3/16/83	13:00	300	10
E4	3/16/83	15:00	300	10
E5	3/22/83	10:00	300	7
H1	3/21/83	15:30	1000	3
H2	3/30/83	16:15	1800	28
H3	3/14/83	9:45	600	12
H4	3/31/83	16:15	1800	30
H5	3/28/83	16:30	1800	30
PB	3/30/83	13:00	1000	3
PK	3/23/83	13:30	1000	3
PL	3/22/83	14:30	300	10
PH	3/23/83	9:45	300	10
PT	3/23/83	11:30	600	5
NPL	3/31/83	10:00	1000	3
NPH	3/30/83	14:30	500	6
PPL	3/31/83	11:30	1000	4
PPH	3/31/83	13:45	600	6
CE2	9/11/83	12:00	300	10
CE4	9/10/83	19:15	300	10
CPB	9/11/83	10:50	500	5
CPK	9/10/83	17:50	300	10
CPL	9/10/83	16:35	300	10
CPH	9/10/83	15:15	300	10
CPT	9/11/83	13:15	300	10
GE2	6/09/83	17:00	300	10
GE4	6/09/83	20:00	300	10
GPB	6/07/83	18:15	1000	5
GPK	6/07/83	10:00	1000	5
GPL	6/07/83	12:15	300	10
GPH	6/07/83	14:45	300	10
GPT	6/07/83	16:30	300	10
RPK	8/27/83	9:00	1000	3
RPL	8/27/83	12:00	300	6
RPH	8/27/83	13:15	300	6
RPT	8/27/83	15:00	300	10
SPB	9/01/83	12:15	300	6
SPK	9/01/83	13:45	500	4
SPL	9/01/83	11:00	300	8
SPH	9/01/83	15:15	300	8
RPB	8/27/83	16:00	1000	3

[a]MCA live time for acquisition of spectra.

Table 7-6. Description of CFMS Measurements (continued)

Pad	Date of Measurement	Time of Measurement	Acquisition Time[a] (sec)	No. of Spectra Collected
SPT	9/01/83	9:00	300	8
TE2	6/13/83	15:45	300	10
TE4	6/13/83	14:00	300	10
TPB	6/13/83	17:20	1000	5
TPK	6/13/83	15:30	1000	5
TPL	6/13/83	10:30	300	10
TPH	6/13/83	12:15	300	10
TPT	6/12/83	18:45	500	8

[a]MCA live time for acquisition of spectra.

7.2.2 Data Reduction

The equations used to relate observed count rates to concentration assignments were defined in Section 2.3.1. Accordingly, the following procedure was used to reduce the CFMS measurement data:

1. For each pad, calculate the mean count rate and its uncertainty in each ROI, for each spectrum collected. The uncertainty is the maximum of either the standard deviation of the measurements about their mean or the statistical counting uncertainty in a single measurement. Results of these calculations for each pad are presented in Table 7-7.

2. Correct the observed count rates for dead time, background, and moisture using equation (2-8) and the left sides of equations (2-5) through (2-7). Dead-time corrections were determined from Figure 7-5, and moisture correction factors were obtained from Table 4-5. The resultant corrected count rates for each pad are presented in Table 7-8; the associated uncertainties reflect both the uncertainties in the observed count rates and in the correction factors.

3. Compute the coefficients for equations (2-5) through (2-7), relating concentrations to count rates, when the concentrations and the exhalation correction factors are those cited in Tables 1-2 and 1-4, respectively. A linear least-squares regression provided the following coefficient values, which were verified by means of separate calculations using selected sets of pads:

$$a_{11} = 0.319$$
$$a_{12} = 0.935$$
$$a_{13} = 0.591$$
$$a_{22} = 1.145$$
$$a_{23} = 1.850$$
$$a_{32} = 0.0246$$
$$a_{33} = 1.018$$

4. Calculate the expected count rates for each pad by evaluating the right side of equations (2-5) through (2-7), using the assigned concentrations and exhalation correction factors cited in Tables 1-2 and 1-4, respectively, and the coefficients determined in Step 3. These expected count rates are presented in Table 7-9.

Table 7-7. CFMS Observed Count Rates

Pad	Spectral-Window Measurement[a]									
	Total Gamma		Potassium		Radium		Thorium		High Energy[b]	
	cps	S	cps	S	cps	S	cps	S	cps	S
E1	350.3	0.2	21.1	1.0	20.8	1.0	1.22	4.1	182.2	0.3
E2	1155.7	0.2	64.5	0.7	72.8	0.7	1.98	4.1	607.0	0.2
E4	5352.5	0.1	292.0	0.4	349.0	0.3	7.03	2.2	2823.1	0.1
E5	12333.7	0.1	684.1	0.3	830.2	0.2	19.14	2.7	6571.8	0.2
H1	66.9	0.5	5.4	1.4	3.0	1.8	0.86	3.4	33.2	0.6
H2	430.2	0.4	18.1	0.6	1.9	1.7	0.39	3.7	71.3	0.3
H3	2309.7	0.1	127.0	0.4	148.4	0.3	3.49	2.2	1222.4	0.1
H4	1714.8	0.1	72.5	0.3	134.9	0.2	65.82	0.3	925.9	0.1
H5	2067.0	0.1	106.7	0.2	123.6	0.4	15.78	1.3	1049.1	0.1
PB	21.6	0.7	1.0	3.2	1.1	3.0	0.26	6.2	8.3	1.1
PK	131.3	0.3	17.5	0.8	1.9	2.3	0.32	5.6	69.9	0.4
PL	1143.1	0.2	63.7	0.7	71.0	0.7	2.07	4.0	599.0	0.2
PH	4578.8	0.1	247.2	0.4	292.4	0.3	6.42	2.3	2400.7	0.1
PT	817.9	0.2	37.1	0.7	62.1	0.5	30.09	0.7	431.9	0.2
NPL	244.3	0.2	15.1	0.8	14.3	0.8	1.10	3.0	126.5	0.3
NPH	624.0	0.2	35.3	0.8	39.1	0.7	1.45	3.7	325.3	0.3
PPL	247.0	0.2	15.0	0.8	14.7	0.8	1.14	3.0	128.7	0.3
PPH	630.6	0.2	35.4	0.7	38.8	0.7	1.38	3.5	328.0	0.3
CE2	1118.8	0.2	61.2	0.8	70.8	0.7	3.32	3.2	583.3	0.2

[a]Uncertainties (S) are one sigma (68 percent confidence interval), and are expressed as a percentage of the observed mean count rate.

[b]The high-energy region of interest is 550 to 3500 keV. These data were not used to verify parameter assignments, but are provided here for reference purposes.

Table 7-7. CFMS Observed Count Rates (continued)

Pad	Spectral-Window Measurement[a]								High Energy[b]	
	Total Gamma		Potassium		Radium		Thorium			
	cps	S	cps	S	cps	S	cps	S	cps	S
CE4	5146.4	0.1	278.1	0.5	338.4	0.4	11.66	2.1	2706.0	0.2
CPB	106.4	1.4	4.9	2.0	7.9	1.6	1.92	3.2	47.9	1.3
CPK	176.1	0.4	20.6	1.3	5.5	2.5	1.28	5.4	93.7	0.6
CPL	1163.1	0.2	64.4	0.7	74.1	0.7	3.83	3.5	607.2	0.2
CPH	4411.6	0.1	239.9	0.5	287.1	0.5	8.46	2.3	2328.7	0.2
CPT	841.7	0.2	38.1	1.1	65.0	0.8	30.58	1.1	446.3	0.4
GE2	1176.1	0.2	66.4	0.8	77.8	1.0	3.85	2.9	626.4	0.3
GE4	5232.7	0.1	282.1	0.3	342.8	0.4	10.16	2.0	2760.3	0.1
GPB	96.2	0.4	4.7	1.8	7.3	1.3	1.79	4.3	44.5	1.0
GPK	163.5	0.3	19.9	0.7	4.5	1.5	1.02	4.1	88.0	0.3
GPL	1353.3	0.1	63.0	1.0	73.1	2.0	3.82	8.3	598.1	0.8
GPH	4551.7	0.1	249.0	0.4	299.1	0.4	7.95	3.4	2391.7	0.1
GPT	866.9	0.3	39.4	0.4	66.3	0.9	31.27	1.0	455.8	0.4
RPB	56.8	0.5	2.9	1.8	4.3	2.1	1.12	4.9	26.7	0.6
RPK	177.1	0.2	20.3	0.7	6.0	1.3	1.44	2.6	94.6	0.3
RPL	1138.1	0.2	64.3	0.7	72.6	0.7	2.88	3.4	597.5	0.2
RPH	4590.0	0.1	253.1	0.5	303.0	0.4	8.58	2.7	2431.1	0.1
RPT	867.3	0.3	39.4	0.9	66.6	1.0	31.64	1.2	459.9	0.3
SPB	71.2	0.7	3.5	3.1	5.1	2.6	1.23	5.1	32.3	1.5
SPK	182.3	0.5	21.0	2.2	6.4	1.8	1.52	6.2	97.3	0.7
SPL	1103.4	0.2	63.3	0.7	70.5	0.7	2.83	3.4	581.6	0.2
SPH	4586.0	0.1	256.6	0.4	304.2	0.3	9.90	1.8	2426.4	0.1
SPT	849.8	0.2	38.4	0.9	65.0	0.7	31.14	1.1	450.4	0.3
TE2	1117.2	0.2	61.6	0.7	71.4	1.0	3.33	3.2	583.7	0.2
TE4	4951.2	0.1	268.3	0.4	324.2	0.3	9.21	2.7	2610.9	0.1
TPB	180.0	1.0	3.9	2.6	6.1	1.4	1.59	4.5	37.1	1.5
TPK	179.3	0.5	20.6	0.7	6.1	1.3	1.44	2.6	96.0	0.4
TPL	1105.7	0.2	61.9	0.8	70.8	0.9	3.05	3.3	577.4	0.2
TPH	4413.3	0.1	239.6	0.4	287.6	0.4	9.12	2.0	2337.1	0.1
TPT	851.2	0.2	38.6	1.0	65.7	0.7	31.13	1.0	452.0	0.2

[a]Uncertainties (S) are one sigma (68 percent confidence interval), and are expressed as a percentage of the observed mean count rate.

[b]The high-energy region of interest is 550 to 3500 keV. These data were not used to verify parameter assignments, but are provided here for reference purposes.

Table 7-8. CFMS Observed Count Rates Corrected for Dead Time, Background, and Moisture

Pad	Spectral-Window Measurement[a]					
	Potassium		Radium		Thorium	
	cps	S	cps	S	cps	S
E1	21.5	1.3	21.1	1.3	1.02	5.5
E2	68.4	1.0	77.2	1.0	1.85	4.9
E4	319.5	1.0	382.0	1.0	7.42	2.5
E5	746.8	0.8	906.4	0.7	20.63	2.8
H1	4.9	2.2	2.1	3.5	0.66	5.7
H2	18.6	1.1	0.9	5.8	0.14	16.6
H3	140.1	1.2	163.5	1.1	3.58	2.7
H4	75.8	0.7	141.9	0.6	69.47	0.6
H5	114.8	0.9	133.1	0.9	16.83	1.6
PK	17.9	1.2	0.9	6.9	0.06	40.1
PL	69.4	1.2	77.3	1.3	2.00	4.8
PH	274.3	1.2	324.3	1.1	6.85	2.6
PT	39.6	1.2	66.8	1.1	32.63	1.2
NPL	15.5	1.4	14.5	1.3	0.92	4.5
NPH	38.1	1.4	42.2	1.3	1.32	4.8
PPL	15.4	1.3	15.0	1.3	0.97	4.4
PPH	38.4	1.4	42.0	1.4	1.25	4.7
CE2	61.0	1.2	68.1	1.2	1.52	8.8
CE4	303.2	1.1	366.4	1.1	10.80	2.8
CPK	16.9	2.0	-2.6	7.8	-0.69	14.5
CPL	64.8	1.2	72.1	1.2	2.08	7.8
CPH	258.2	1.1	306.6	1.1	7.19	3.2
CPT	36.3	1.6	62.5	1.3	31.29	1.5
GE2	70.7	1.6	80.6	1.8	2.36	6.7
GE4	305.4	1.0	369.3	1.0	9.22	2.8
GPK	16.3	1.3	-3.0	4.2	-0.82	11.4
GPL	64.1	1.5	72.3	2.4	2.23	16.1
GPH	267.1	0.9	318.7	0.9	6.73	4.6
GPT	37.8	1.1	64.1	1.4	32.01	1.4
RPK	19.0	1.3	1.9	7.1	0.35	20.8
RPL	66.8	1.2	74.3	1.2	1.91	6.4
RPH	274.0	1.1	326.8	1.0	8.16	3.3
RPT	39.2	1.2	66.8	1.3	32.71	1.5
SPK	18.8	2.8	1.4	13.5	0.31	39.0
SPL	65.5	1.3	71.6	1.2	1.75	7.2

[a]Uncertainties (S) are one sigma (68 percent confidence interval), and are expressed as a percentage of the reported mean count rate.

Table 7-8. CFMS Observed Count Rates Corrected for Dead Time, Background, and Moisture (continued)

Pad	Spectral-Window Measurement[a]					
	Potassium		Radium		Thorium	
	cps	S	cps	S	cps	S
SPH	277.2	1.0	327.6	1.0	9.49	2.3
SPT	37.8	1.3	64.7	1.2	32.30	1.4
TE2	64.3	1.4	72.7	1.6	1.94	7.4
TE4	303.2	1.4	364.1	1.4	8.72	3.6
TPK	17.9	1.3	0.0	99.9	-0.16	53.8
TPL	63.5	1.3	70.8	1.4	1.60	8.5
TPH	259.7	1.0	309.9	1.0	8.29	1.4
TPT	38.0	1.5	65.1	1.2	32.23	1.4

[a]Uncertainties (S) are one sigma (68 percent confidence interval), and are expressed as a percentage of the reported mean count rate.

Table 7-9. Expected Count Rates

Pad	Spectral-Window Count Rate[a]					
	Potassium		Radium		Thorium	
	cps	S	cps	S	cps	S
Radium-Enriched Pads						
NPL	13.1	5.6	12.2	0.9	0.93	1.4
PPL	15.1	4.9	14.8	0.9	0.91	1.5
E1	22.3	4.0	22.6	0.8	1.19	1.7
NPH	38.2	1.9	42.9	0.8	1.58	2.4
PPH	33.0	2.2	38.6	0.8	1.42	2.3
E2	72.1	1.4	83.2	0.8	2.61	2.8
CE2	65.3	1.4	75.2	0.8	2.35	2.8
GE2	69.1	1.3	80.0	0.8	2.25	3.1
TE2	63.3	1.5	72.7	0.8	2.21	2.9
PL	72.7	1.4	83.5	0.8	2.40	3.1
CPL	61.7	1.7	69.7	0.8	2.10	2.9

[a]Uncertainties (S) are one sigma (68 percent confidence interval), and are expressed as a percentage of the count rate.

Table 7-9. Expected Count Rates (continued)

Pad	Spectral-Window Count Rate[a]					
	Potassium		Radium		Thorium	
	cps	S	cps	S	cps	S
GPL	64.1	1.6	72.8	0.8	2.03	3.2
TPL	65.8	1.6	75.0	0.8	2.13	3.1
RPL	73.1	1.5	83.6	0.8	2.41	3.0
SPL	62.0	1.7	69.9	0.8	1.92	3.2
H3	150.8	0.9	180.7	0.8	4.61	3.5
PH	266.9	0.9	321.0	0.8	7.67	3.7
CPH	267.4	0.9	321.9	0.8	7.65	3.7
GPH	265.1	0.9	318.7	0.8	7.41	3.8
TPH	239.4	0.9	287.6	0.8	6.82	3.7
RPH	244.4	0.9	293.3	0.8	6.87	3.8
SPH	258.2	0.9	310.4	0.8	7.46	3.7
E4	351.1	0.9	425.3	0.8	9.91	3.8
CE4	299.1	0.9	361.8	0.8	8.57	3.7
GE4	298.7	0.9	361.5	0.8	8.53	3.8
TE4	299.3	0.9	362.3	0.8	8.48	3.8
E5	741.1	0.9	901.2	0.8	20.23	4.0
Potassium-Enriched Pads						
PK	16.8	21.7	0.7	2.7	0.18	1.1
CPK	16.9	21.5	0.9	2.4	0.20	1.2
GPK	17.1	21.6	0.7	2.3	0.15	1.2
TPK	17.0	21.8	0.6	2.3	0.13	1.2
RPK	17.1	21.6	0.7	2.4	0.15	1.2
SPK	17.3	21.8	0.5	2.7	0.04	1.4
H2	17.7	21.6	0.8	2.4	0.18	1.3
Thorium-Enriched Pads						
PT	36.9	8.7	63.2	5.6	31.74	1.2
CPT	36.8	8.6	62.9	5.6	31.24	1.2
GPT	36.0	8.6	61.1	5.6	30.49	1.2
TPT	36.7	8.7	62.8	5.7	31.74	1.2
RPT	37.1	8.7	63.5	5.7	31.98	1.2
SPT	37.8	8.6	64.9	5.5	32.13	1.2
H4	73.6	9.7	138.1	5.6	69.49	1.2

[a]Uncertainties (S) are one sigma (68 percent confidence interval), and are expressed as a percentage of the count rate.

7.2.3 Observations

This section of the report was intended to demonstrate that the CFMS measurements verified the assigned concentrations. The CFMS data, however, were not as useful for this purpose as had been anticipated. Before examining the verification data, it is worthwhile to describe an inherent limitation of NaI detector systems, and to make one observation regarding the raw CFMS data.

For a pad containing one enriched radioelement, it is difficult to verify the concentrations of the two unenriched radioelements in the pad using a NaI detector system. This limitation is apparent from an examination of the data presented in Table 7-10. The table shows the percentage of the count rate observed in each spectral window, due to each radioelement, for typical pads, based on previous calibrations of the CFMS detector. Note that, in almost all cases, the primary enriched radioelement dominates the observed count rate in all three spectral windows. The potassium pads are the exception because the potassium 'enrichment' is not large in terms of gamma-ray intensity and the potassium gamma-ray flux does not contribute to count rates in the radium and thorium windows. The end result is that, in any given spectral window, count rates contributed by the nonprimary radioelements are difficult to observe because large subtractions must be made to obtain small differences.

With respect to the raw CFMS data, it is important to note that the measured gamma-ray activities of the background pads are contaminated in certain cases. An examination of the count rates of the six background (xPB) pads (Table 7-7) reveals that the background measurements for the field sites are significantly greater than those for Grand Junction. Because of exposed sources and other pertinent history at Grand Junction, and due to geologic conditions at some of the field sites, we would expect the opposite. Note also that the count rates in the radium and thorium windows for the potassium pads at certain field sites (CPK, GPK, and TPK) are less than corresponding count rates from the respective background pad (CPB, GPB, and TPB). Since the potassium pads contain more radium and thorium than the background pads, these differences should be reversed; the fact that they are not is not explained by counting uncertainties. We suspect that the elevated background measurements at certain field sites were due to a neutron source carried on the CFMS truck for measuring moisture in the subsurface calibration models at these sites. During background measurements at Grand Junction, this source was not on the truck. Although the source was shielded by neutron-absorbing material during pad measurements at the field sites, the source and shield were within 5 to

Table 7-10. Percentage Contribution to Spectral Windows Due to Each Radioelement for Typical Calibration Pads

Type of Enriched Pad[a]	Percentage Contribution to Each Spectral Window						
	Potassium Window			Radium Window		Thorium Window	
	K	Ra	Th	Ra	Th	Ra	Th
Potassium	95	4	1	65	35	7	93
Radium							
Low	18	79	3	94	6	37	63
Medium	6	93	1	98	2	68	32
High	2	98	-	100	-	90	10
Thorium	10	16	74	11	89	-	100

[a]Radioelement concentrations, in pCi/g, typical of those contained in the calibration pads are the following:

	K-40	Ra-226	Th-232
Potassium-Enriched	52	0.7	0.2
Radium-Enriched			
Low	13	18	0.8
Medium	13	67	0.8
High	13	280	0.8
Thorium-Enriched	13	6.7	33

20 feet of the detector. The truck, and hence the neutron source, was not repeatably positioned with respect to any of the pads, making it impossible to subsequently correct for gamma radiation emitted by this source. As a consequence, concentrations derived from the CFMS data for the low-gamma-activity pads, including all potassium pads, are degraded by this contamination, and are therefore not very useful for verification purposes.

For purposes of verifying the concentration assignments, expected count rates and their uncertainties for each pad were determined as discussed above (see Table 7-9). The uncertainties were computed strictly from the least-squares regression used to determine the coefficients (Walpole and Myers, 1972); they are therefore a measure of the goodness of fit of the regression and do not reflect propagation of uncertainties associated with the

concentration assignments, exhalation correction factors, or moisture correction factors. The expected and observed count rates were compared using two methods (Table 7-11). One comparison is the ratio of the difference between the observed and expected count rates to the expected count rate. This ratio is expressed as a percentage, e(%), and represents the relative difference between the two count rates. Pursuant to our objective of verifying the assigned concentrations to within a few percent, this method permits comparison of the expected and observed count rates on the basis of percentage difference. However, a large percentage difference may not be statistically significant. The second comparison, therefore, is the ratio of the difference between the observed and expected count rates to the uncertainty; that is, it is the difference between the two count rates expressed as a fraction of the measurement uncertainty (standard deviation). This ratio is denoted e(s). If there were no difference statistically between the two count rates, we would expect e(s) to be between +3 and -3, 99 percent of the time. Comparisons made using these two methods permit simultaneous comparisons of absolute errors, e(%), in percentages, and statistical errors, e(s), in fractions of expected standard deviation. A large value for e(%), associated with an e(s) value in excess of 3, indicates a significant difference between the two count rates.

Examination of e(s) for all spectral windows (Table 7-11) indicates that many of the differences can not be explained as variations due to counting statistics only, i.e., 99 percent of them are not less than or equal to 3. Even so, the following observations can be made for purposes of verification.

Thorium-Enriched Pads

- The observed count rates agree with the expected count rates to within 7.5 percent and 3 sigmas for all three windows. The comparisons thus indicate that the assignments of thorium concentrations for the thorium pads are consistent to within 7.5 percent.

Potassium-Enriched Pads

- The contamination described earlier significantly affected the observed count rates, especially for the radium and thorium windows. As a consequence, only the potassium-window count-rate comparisons were used for purposes of verification for these pads. Note that the values for e(%) are within 12 percent, with those for RPK and SPK being the highest. An increase in background count rate of not more than 1 cps for

the potassium window, which is within the measured background count rates of the other sites, will yield e(%) values within 6 percent for these two pads (RPK and SPK). We suspect therefore that the contamination in the measurements is the primary source of the disparity between the expected and the observed count rates. We do not conclude that the assigned concentrations are in error by this amount.

Radium-Enriched Pads

- For all three windows, one-third to one-half of the e(s) values are greater than 3, indicating that either the expected uncertainties are low [see footnote (b) of Table 7-11] or that other errors are significant. We suspect that a combination of these two possibilities is the actual case.

- For the radium window, e(%) is less than 12 percent, except on pad NPL where the value is 18.9 percent. For the potassium window, e(%) is less than 11 percent, except on pads NPL (18.3 percent), PPH (16.4 percent), and SPH (13.4 percent). As expected, the values of e(%) for the potassium and radium windows are strongly correlated, because radium dominates the count rates in both windows. We attribute part of the variance that exists in the data for both windows to uncertainties in the radon-exhalation correction. As shown in Figure 7-6, there is no definite correlation between concentration and e(%), so problems due to errors in background, dead-time correction, or the regression coefficients are eliminated, leaving radon exhalation as the most likely source of variance.

- For the thorium window, e(%) is larger than for the other windows, but generally less than approximately 30 percent. We attribute these high e(%) values to slight gain drifts in the CFMS, which occur because the count rate in this window is primarily due to radium and because the count rate is sensitive to the position of the lower boundary of the thorium window. The lower boundary, at 2475 keV, falls near the peak of the 2448-keV line from Bi-214.

- In conclusion, we estimate that the assignments of radium-226 concentrations have been verified to within 6 percent. Although the measurements only directly verified the assignments to within roughly 12 percent (with a few exceptions), we attribute the additional 6 percent variation to uncertainty in radon-exhalation corrections.

Table 7-11. Comparisons of Expected and Observed Count Rates

Pad	Potassium Window		Radium Window		Thorium Window	
	e(%)[a]	e(s)[b]	e(%)[a]	e(s)[b]	e(%)[a]	e(s)[b]
Radium-Enriched Pads						
NPL	18.3	3.1	18.9	10.5	-10.8	-0.2
PPL	2.0	0.4	1.4	0.8	6.6	1.5
E1	-3.6	-0.9	-6.6	-4.5	-14.3	-2.8
NPH	-0.3	-0.1	-1.6	-1.1	-16.5	-3.7
PPH	16.4	6.0	8.8	5.2	-12.0	-2.4
E2	-5.1	-3.0	-7.2	-5.9	-29.1	-6.3
CE2	-6.6	-3.7	-9.4	-7.0	-35.3	-5.5
GE2	2.3	1.1	0.7	0.4	4.9	0.6
TE2	1.6	0.8	0	0	-12.2	-1.7
PL	-4.5	-2.4	-7.4	-5.1	-16.7	-3.3
CPL	5.0	2.4	3.4	2.3	-1.0	-0.1
GPL	0	0	-0.7	-0.3	9.9	0.6
TPL	-3.5	-1.7	-5.6	-3.6	-24.5	-3.5
RPL	-8.5	-4.6	-11.1	-8.4	-20.7	-3.6
SPL	5.6	2.6	2.4	1.7	-8.9	-1.2
H3	-7.1	-5.0	-9.5	-7.4	-22.3	-5.4
PH	2.8	1.8	1.0	0.7	-10.7	-2.4
CPH	-3.4	-2.5	-4.8	-3.6	-6.0	-1.3
GPH	0.8	0.6	0	0	-10.1	-1.8
TPH	8.5	6.0	7.8	5.8	21.6	4.3
RPH	6.1	4.1	5.3	4.0	9.4	1.8
SPH	13.4	9.3	11.7	8.5	38.1	7.7
E4	-9.0	-7.0	-10.2	-8.5	-25.2	-5.9
CE4	1.4	1.0	1.3	0.9	26.0	5.1
GE4	2.2	1.9	2.2	1.7	8.1	1.7
TE4	1.3	0.8	0.5	0.3	2.8	0.5
E5	0.8	0.6	0.6	0.5	2.0	0.4

[a] e(%) is the difference between the observed and expected count rates, expressed as a percentage of the expected count rate.

[b] e(s) is the difference between the observed and expected count rates, expressed as a multiple of the measurement uncertainty.

Table 7-11. Comparisons of Expected and Observed Count Rates (continued)

Pad	Potassium Window		Radium Window		Thorium Window	
	e(%)[a]	e(s)[b]	e(%)[a]	e(s)[b]	e(%)[a]	e(s)[b]
Potassium-Enriched Pads						
PK	6.5	0.3	28.6	3.3	-66.7	-6.0
CPK	0	0	-100.0	-17.5	-100.0	-8.9
GPK	-4.7	-0.2	-100.0	-28.5	-100.0	-9.7
TPK	5.3	0.2	-100.0	-4.3	-100.0	-3.2
RPK	11.1	0.5	-100.0	8.5	-100.0	2.9
SPK	8.7	0.4	-100.0	4.5	-100.0	2.3
H2	5.1	0.2	12.5	1.7	-22.2	-2.0
Thorium-Enriched Pads						
PT	7.3	0.8	5.7	1.0	2.8	1.6
CPT	-1.4	-0.2	-0.6	-0.1	0.2	0.1
GPT	5.0	0.6	4.9	0.8	5.0	2.6
TPT	3.5	0.4	3.7	0.6	1.5	0.8
RPT	5.7	0.6	5.2	0.9	2.3	1.2
SPT	0	0	-0.3	-0.1	0.5	0.3
H4	3.0	0.3	2.8	0.5	0	0

[a] e(%) is the difference between the observed and expected count rates, expressed as a percentage of the expected count rate.

[b] e(s) is the difference between the observed and expected count rates, expressed as a multiple of the measurement uncertainty.

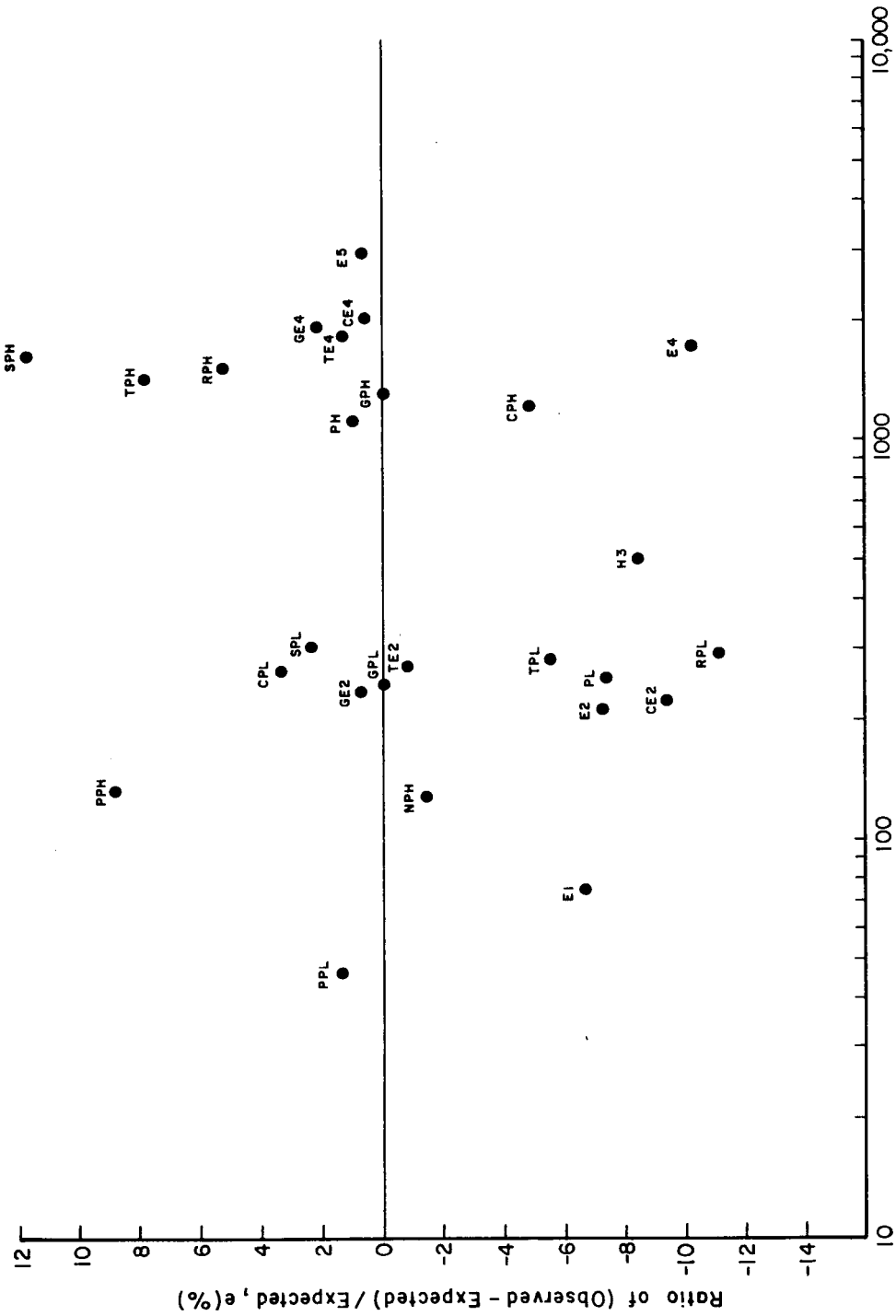

Figure 7-6. Plot of the Percentage Difference Between Observed and Expected Count Rates Versus Uranium Concentration for the Radium-Enriched Pads

8.0 ACKNOWLEDGMENTS

The authors gratefully acknowledge the extremely able assistance of B. J. Edwardson, whose careful and thorough editing significantly improved the quality of this report. We also acknowledge the capable technical assistance of J. Burnham who set up, maintained, and operated the high-resolution gamma-ray spectroscopy system; B. E. Heistand and J. E. Krabacher who operated the CFMS and helped reduce the data; and G. Dechant and E. Reid who prepared and assayed the concrete samples from the pads. We appreciate the comments of J. R. Duray, J. Pacer, L. Ball, and B. E. Heistand, all of whom reviewed the report for technical content. We are grateful to M. G. White, L. Ball, J. R. Duray, and the Office of Remedial Action and Waste Technology in general for providing funding and other support for this study. We also wish to thank R. Osterstock, D. Emilia, and A. Girdley, all of Bendix Field Engineering Corporation, for their support throughout the course of this study.

9.0 REFERENCES

Bevington, P. R., 1969. Data Reduction and Error Analysis for the Physical Sciences, McGraw-Hill, New York.

Dechant, G., and S. Donivan, 1984. Calibration and Performance of a High-Resolution Gamma-Spectroscopy System, GJBX-4(84), Grand Junction Area Office, U.S. Department of Energy, Grand Junction, Colorado.

George, D. C., 1982. 'Total Count Gamma-Ray Logging - Correction Factors and Logging Model Grade Assignments,' in Uranium Exploration Methods, Proceedings, Review of the NEA/IAEA R&D Programme, Organization for Economic Cooperative Development, Nuclear Energy Agency with the International Atomic Energy Agency, Paris, 1-4 June 1982.

George, D. C., and L. Knight, 1982. Field Calibration Facilities for Environmental Measurements of Radium, Thorium, and Potassium, GJ/TMC-01(82), Technical Measurements Center, U.S. Department of Energy, Grand Junction, Colorado.

George, D. C., B. E. Heistand, and J. E. Krabacher, 1983. Grade Assignments for Models Used for Calibration of Gross-Count Gamma-Ray Logging Systems, GJBX-39(83), Grand Junction Office, U.S. Department of Energy, Grand Junction, Colorado.

Gunnink, Ray, 1979. 'Computer Techniques for Analysis of Gamma-Ray Spectra,' in Computers in Activation Analysis and Gamma-Ray Spectroscopy, Proceedings of the American Nuclear Society Topical Conference, Mayaguez, Puerto Rico, April 30-May 4, 1978, available from the U.S. Department of Energy Technical Information Center.

Heistand, B. E., and D. C. George, 1981. Statistical Analysis of Laboratory Assay Data for Use in Grade Reassignment of GJO Models, BFEC-8-1981, Bendix Field Engineering Corporation, Grand Junction, Colorado, internal report.

Kohman, T. P., 1949. 'A General Method for Determining Coincidence Corrections of Counting Instruments,' in The Transuranic Elements, Part II, G. T. Seaborg, J. J. Katz, and W. M. Manning (eds.), McGraw-Hill, New York.

Koizumi, C. J., 1981. Formation Moisture Study for the Ore Zone of the KUT Water Factor Calibration Model, BFEC-1981-6, Bendix Field Engineering Corporation, Grand Junction, Colorado, internal report.

Lederer, C. M., and V. S. Shirley (eds.), 1978. Table of Isotopes, Seventh Edition, John Wiley and Sons, New York.

Mathews, M. A., and K. L. Kosanke, 1978. Gross Gamma-Ray Calibration Blocks, GJBX-59(78), Grand Junction Area Office, U.S. Department of Energy, Grand Junction, Colorado.

Murri, R., E. Novak, and C. Ruzycki, 1983. Mobile Gamma Spectroscopy System Operation, BFEC-1983-1, Bendix Field Engineering Corporation, Grand Junction, Colorado, internal report.

Novak, E. F., 1985. Radiometric Monitoring of the Airport Pads at Walker Field, Grand Junction, Colorado, Over the Period October 1978 to November 1981, U.S. Department of Energy, Grand Junction, Colorado, in preparation.

Siegbahn, Kai, 1968. Alpha-, Beta- and Gamma-ray Spectroscopy, Vol. I, North-Holland Publishing Company, Amsterdam.

Stromswold, D. C., 1978. Monitoring of the Airport Calibration Pads at Walker Field, Grand Junction, Colorado, for Long-Term Radiation Variations, GJBX-99(78), Grand Junction Area Office, U.S. Department of Energy, Grand Junction, Colorado.

Trahey, N. M., A. M. Voeks, and M. D. Soriano, 1982. Grand Junction/New Brunswick Laboratory Interlaboratory Measurement Program, Part I - Evaluation, Part II - Methods Manual, NBL-303, New Brunswick Laboratory, U.S. Department of Energy, Argonne, Illinois.

Troxler Electronic Laboratories, Inc., 1980. 3400-B Series Instruction Manual, Surface Moisture-Density Gauges, Research Triangle Park, North Carolina.

U.S. Department of Health, Education, and Welfare, Bureau of Radiological Health, 1970. Radiological Health Handbook, Revised Edition, U.S. Government Printing Office, Washington, D.C.

Walpole, R. E., and R. H. Myers, 1972. Probability and Statistics for Engineers and Scientists, MacMillan Publishing Company, Inc., New York.

Ward, D. L., 1978. Construction of Calibration Pads Facility, Walker Field, Grand Junction, Colorado, GJBX-37(78), Grand Junction Area Office, U.S. Department of Energy, Grand Junction, Colorado.

Wilson, R. D., and D. C. Stromswold, 1981. Spectral Gamma-Ray Logging Studies, GJBX-21(81), Grand Junction Area Office, U.S. Department of Energy, Grand Junction, Colorado.

PUBLICATIONS
Issued by
TECHNICAL MEASUREMENTS CENTER
Bendix Field Engineering Corporation
for
U.S. Department of Energy
Office of Remedial Action and Waste Technology
Idaho Operations Office
Grand Junction Projects Office
November 1985

Number	Title (Authors)
GJ/TMC-01*†	Field Calibration Facilities for Environmental Measurement of Radium, Thorium, and Potassium. (D. C. George and L. Knight)
GJ/TMC-02	Review of Selected DOE Remedial Action Field Measurement Procedures for the Summer of 1982. (TMC Staff)
GJ/TMC-03*	Abbreviated Total-Count Logging Procedures for Use in Remedial Action. (D. C. George and R. K. Price)
GJ/TMC-04*	Evaluation of Methods for the Estimation of Indoor Radon Daughter Concentrations for Remedial Action Programs. (G. H. Langner, Jr., J. C. Pacer, V. G. Johnson, and M. A. Gillings)
GJ/TMC-05*	Feasibility Study of the Prompt Pb-214, Bi-214 Gamma Method for Determining Radon Migration Through Tailings. (L. R. Stieff, The Stieff Research and Development Co., Inc., Kensington, Maryland)
GJ/TMC-06*	Surface Gamma-Ray Measurement Protocol. (S. J. Marutzky, W. D. Steele, and B. N. Key)
GJ/TMC-07*	Procedures for Field Chemical Analyses of Water Samples. (N. Korte and D. Ealey)

---

*Available from
National Technical Information Service
U.S. Department of Commerce
5285 Port Royal Road
Springfield, Virginia 22161
703/487-4600

†To be updated.

PUBLICATIONS
Issued by
TECHNICAL MEASUREMENTS CENTER
(continued)

Number	Title (Authors)
GJ/TMC-08*	Procedures for the Collection and Preservation of Groundwater and Surface Water Samples and for the Installation of Monitoring Wells: Second Edition. (N. Korte and P. Kearl)
GJ/TMC-10*	Development of Solid Radium-226 Reference Materials. (R. B. Chessmore and P. R. Engelder)
GJ/TMC-13*	Procedures for Sampling Radium-Contaminated Soils. (H. L. Fleischhauer)
GJ/TMC-14*	Procedures for Reconnaissance Stream-Sediment Sampling. (H. L. Fleischhauer and P. R. Engelder)
GJ/TMC-15*	A Feasibility Study of the Use of Nuclear-Emulsion Techniques in the Study of Drill Core and Water Samples from the Monticello Mill, Monticello, Utah. (L. R. Stieff, The Stieff Research and Development Co., Inc., Kensington, Maryland)
GJ/TMC-16*	Test and Evaluation of Selected Instruments for Surface Gamma-Ray Measurements. (B. N. Key)
GJ/TMC-17*	Calibration-Pad Parameter Assignments for In-Situ Gamma-Ray Measurements of Radium, Thorium, and Potassium. (D. C. George, E. F. Novak, and R. K. Price)
GJ/TMC-18*	Operating Manual for the Radon-Daughter Chamber. (T. Nelson and G. H. Langner, Jr.)
GJ/TMC-19*	Laboratory Intercomparison of Analytical Results on Samples Contaminated by Uranium Mill Tailings. (N. Korte, M. Hollenbach, and S. Donivan)
GJ/TMC-20	Radon-Daughter Chamber Instrumentation System Reference Manual. (L. Johnson and R. Showalter)

*Available from
National Technical Information Service
U.S. Department of Commerce
5285 Port Royal Road
Springfield, Virginia 22161
703/487-4600

PUBLICATIONS
Issued by
TECHNICAL MEASUREMENTS CENTER
(continued)

Number	Title (Authors)
GJ/TMC-22*	Development of Solid Thorium-232 Reference Materials. (P. R. Engelder, S. Donivan, and R. B. Chessmore)
GJ/TMC-23	Gamma-Ray Instrument Calibration Comparison Workshop. (W. D. Steele, D. C. George, and J. L. Burnham)

*Available from
National Technical Information Service
U.S. Department of Commerce
5285 Port Royal Road
Springfield, Virginia 22161
703/487-4600